

**NOVEMBER 2014**

**M.Sc. IN MECHANICAL**

**MUSTAFA BARBAR**

**UNIVERSITY OF GAZIANTEP  
GRADUATE SCHOOL OF  
NATURAL & APPLIED SCIENCES**

**APPLICATION OF MESHFREE EFG METHOD IN PLATE PROBLEMS**

**M.Sc. THESIS  
IN  
MECHANICAL ENGINEERING**

**BY  
MUSTAFA BARBAR  
NOVEMBER 2014**

**Application of Meshfree EFG Method in Plate Problems**

**M.Sc. Thesis**

**in**

**Mechanical Engineering**

**University of Gaziantep**

**Supervisor**

**Assist. Prof. Dr. Ö. Yavuz BOZKURT**

**BY**

**Mustafa BARBAR**

**November 2014**

© 2014 [Mustafa BARBAR]

REPUBLIC OF TURKEY  
UNIVERSITY OF GAZIANTEP  
GRADUATE SCHOOL OF NATURAL & APPLIED SCIENCES  
MECHANICAL ENGINEERING

Name of the thesis: Application of Meshfree EFG method in Plate Problems


Name of student : Mustafa BARBAR

Exam Date : 27.11.2014

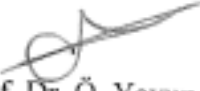
Approval of the Graduate School of Natural and Applied Sciences

  
Prof. Dr. Metin BÉDİR  
Director

I certify that this thesis satisfies all the requirements as a thesis for the degree of Master of Science.

  
Prof. Dr. M. Sait SÖYLEMEZ  
Head of Department

This is to certify that we have read this thesis and that in our opinion it is fully adequate, in scope and quality, as a thesis for the degree of Master of Science.

  
Assist. Prof. Dr. Ö. Yavuz BOZKURT  
Supervisor

Examining Committee Members:

Prof.Dr. Bahattin KANBER

Assist. Prof. Dr. Ö. Yavuz BOZKURT

Assist. Prof. Dr. İbrahim GÖV

Signature  
  
  


**I hereby declare that all information in this document has been obtained and presented in accordance with academic rules and ethical conduct. I also declare that, as required by these rules and conduct, I have cited and referenced all material and results that are not original to this work.**

Mustafa BARBAR

## **ABSTRACT**

### **APPLICATION OF MESHFREE EFG METHOD IN PLATE PROBLEMS**

BARBAR, Mustafa

M.Sc. in Mechanical Eng.

Supervisor: Assist. Prof. Dr. Ö. Yavuz BOZKURT

Nov 2014, 119 pages

In this work, the effects of selectable parameters of Element-Free Galerkin Method (EFGM); such as type of weight functions, size of support domain, number of gauss points, number of monomials and value of penalty coefficient, on the solution accuracy of the Reissner-Mindlin plate bending problems are investigated.

An EFGM source code using MATLAB has been written for the solutions of plate bending problems. Several plate bending problems were solved using the MATLAB source code and the results of EFGM solutions are compared with the results of analytical solutions.

**Keywords:** Meshfree Methods, Element Free Galerkin Method, Moving least squares, EFGM, plate bending.

## ÖZET

### PLAKA PROBLEMLERİ İÇİN ELEMAN BAĞIMSIZ GALERKİN YÖNTEMİ UYGULAMASI

BARBAR, Mustafa

Yüksek Lisans Tezi, Mak Müh. Bölümü

Tez Yöneticisi: Yrd.Doç.Dr. Ömer Yavuz BOZKURT

Kasım 2014, 119 sayfa

Bu çalışmada, Eleman Serbest Galerkin Yönteminin (EFGM) ağırlık fonksiyon türü, destek etki büyüklüğü, arka plan hücrelerindeki entegrasyon nokta sayısı, monomiyallerin derecesi ve ceza katsayısı değeri gibi seçilebilir parametrelerinin plaka bükme problemlerinde çözüm doğruluğuna etkisi araştırılmıştır.

MATLAB kullanarak, plaka bükme problemlerinin çözümleri için bir EFGM kaynak kodu yazılmıştır. Çeşitli plaka bükme problemleri, MATLAB kaynak kodu kullanılarak çözülmüş ve EFGM çözümlerinin sonuçları analitik sonuçları ile karşılaştırılmıştır.

**Keywords:** Ağsız yöntemler, Eleman Bağımsız Galerkin Yöntemi, Hareketli en küçük kareler yöntemi, EFGM, plaka bükme.

To my parents . . .



## **ACKNOWLEDGEMENTS**

I want to express my honest respect to my supervisor Assist. Prof. Ö. Yavuz BOZKURT for his advises and suggestions to have this thesis.

Finally I want to thanks my mother, my father, my brothers (Mohammed Omeed EZZULDDIN and Taha) and especially thanks to my friend Research Asst. Özkan ÖZBEK. Also I like to thank my friends (Ömer ALI and Mustafa KAMAL) for their reassurance and support.

## TABLE OF CONTENTS

	<b>Page</b>
ABSTRACT .....	v
ÖZET .....	vi
ACKNOWLEDGEMENTS .....	viii
TABLE OF CONTENTS .....	ix
LIST OF FIGURES .....	xi
LIST OF TABLES .....	xvi
CHAPTER 1 .....	1
INTRODUCTION .....	1
1.1. General Introduction .....	1
1.2. Research Objectives and Tasks .....	2
1.3. Layout of Thesis .....	2
CHAPTER 2 .....	3
LITERATURE SURVEY .....	3
2.1. Introduction .....	3
2.2. General Review of Some Mesh-free Methods .....	3
2.2.1. Smoothed Particle Hydrodynamics Method .....	3
2.2.2. Diffuse Element Method .....	3
2.2.3. Point Interpolation Method .....	4
2.2.4. Meshless Local-Petrov Galerkin .....	5
2.3. Element-Free Galerkin Method .....	5
2.4. Element-Free Galerkin Method in the Solution of Plate Bending Problems .....	7
2.5. Conclusions on Literature Survey .....	8
CHAPTER 3 .....	9
PLATE THEORIES .....	9
3.1. Introduction .....	9
3.2. Review of The Plate Theories .....	9
3.2.1. Kirchhoff Plate Theory .....	9
3.2.2. Reissner-Mindlin Plate Theory .....	12
CHAPTER 4 .....	17
ELEMENT FREE GALERKIN METHOD FOR MINDLIN-REISSNER PLATE BENDING PROBLEMS .....	17

4.1. Introduction .....	17
4.2. Short Description of Implementation Procedure for Galerkin Meshfree Methods.....	17
4.2.1. Basic Definitions for Meshfree Methods .....	18
4.2.1.1. Local Domains (Support and Influence Domains) .....	18
4.2.1.2. Background cells.....	18
4.3. Formulation of Moving least-squares (MLS) shape functions .....	19
4.4. Governing equations and weak form .....	21
CHAPTER 5 .....	26
NUMERICAL EXPERIMENTS AND DISCUSSIONS .....	26
5.1. Introduction .....	26
5.2. Simply supported square plate under transverse centric point load.....	26
5.3. Simply supported square plate under uniform load. ....	45
5.4. Clamped circular plate under uniform load. ....	79
CHAPTER 6 .....	112
CONCLUSIONS AND RECOMMENDATIONS .....	112
REFERENCES.....	113

## LIST OF FIGURES

	<b>Page</b>
Figure 3.1. Plate subjected to transverse loads.....	9
Figure 3.2. Deformation according to Kirchhoff plate cross-section a) $y - z$ plane b) $x - z$ plane.....	10
Figure 3.3. Free body diagram of the plate element .....	12
Figure 3.4. A typical Reissner-Mindlin plate .....	13
Figure 3.5. Deformation according to Reissner-Mindlin cross-section a) $y - z$ plane b) $x - z$ plane.....	13
Figure 4.1. Support Domain; the centre is a quadrature point .....	19
Figure 5.1. Simply supported square plate under transverse centric point load.....	27
Figure 5.2. The EFGM models for a) regular node distributions, b) irregular node distributions.....	27
Figure 5.3. Variations of normalized central deflections $w_c/(pL^4/100D)$ against $n_g$ for simply supported square plate under transverse centric point load using cubic spline weight functions and regular node distribution with $\alpha_p = 6$ .....	30
Figure 5.4. Variations of normalized central deflections $w_c/(pL^4/100D)$ against $n_g$ for simply supported square plate under transverse centric point load using cubic spline weight functions and irregular node distribution with $\alpha_p = 6$ .....	32
Figure 5.5. Variations of normalized central deflections $w_c/(pL^4/100D)$ against $\alpha_p$ for simply supported square plate under transverse centric point load using cubic spline weight functions and regular node distribution with $n_g = 5$ .....	34
Figure 5.6. Variations of normalized central deflections $w_c/(pL^4/100D)$ against $\alpha_p$ for simply supported square plate under transverse centric point load using cubic spline weight functions and irregular node distribution with $n_g = 5$ .....	36
Figure 5.7. Variations of normalized central deflections $w_c/(pL^4/100D)$ against $n_g$ for simply supported square plate under transverse centric	

point load using quartic spline weight functions and regular node distribution with $\alpha_p = 6$ .....	38
Figure 5.8. Variations of normalized central deflections $w_c/(pL^4/100D)$ against $n_g$ for simply supported square plate under transverse centric point load using quartic spline weight functions and irregular node distribution with $\alpha_p = 6$ .....	40
Figure 5.9. Variations of normalized central deflections $w_c/(pL^4/100D)$ against $\alpha_p$ for simply supported square plate under transverse centric point load using quartic spline weight functions and regular node distribution with $n_g = 5$ .....	42
Figure 5.10. Variations of normalized central deflections $w_c/(pL^4/100D)$ against $\alpha_p$ for simply supported square plate under transverse centric point load using quartic spline weight functions and irregular node distribution with $n_g = 5$ .....	44
Figure 5.11. Simply supported square plate under uniform load.....	45
Figure 5.12. The EFGM models for a) regular node distributions, b) irregular node distributions.....	45
Figure 5.13. Variations of normalized central deflections $w_c/(pL^4/100D)$ against $n_g$ for simply supported square plate subjected to uniform load using cubic spline weight functions and regular node distribution with $\alpha_p = 6$ .....	48
Figure 5.14. Variations of normalized central moments $M_c/(pL^2/10)$ against $n_g$ for simply supported square plate subjected to uniform load using cubic spline weight functions and regular node distribution with $\alpha_p = 6$ .....	50
Figure 5.15. Variations of normalized central deflections $w_c/(pL^4/100D)$ against $n_g$ for simply supported square plate subjected to uniform load using cubic spline weight functions and irregular node distribution with $\alpha_p = 6$ .....	52
Figure 5.16. Variations of normalized central moments $M_c/(pL^2/10)$ against $n_g$ for simply supported square plate subjected to uniform load using cubic spline weight functions and irregular node distribution with $\alpha_p = 6$ .....	54
Figure 5.17. Variations of normalized central deflections $w_c/(pL^4/100D)$ against $\alpha_p$ for simply supported square plate subjected to uniform load using cubic spline weight functions and regular node distribution with $n_g = 5$ .....	56
Figure 5.18. Variations of normalized central moments $M_c/(pL^2/10)$ against $\alpha_p$ for simply supported square plate subjected to uniform	

load using cubic spline weight functions and regular node distribution with $n_g = 5$ .....	58
Figure 5.19. Variations of normalized central deflections $w_c/(pL^4/100D)$ against $\alpha_p$ for simply supported square plate subjected to uniform load using cubic spline weight functions and irregular node distribution with $n_g = 5$ .....	60
Figure 5.20. Variations of normalized central moments $M_c/(pL^2/10)$ against $\alpha_p$ for simply supported square plate subjected to uniform load using cubic spline weight functions and irregular node distribution with $n_g = 5$ .....	62
Figure 5.21. Variations of normalized central deflections $w_c/(pL^4/100D)$ against $n_g$ for simply supported square plate subjected to uniform load using quartic spline weight functions and regular node distribution with $\alpha_p = 6$ .....	64
Figure 5.22. Variations of normalized central moments $M_c/(pL^2/10)$ against $n_g$ for simply supported square plate subjected to uniform load using quartic spline weight functions and regular node distribution with $\alpha_p = 6$ .....	66
Figure 5.23. Variations of normalized central deflections $w_c/(pL^4/100D)$ against $n_g$ for simply supported square plate subjected to uniform load using quartic spline weight functions and irregular node distribution with $\alpha_p = 6$ .....	68
Figure 5.24. Variations of normalized central moments $M_c/(pL^2/10)$ against $n_g$ for simply supported square plate subjected to uniform load using quartic spline weight functions and irregular node distribution with $\alpha_p = 6$ .....	70
Figure 5.25. Variations of normalized central deflections $w_c/(pL^4/100D)$ against $\alpha_p$ for simply supported square plate subjected to uniform load using quartic spline weight functions and regular node distribution with $n_g = 5$ .....	72
Figure 5.26. Variations of normalized central moments $M_c/(pL^2/10)$ against $\alpha_p$ for simply supported square plate subjected to uniform load using quartic spline weight functions and regular node distribution with $n_g = 5$ .....	74
Figure 5.27. Variations of normalized central deflections $w_c/(pL^4/100D)$ against $\alpha_p$ for simply supported square plate subjected to uniform load using quartic spline weight functions and irregular node distribution with $n_g = 5$ .....	76

Figure 5.28. Variations of normalized central moments $M_c/(pL^2/10)$ against $\alpha_p$ for simply supported square plate subjected to uniform load using quartic spline weight functions and irregular node distribution with $n_g = 5$ .....	78
Figure 5.29. Clamped circular plate under uniform load.....	79
Figure 5.30. The EFGM models for a) regular node distributions, b) irregular node distributions.....	79
Figure 5.31. Variations of normalized central deflections $w_c/(pL^4/100D)$ against $n_g$ for clamped circular plate subjected to uniform load using cubic spline weight functions and regular node distribution with $\alpha_p = 6$ .....	81
Figure 5.32. Variations of normalized central moments $M_c/(pL^2/10)$ against $n_g$ for clamped circular plate subjected to uniform load using cubic spline weight functions and regular node distribution with $\alpha_p = 6$ .....	83
Figure 5.33. Variations of normalized central deflections $w_c/(pL^4/100D)$ against $n_g$ for clamped circular plate subjected to uniform load using cubic spline weight functions and irregular node distribution with $\alpha_p = 6$ .....	85
Figure 5.34. Variations of normalized central moments $M_c/(pL^2/10)$ against $n_g$ for clamped circular plate subjected to uniform load using cubic spline weight functions and irregular node distribution with $\alpha_p = 6$ .....	87
Figure 5.35. Variations of normalized central deflections $w_c/(pL^4/100D)$ against $\alpha_p$ for clamped circular plate subjected to uniform load using cubic spline weight functions and regular node distribution with $n_g = 5$ .....	89
Figure 5.36. Variations of normalized central moments $M_c/(pL^2/10)$ against $\alpha_p$ for clamped circular plate subjected to uniform load using cubic spline weight functions and regular node distribution with $n_g = 5$ .....	91
Figure 5.37. Variations of normalized central deflections $w_c/(pL^4/100D)$ against $\alpha_p$ for clamped circular plate subjected to uniform load using cubic spline weight functions and irregular node distribution with $n_g = 5$ .....	93
Figure 5.38. Variations of normalized central moments $M_c/(pL^2/10)$ against $\alpha_p$ for clamped circular plate subjected to uniform load using cubic spline weight functions and irregular node distribution with $n_g = 5$ .....	95

Figure 5.39. Variations of normalized central deflections $w_c/(pL^4/100D)$ against $n_g$ for clamped circular plate subjected to uniform load using quartic spline weight functions and regular node distribution with $\alpha_p = 6$ .....	97
Figure 5.40. Variations of normalized central moments $M_c/(pL^2/10)$ against $n_g$ for clamped circular plate subjected to uniform load using quartic spline weight functions and regular node distribution with $\alpha_p = 6$ .....	99
Figure 5.41. Variations of normalized central deflections $w_c/(pL^4/100D)$ against $n_g$ for clamped circular plate subjected to uniform load using quartic spline weight functions and irregular node distribution with $\alpha_p = 6$ .....	101
Figure 5.42. Variations of normalized central moments $M_c/(pL^2/10)$ against $n_g$ for clamped circular plate subjected to uniform load using quartic spline weight functions and irregular node distribution with $\alpha_p = 6$ .....	103
Figure 5.43. Variations of normalized central deflections $w_c/(pL^4/100D)$ against $\alpha_p$ for clamped circular plate subjected to uniform load using quartic spline weight functions and regular node distribution with $n_g = 5$ .....	105
Figure 5.44. Variations of normalized central moments $M_c/(pL^2/10)$ against $\alpha_p$ for clamped circular plate subjected to uniform load using quartic spline weight functions and regular node distribution with $n_g = 5$ .....	107
Figure 5.45. Variations of normalized central deflections $w_c/(pL^4/100D)$ against $\alpha_p$ for clamped circular plate subjected to uniform load using quartic spline weight functions and irregular node distribution with $n_g = 5$ .....	109
Figure 5.46. Variations of normalized central moments $M_c/(pL^2/10)$ against $\alpha_p$ for clamped circular plate subjected to uniform load using quartic spline weight functions and irregular node distribution with $n_g = 5$ .....	109



## LIST OF TABLES

	Page
Table 5.1. Normalized central deflections $w_c/(pL^4/100D)$ of simply supported square plate under transverse centric point load for regular node distribution using cubic spline weight function with $\alpha_p = 6$ .....	29
Table 5.2. Normalized central deflections $w_c/(pL^4/100D)$ of simply supported square plate under transverse centric point load for irregular node distribution using cubic spline weight function with $\alpha_p = 6$ .....	31
Table 5.3. Variations of normalized central deflections $w_c/(pL^4/100D)$ of simply supported square plate under transverse centric point load using regular node distribution using cubic spline weight function with $n_g = 5$ .....	33
Table 5.4. Variations of normalized central deflections $w_c/(pL^4/100D)$ of simply supported square plate under transverse centric point load using irregular node distribution using cubic spline weight function with $n_g = 5$ .....	35
Table 5.5. Variations of normalized central deflections $w_c/(pL^4/100D)$ of simply supported square plate under transverse centric point load using regular node distribution using quartic spline weight function with $\alpha_p = 6$ .....	37
Table 5.6. Variations of normalized central deflections $w_c/(pL^4/100D)$ of simply supported square plate under transverse centric point load using irregular node distribution using quartic spline weight function with $\alpha_p = 6$ .....	39
Table 5.7. Variations of normalized central deflections $w_c/(pL^4/100D)$ of simply supported square plate under transverse centric point load using regular node distribution using quartic spline weight function with $n_g = 5$ .....	41
Table 5.8. Variations of normalized central deflections $w_c/(pL^4/100D)$ of simply supported square plate under transverse centric point load using irregular node distribution using quartic spline weight function with $n_g = 5$ .....	43
Table 5.9. Normalized central deflections $w_c/(pL^4/100D)$ of simply supported square plate subjected to uniform transverse load for regular node distribution using cubic spline weight function with $\alpha_p = 6$ .....	47
Table 5.10. Normalized central moments $M_c/(pL^2/10)$ of simply supported square plate subjected to uniform transverse load for	

regular node distribution using cubic spline weight function with $\alpha_p = 6$ .....	49
Table 5.11. Normalized central deflections $w_c/(pL^4/100D)$ of simply supported square plate subjected to uniform transverse load for irregular node distribution using cubic spline weight function with $\alpha_p = 6$ .....	51
Table 5.12. Normalized central moments $M_c/(pL^2/10)$ of simply supported square plate subjected to uniform transverse load for irregular node distribution using cubic spline weight function with $\alpha_p = 6$ .....	53
Table 5.13. Variations of normalized central deflections $w_c/(pL^4/100D)$ of simply supported square plate subjected to uniform transverse load using regular node distribution using cubic spline weight function with $n_g = 5$ .....	55
Table 5.14. Variations of normalized central moments $M_c/(pL^2/10)$ of simply supported square plate subjected to uniform transverse load using regular node distribution using cubic spline weight function with $n_g = 5$ .....	57
Table 5.15. Variations of normalized central deflections $w_c/(pL^4/100D)$ of simply supported square plate subjected to uniform transverse load using irregular node distribution using cubic spline weight function with $n_g = 5$ .....	59
Table 5.16. Variations of normalized central moments $M_c/(pL^2/10)$ of simply supported square plate subjected to uniform transverse load using irregular node distribution using cubic spline weight function with $n_g = 5$ .....	61
Table 5.17. Variations of normalized central deflections $w_c/(pL^4/100D)$ of simply supported square plate subjected to uniform transverse load using regular node distribution using quartic spline weight function with $\alpha_p = 6$ .....	63
Table 5.18. Variations of normalized central moments $M_c/(pL^2/10)$ of simply supported square plate subjected to uniform transverse load using regular node distribution using quartic spline weight function with $\alpha_p = 6$ .....	65
Table 5.19. Variations of normalized central deflections $w_c/(pL^4/100D)$ of simply supported square plate subjected to uniform transverse load using irregular node distribution using quartic spline weight function with $\alpha_p = 6$ .....	67

Table 5.20. Variations of normalized central moments $M_c/(pL^2/10)$ of simply supported square plate subjected to uniform transverse load using irregular node distribution using quartic spline weight function with $\alpha_p = 6$ .....	69
Table 5.21. Variations of normalized central deflections $w_c/(pL^4/100D)$ of simply supported square plate subjected to uniform transverse load using regular node distribution using quartic spline weight function with $n_g = 5$ .....	71
Table 5.22. Variations of normalized central moments $M_c/(pL^2/10)$ of simply supported square plate subjected to uniform transverse load using regular node distribution using quartic spline weight function with $n_g = 5$ .....	73
Table 5.23. Variations of normalized central deflections $w_c/(pL^4/100D)$ of simply supported square plate subjected to uniform transverse load using irregular node distribution using quartic spline weight function with $n_g = 5$ .....	75
Table 5.24. Variations of normalized central moments $M_c/(pL^2/10)$ of simply supported square plate subjected to uniform transverse load using irregular node distribution using quartic spline weight function with $n_g = 5$ .....	77
Table 5.25. Normalized central deflections $w_c/(pL^4/100D)$ of clamped circular plate subjected to uniform transverse load for regular node distribution using cubic spline weight function with $\alpha_p = 6$ .....	80
Table 5.26. Normalized central moments $M_c/(pL^2/10)$ of clamped circular plate subjected to uniform transverse load for regular node distribution using cubic spline weight function with $\alpha_p = 6$ .....	82
Table 5.27. Normalized central deflections $w_c/(pL^4/100D)$ of clamped circular plate subjected to uniform transverse load for irregular node distribution using cubic spline weight function with $\alpha_p = 6$ .....	84
Table 5.28. Normalized central moments $M_c/(pL^2/10)$ of clamped circular plate subjected to uniform transverse load for irregular node distribution using cubic spline weight function with $\alpha_p = 6$ .....	86
Table 5.29. Variations of normalized central deflections $w_c/(pL^4/100D)$ of clamped circular plate subjected to uniform transverse load using regular node distribution using cubic spline weight function with $n_g = 5$ .....	88

Table 5.30. Variations of normalized central moments $M_c/(pL^2/10)$ of clamped circular plate subjected to uniform transverse load using regular node distribution using cubic spline weight function with $n_g = 5$ .....	90
Table 5.31. Variations of normalized central deflections $w_c/(pL^4/100D)$ of clamped circular plate subjected to uniform transverse load using irregular node distribution using cubic spline weight function with $n_g = 5$ .....	92
Table 5.32. Variations of normalized central moments $M_c/(pL^2/10)$ of clamped circular plate subjected to uniform transverse load using irregular node distribution using cubic spline weight function with $n_g = 5$ .....	94
Table 5.33. Variations of normalized central deflections $w_c/(pL^4/100D)$ of clamped circular plate subjected to uniform transverse load using regular node distribution using quartic spline weight function with $\alpha_p = 6$ .....	96
Table 5.34. Variations of normalized central moments $M_c/(pL^2/10)$ of clamped circular plate subjected to uniform transverse load using regular node distribution using quartic spline weight function with $\alpha_p = 6$ .....	98
Table 5.35. Variations of normalized central deflections $w_c/(pL^4/100D)$ of clamped circular plate subjected to uniform transverse load using irregular node distribution using quartic spline weight function with $\alpha_p = 6$ .....	100
Table 5.36. Variations of normalized central moments $M_c/(pL^2/10)$ of clamped circular plate subjected to uniform transverse load using irregular node distribution using quartic spline weight function with $\alpha_p = 6$ .....	102
Table 5.37. Variations of normalized central deflections $w_c/(pL^4/100D)$ of clamped circular plate subjected to uniform transverse load using regular node distribution using quartic spline weight function with $n_g = 5$ .....	104
Table 5.38. Variations of normalized central moments $M_c/(pL^2/10)$ of clamped circular plate subjected to uniform transverse load using regular node distribution using quartic spline weight function with $n_g = 5$ .....	106
Table 5.39. Variations of normalized central deflections $w_c/(pL^4/100D)$ of clamped circular plate subjected to uniform transverse load using irregular node distribution using quartic spline weight function with $n_g = 5$ .....	108

Table 5.40. Variations of normalized central moments $M_c/(pL^2/10)$ of clamped circular plate subjected to uniform transverse load using irregular node distribution using quartic spline weight function with $n_g = 5$ .....	110
--	-----

# CHAPTER 1

## INTRODUCTION

### 1.1 General Introduction

The Finite Element Method (FEM), Boundary Element Method (BEM), and Finite Difference Method (FDM) are the popular methods in the field of numerical simulation methods. These methods are successfully used in the solutions of several engineering and scientific problems. The most important reasons behind this success are unified formulations for different approximation schemes, ability to tackle problems with irregular boundaries, ability to deal with complex boundary conditions, easy modifications to improve solution quality and handling non-linear problems with linear approximations.

Despite these impressive features, FEM and BEM has the following shortcomings;

- Inadequate results near the boundary of the problem domain,
- Requirement of re-meshing for the regions enclosing geometry changes,
- Discontinuities for derivatives of field variables at the boundaries of elements,  
and
- Mesh quality dependent solution.

The discretization scheme of FEM and BEM is the origin of these shortcomings. Meshfree methods are the recently developed numerical methods to eliminate/alleviate the issues mentioned above using a new discretization approach. In Meshfree methods, the problem domain and its boundaries are defined by a set of arbitrarily scattered nodes. The interpolation of field variables are carried out using momentarily selected field nodes for construction of local domains. Obtaining a numerical method superior over the conventional numerical methods, by means of removing errors caused by the mesh, is the aim of Meshfree methods. However, these methods are new and in the development stage. They have some issues such as stability, efficiency, etc. to be solved.

## **1.2 Research Objectives and Tasks**

The main objective of this study is the investigation of effects of selectable parameters of EFGM, such as weight functions, size of support domain, number of gauss points in a background cell, value of penalty coefficient and order of monomials, on the accuracy of plate bending problems.

The research tasks can be shown as follows:

- I. Revise of the Element-Free Galerkin methods in the literature.
- II. Revise of the Moving Least Squares approximation scheme in the literature.
- III. Construction of shape functions using the Moving Least Squares.
- IV. Implementation of the MLS shape functions to EFG method.
- V. Development of a MATLAB source code to implement the EFGM in plate problems.
- VI. Solution of plate bending problems using the EFG method.
- VII. Investigation of effects of the selectable parameters.

## **1.3 Layout of Thesis**

A short literature review about the Meshfree methods and a special review for element free Galerkin method are presented in chapter two. The basic concepts of element free Galerkin method is summarized in chapter three. In chapter four, solutions of some benchmark problems using different values of selectable parameters and the discussions of the results are presented. The conclusions are introduced in chapter five.

## **CHAPTER 2**

### **LITERATURE SURVEY**

#### **2.1 Introduction**

A brief literature review related with Meshfree methods is given in this section. According to the interpolation and integration techniques used in, several types of meshfree methods can be found in the literature. Some of them are Smoothed Particle Hydro-dynamics (SPH) [1,2], Diffuse Element Method (DEM) [3], Element-Free Galerkin Method [4], Reproducing Kernel Particle Method (RPKM) [5], Point Interpolation Method (PIM) [6], Meshless Local-Petrov Galerkin (MLPG) [7], Natural Element Method [8] and Finite Particle Method (FPM) [9].

The brief reviews of the SPH method, the DEM, the PIM and the MLPG method are presented in Section 2.2. The literature review of EFGM, subject of the study, is represented in Section 2.3.

#### **2.2 General Review of Some Mesh-Free Methods**

##### **2.2.1 Smoothed Particle Hydrodynamics Method**

The SPH method which can be considered as the ancestor of meshfree methods was proposed by Lucy [1], Gingold and Monaghan [2]. It was developed to understand the astrophysical phenomena by means of numerical simulation. A set of moving particles which doesn't have any predefined relations are used to represent physical problem domain. The mathematical model of physical problem is constructed using partial differential equations which are transformed into selected finite integral form to compute integral over the particles [10]. Since its inception, SPH has a constantly evolving application areas such as fluid dynamics [11], explosion [12], large deformations and fracture in solid continuums [13]. However, SPH method is not foolproof; it has stability and consistency problems, especially in solid mechanics [14].

##### **2.2.2 Diffuse Element Method**

The DEM proposed by Nayroles et al [3] is the initial example of meshfree methods based on Galerkin weak form. The difference between FEM and DEM is the



field approximation. The field approximation of the DEM is obtained for local domains using Moving Least Squares (MLS) approximation and these local domains contain varying numbers of nodes [3].

### **2.2.3 Point Interpolation Method**

PIM is a meshfree method which was firstly proposed by Liu [6]. The field variables at a point are interpolated from the field values of local domain of the point. The interpolation functions are constructed using polynomials selected from the Pascal's triangle [15]. The interpolation functions possess the delta Kronecker property which simplifies the enforcement of boundary conditions by eliminating extra algorithm requirements for implementation of boundary conditions as in some meshfree methods [16]. This simplifies the computation procedure of the PIM and it also increases the computational efficiency of the PIM.

Besides the advantages of PIM, singularity of moment matrix is the gap of PIM which avoids the construction of interpolation functions [17]. Some algorithms have been proposed to overcome the singularity problem such as transformation of coordinates of points in a local domain [18], matrix triangularization algorithm [19] and diagonal offset algorithm [20]. However, these methods cannot guarantee the elimination of singularity problem permanently.

The replacement of polynomial basis function with radial basis function is another method to handle the singularity problem of PIM [21]. The PIM based on radial basis function is called as Radial Point Interpolation Method (RPIM) [22]. It solves the singularity problem and some order of monomials can be added to guarantee the elimination of singularity problem permanently. However, the accuracy and computational efficiency of RPIM is less than the PIM.

The applications of PIM to various engineering problems, such as 2D and 3D problems [22], beams and shells [22], static deformation problems [22], buckling [23], thermoplastic problems [24], plate bending problems [25], dynamic response of thin and thick plates [26] and composite laminated plates [27] are found in the literature.

#### **2.2.4 Meshless Local-Petrov Galerkin**

Meshless local Petrov-Galerkin method (MLPG) is a real meshfree method which doesn't require any background cells (or elements) for interpolation or integration process. This method was proposed by Atluri and Zhu [7], and later developed by Atluri and Shen [28]. The replacement of global weak form with the local weak forms generated by using overlapping local domains is the main difference between (MLPG) and finite element method. Integration of the weak form is performed on the local sub-domains with ordinary geometrical shapes, therefore there is need to background cells (or elements) for integration or interpolation purposes. Element connectivity is not a necessity and only nodal information is required, which leads to a simple and suitable pre-processing. Because of this, wide range of engineering applications of the MLPG can be found in the literature, such as 2-D elasto-statics [22], plate problems [29]; 2-D elasto-dynamics [30], fluid mechanics [31], large deformation problems [32]; convection-diffusion problems [31], fracture mechanics, [33]; analyses of shell deformations [22]; and dynamics problems [21].

#### **2.3 Element-Free Galerkin Method**

The original EFG method was proposed by Belytschko et al. [4]. The approximation procedure of EFGM is based only on nodes, so it doesn't require any mesh generation or remeshing operations. However, a set of background cells is used to take integral of Galerkin weak form. By comparing this method with the finite element method, it's shown that the EFG method has the advantages of rapid convergence [34, 36], and also a smooth stress solution can be obtained without post-processing. However, the computational cost of EFG method is higher than of FEM [28]. This is because the node searching has to be performed and a set of algebraic equations should be solved to compute the MLS shape functions for each sampling point and also the requirement of more nodes for the construction of the MLS shape functions lead to larger band width for the resultant system matrix [22].

In the EFGM, the problem domain and its boundaries are represented by a set of arbitrary distributed nodes. The irregularity of node distribution does not suffer much degradation in accuracy [22]. Because of that, EFGM becomes one of the promising meshfree methods. The accuracy of the EFGM have been reported as good by scientists [21].

Despite the above significant advantages, the Kronecker delta criterion cannot be satisfied by MLS approximation and there is no resemblance between the essential boundary conditions in the EFG method and the conventional FEM. To solve this problem, in the last previous years, many specified techniques for the enforcement of essential boundary conditions in mesh-free methods have been proposed. Such as the penalty method [36], the Lagrange multiplier method [37], coupling of EFGM with FEM [38], and employment of singular weight functions [39].

The EFGM has been successfully applied to a large assortment of problems, including solid mechanics, fluid mechanics, heat transfer, and electromagnetic field problems. In solid mechanics, a variety of elastic and plastic applications of EFG method can be found for two-dimensional (2-D) and three-dimensional (3-D) problems such as; plane stress [40], plane strain [41], axisymmetric [42], beams [43], shell [44] and plate problems [45]. Fluid-structure interaction problems [46], incompressible flow problems [48], free surface flow [49] problems are some of the fluid mechanics applications of EFG method. The successful applications of heat transfer problems can be summarized as steady state and transient heat conduction analyses [2, 5], axisymmetric heat transfer problems [10], heat transfer of composite slabs [12], heat flow [11], and moving heat source problems [13]. The simple list of electromagnetic field applications are 3D electromagnetic field [50], static and quasi-static electromagnetic field [51], 2D electromagnetic wave scattering [52], electromagnetic scattering [53], axisymmetric electromagnetic [54] problems.

EFGM serves high convergence rates, stable solutions, and, application flexibility by the elimination of mesh requirement. Because of these, EFGM has become one of the best choice to solve fracture mechanics and crack propagation problems. In the EFGM, a growing crack can be modelled easily by extending the surfaces that match to the crack without the need for remeshing. Several fracture mechanics and crack growth analysis [55, 56] using EFGM can be found in the literature. Also, many arguments on the implementation advantages of the EFG and other meshfree methods over FEM in solving crack propagation problems have been reported [57]. For example, Belytschko et al. [58] state that, in the recent years, finite element schemes with remeshing have been used to solve growing crack problems.

In addition, many techniques have been proposed of coupling EFG method with FEM [38]. All these applications and extensions denote that the EFG method is progressively becoming a mature and practical computational approach within the group of computational mechanics, the benefit behind using the MLS approximation is to achieve stability in function approximation, and use of Galerkin procedure to provide stable and well behaved discretized global system equations.

## **2.4 Element-Free Galerkin Method in the Solution of Plate Bending Problems**

The plate structures have a variety of engineering applications with several geometries and loading conditions. Because of this, the analysis of plates are very important for engineers. The analytical solutions of plate's structures for complex geometries and complex loading conditions are very difficult. The numerical solutions have been developed using different schemes such as; FEM, BEM, and meshfree methods.

The EFG method is one of the meshfree methods that widely used in the analysis of plate structures. Krysl and Belytschko have used it for the static analysis of thin plates [45]. The EFG method has been also used for the bending analysis of Kirchhoff plates [59], Mindlin-Reissner plates [60], laminated composite plates [61], and thick plates [62]. The buckling [63], vibration [64], elasto-plastic [65], and crack [66] analysis of plates are found in the literature.

The EFG method has shear locking issue for the higher order plate theories [67]. To eliminate shear locking issue, several techniques were proposed such as; use of higher order basis [68] and use of first derivatives of shape functions as shape functions for rotations [69]

## **2.5 Conclusions on Literature Survey**

The literature review shows that the EFG method has some selectable parameters that affect the accuracy of solutions such as;

- size of support domain,
- number of polynomial basis,
- type of weight function,
- number of integration points and
- value of penalty coefficient.

The effects of these selectable parameters on the accuracy of the solution of Reissner-Mindlin plate bending are not well defined and examined.

## CHAPTER 3

### PLATE THEORIES

#### 3.1 Introduction

A plate is a flat structure and has a very small thickness in comparison to the other two dimensions. The applied forces of a plate are transverse loads through bending.

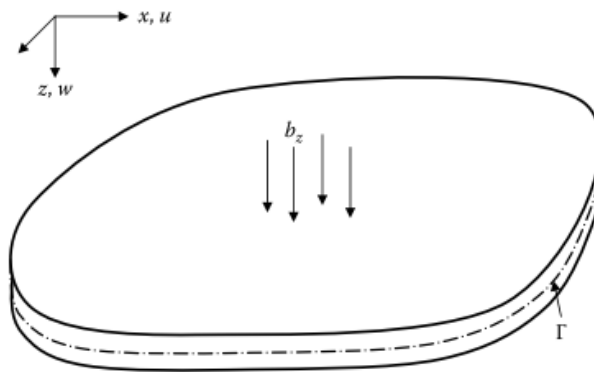


**Figure 3.1.** Plate subjected to transverse loads.

In the literature, several theories are present to analyse the deflections and stresses in plates. However, in this section, short reviews of two plate theories are presented about bending of the plates. These theories are as follows;

- Kirchhoff plate theory,
- Reissner-Mindlin plate theory.

The Kirchhoff and Reissner-Mindlin plate theories are presented with governing equations in the following parts of the chapter.

#### 3.2 Review of The Plate Theories

##### 3.2.1 Kirchhoff Plate Theory

The Kirchhoff plate theory is also known as the classical plate theory (CPT). It is used for thin plates. It is based upon assumptions initiated for beams by Bernoulli but

first applied to plates and shells by Kirchhoff. Basically, three assumptions are used to reduce the equations of three dimensional theory of elasticity to two dimensions [70]:

- Normal to the mid-plane before deformation remain straight and normal to the mid-plane after deformation.
- Transverse direct and shear stress effects are negligible.
- Deflections are small compared with the plate thickness.

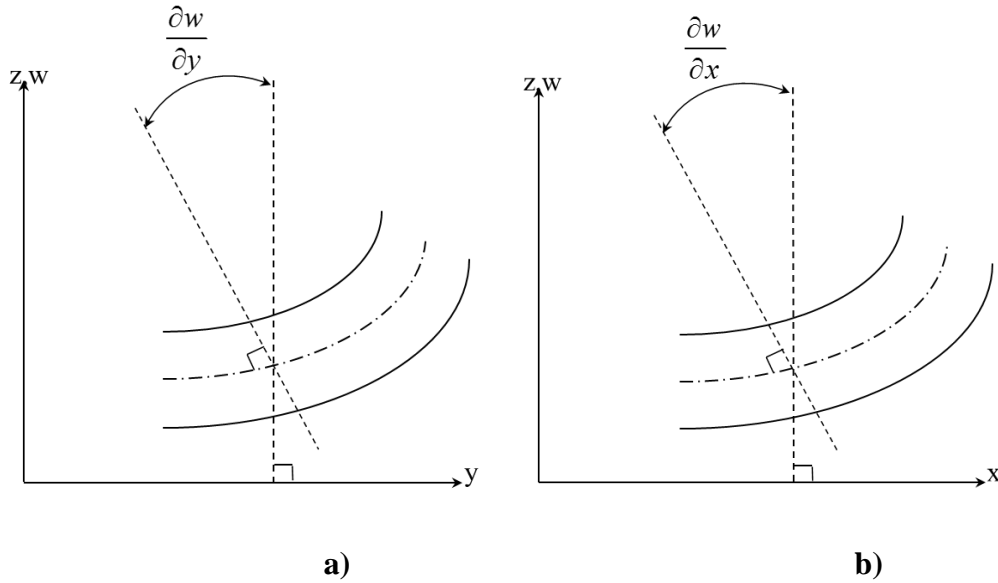


**Figure 3.2.** Deformation according to Kirchhoff plate cross-section  
**a)**  $y - z$  plane, **b)**  $x - z$  plane

The displacements of in-plane axes  $x$  and  $y$  are  $u$  and  $v$  that can be expressed as

$$u = -z \frac{\partial w}{\partial x} \quad (3.1)$$

$$v(x, y, z) = -z \frac{\partial w}{\partial y} \quad (3.2)$$

where  $z$  is the direction of the plate thickness.

Since transverse shear deformations are neglected, the strains can be written as

$$\{ \epsilon_x \ \epsilon_y \ \gamma_{xy} \} = -z \{ K_x \ K_y \ K_{xy} \} \quad (3.3)$$

where  $K$ , is the curvature,

$$\{K\}^T = \{ K_x \ K_y \ K_{xy} \} = \left\{ \frac{\partial^2 w}{\partial x^2} \ \frac{\partial^2 w}{\partial y^2} \ 2 \frac{\partial^2 w}{\partial x \partial y} \right\} \quad (3.4)$$

From substituting Eq.(3.3) into equation of  $\{\sigma\} = [D]\{\epsilon\}$  is the plane stress constitutive equation for an isotropic material; the equation becomes in following form

$$\{ \sigma \} = -z[D]\{K\} \quad (3.5)$$

in which  $\{ \sigma \} = \{ \sigma_x \ \sigma_y \ \tau_{xy} \}$  and  $[D]$  is the material property matrix,

$$[D] = \frac{E}{1 - \nu^2} \begin{bmatrix} 1 & \nu & 0 \\ \nu & 1 & 0 \\ 0 & 0 & \frac{1 - \nu}{2} \end{bmatrix} \quad (3.6)$$

Moments are defined as

$$\{ M \} = \int_{-h/2}^{h/2} \{ \sigma \} z \, dz \quad (3.7)$$

where  $\{ M \} = \{ M_x \ M_y \ M_{xy} \}$  and  $h$  is the thickness of plate.

Substituting of Eq. (3.5) into Eq. (3.7),

$$\{ M \} = -[D]\{K\} \quad (3.8)$$

where

$$[\bar{D}] = \frac{h^3}{12} [D] \quad (3.9)$$

Equilibrium equations are obtained from the free body diagram as shown in Fig. 3.2. Moment equilibriums about the  $y$  – and  $x$  –axes and force equilibrium about the  $z$  –axis, after neglecting higher order terms, can be written as

$$\frac{\partial M_x}{\partial x} + \frac{\partial M_{xy}}{\partial y} - Q_x = 0 \quad (3.9)$$

$$\frac{\partial M_{xy}}{\partial x} + \frac{\partial M_y}{\partial y} - Q_y = 0 \quad (3.10)$$

$$\frac{\partial Q_x}{\partial x} + \frac{\partial Q_y}{\partial y} + p = 0 \quad (3.11)$$



where  $Q_x$  and  $Q_y$  are the shear forces and  $p$  is the distributed pressure load.

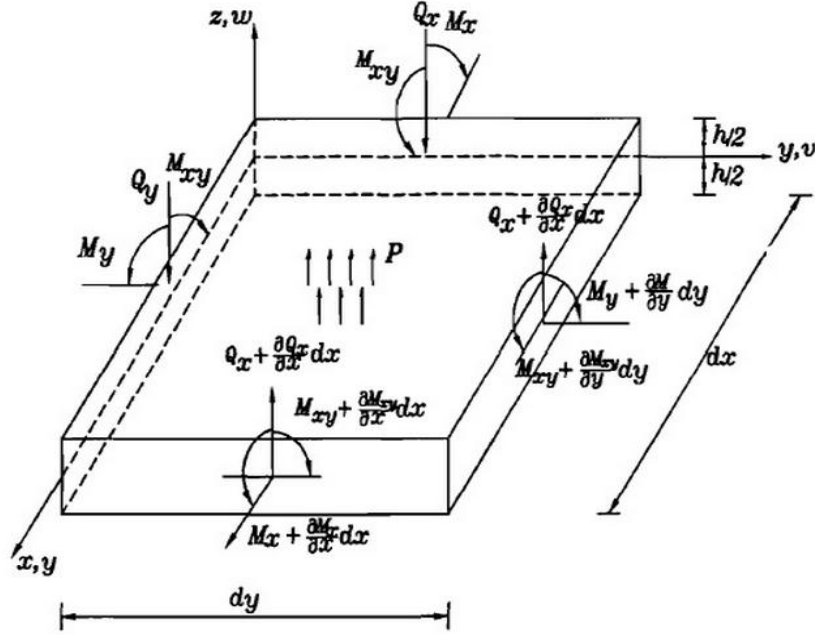


**Figure 3.3.** Free body diagram of the plate element

The shear forces are neglected from Eq. (3.9) and Eq. (3.11) gives

$$\frac{\partial^2 M_x}{\partial x^2} + 2 \frac{\partial^2 M_{xy}}{\partial x \partial y} + \frac{\partial^2 M_y}{\partial y^2} + p = 0 \quad (3.12)$$

When combining of Eq. (3.4), Eq. (3.8) and Eq. (3.12), the biharmonic governing equation for plate bending is produced in terms of the transverse displacement  $w$ .

$$\frac{\partial^4 w}{\partial x^4} + 2 \frac{\partial^4 w}{\partial x^2 \partial y^2} + \frac{\partial^4 w}{\partial y^4} = \frac{p}{D_r} \quad (3.13)$$

where  $D_r = \frac{Eh^3}{12(1-\nu^2)}$  is the rigidity of the plate.

### 3.2.2 Reissner-Mindlin Plate Theory

Reissner-Mindlin plate theory can be also called as the first shear deformation theory (FSDT). It is used for thick plates. In thick plates, Kirchhoff hypothesis cannot supply efficient solution in the analysis since Kirchhoff plate element cannot rotate independently of the position of the mid-surface. In Reissner-Mindlin plate theory, the shear deformations become significant and must be included in the analysis.

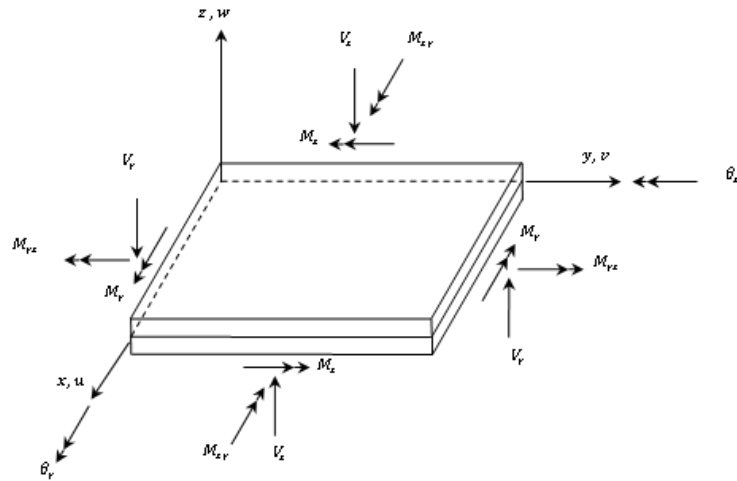


**Figure 3.4.** A typical Reissner-Mindlin plate

The Reissner–Mindlin plate theory, as shown in Fig. 3.3, is used for analysis of thick plates, where the shear deformations are considered, rotation and lateral deflections are decoupled. It does not need the cross-sections to be perpendicular to the axial forces after deformation. It basically depends on following assumptions [70]:

- Normal to the mid-plane before deformation remain straight but not necessarily normal to the mid-plane after deformation.
- Stresses normal to the mid-plane may be neglected.
- Deflections are small compared with the plate thickness.

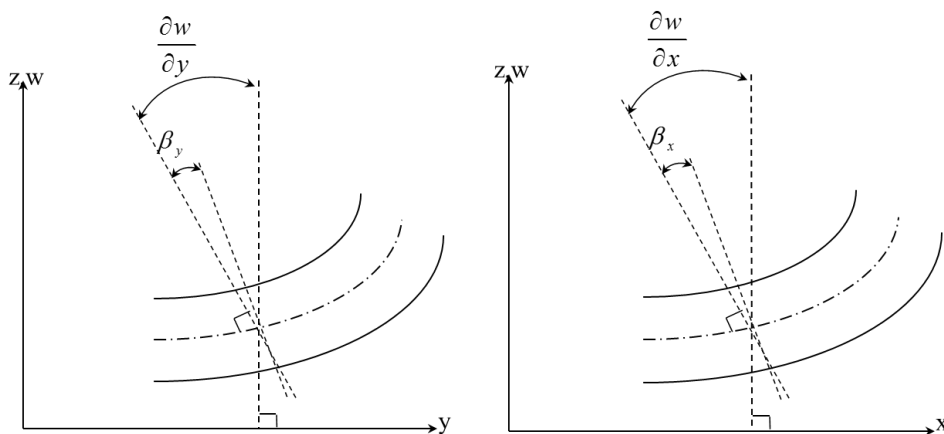


**Figure 3.5.** Deformation according to Reissner-Mindlin plate cross-section  
**a)  $y - z$  plane b)  $x - z$  plane**

The internal energy equation of the Reissner-Mindlin plate have to include transverse shear energy and bending energy.

$$U = \frac{1}{2} \int_{\Omega} \{\sigma_b\}^T \{\epsilon_b\} dV + \frac{K}{2} \int_{\Omega} \{\sigma_s\}^T \{\epsilon_s\} dV \quad (3.14)$$

where bending stresses and strains are

$$\{\sigma_b\} = \{\sigma_x \ \sigma_y \ \tau_{xy}\}^T \quad (3.15)$$

$$\{\epsilon_b\} = \{\epsilon_x \ \epsilon_y \ \gamma_{xy}\}^T \quad (3.16)$$

and transverse shear components are

$$\{\sigma_s\} = \{\tau_{xz} \ \tau_{yz}\}^T \quad (3.17)$$

$$\{\epsilon_s\} = \{\gamma_{xz} \ \gamma_{yz}\}^T \quad (3.18)$$

also  $K$ , is the shear energy correction factor, equals to 5/6. Substituting the constitutive equations, getting

$$U = \frac{1}{2} \int_{\Omega} \{\epsilon_b\}^T [D_b] \{\epsilon_b\} dV + \frac{K}{2} \int_{\Omega} \{\epsilon_s\}^T [D_s] \{\epsilon_s\} dV \quad (3.19)$$

in which

$$[D_b] = \frac{E}{1-\nu^2} \begin{bmatrix} 1 & \nu & 0 \\ \nu & 1 & 0 \\ 0 & 0 & \frac{1-\nu}{2} \end{bmatrix} \quad (3.20)$$

and

$$[D_s] = \begin{bmatrix} G & 0 \\ 0 & G \end{bmatrix} \quad (3.21)$$

The displacements of parallel to the undeformed neutral surface,  $u$  and  $v$ , can be expressed by

$$u = -z\theta_x(x, y) \quad (3.22)$$

$$v = -z\theta_y(x, y) \quad (3.23)$$

where  $\theta_x$  and  $\theta_y$  are the normal rotations of the cross section of the plate about the  $y$  – and  $x$  –axis and can be expressed as

$$\theta_x = \frac{\partial w}{\partial x} - \gamma_{xz} \quad (3.24)$$

$$\theta_y = \frac{\partial w}{\partial y} - \gamma_{yz} \quad (3.25)$$

The transverse displacement can be written as

$$w = w(x, y) \quad (3.24)$$

The strains are expressed as

$$\varepsilon = [\epsilon_x \ \epsilon_y \ \gamma_{xy} \ \gamma_{xz} \ \gamma_{yz}]^T \quad (3.25)$$

where the curvatures are given as

$$\epsilon_x = -\frac{\partial \theta_x}{\partial x} \quad (3.26)$$

and

$$\epsilon_y = -\frac{\partial \theta_y}{\partial y} \quad (3.27)$$

and the twisting curvature is

$$\gamma_{xy} = -\left(\frac{\partial \theta_y}{\partial x} + \frac{\partial \theta_x}{\partial y}\right) \quad (3.28)$$

The shear strains are expressed as

$$\gamma_{xz} = \left(\frac{\partial w}{\partial x} - \theta_x\right) \quad (3.29)$$

and

$$\gamma_{yz} = \left(\frac{\partial w}{\partial y} - \theta_y\right) \quad (3.30)$$

The constitutive relationships are given in the form

$$\underline{\sigma} = \underline{D} \underline{\varepsilon} \quad (3.31)$$

where

$$\underline{\sigma} = [M_x \ M_y \ M_{xy} \ Q_x \ Q_y]^T \quad (3.32)$$

in which  $M_x$  and  $M_y$  are the direct bending moments and  $M_{xy}$  is the twisting moment.

The quantities  $Q_x$  and  $Q_y$  are the shear forces in the  $x - z$  and  $y - z$  planes.

For an isotropic material  $\underline{D}$  is given as

$$\underline{D} = \begin{bmatrix} D & \nu D & 0 & 0 & 0 \\ \nu D & D & 0 & 0 & 0 \\ 0 & 0 & \frac{(1-\nu)D}{2} & 0 & 0 \\ 0 & 0 & 0 & S & 0 \\ 0 & 0 & 0 & 0 & S \end{bmatrix} \quad (3.33)$$

in which for a plate of thickness  $t$

$$D = \frac{Et^3}{12(1-\nu^2)} \quad (3.34)$$

and

$$S = \frac{Gt}{1.2} \quad (3.35)$$

where  $G$  is the shear modulus and the factor 1.2 is a correction term.

The form of the body force can be expressed as

$$\underline{b} = [q \ 0 \ 0]^T \quad (3.36)$$

where  $q$  is the distributed loading per unit area. The boundary tractions are not considered.

An elemental plate area is given as

$$d\Omega = dx dy \quad (3.37)$$

## **CHAPTER 4**

### **ELEMENT FREE GALERKIN METHOD**

#### **FOR MINDLIN-REISSNER PLATE BENDING PROBLEMS**

#### **4.1 Introduction**

Element free Galerkin method, developed by Belytschko et al. [4], is a popular meshfree method. The problem domain and its boundaries are described by arbitrary scattered nodes. The moving least square (MLS) approximation scheme is used for the interpolation field variables. The MLS shape functions do not possess the Kronecker delta function property which requires extra algorithms for the application of boundary conditions. Several algorithms have been developed for the implementation of boundary conditions.

In this chapter, implementation procedure of meshfree methods for the solution of solid mechanic problems is briefly described in section 2.2. The construction of MLS shape functions is reviewed in section 2.3. The solution of Mindlin-Reissner plate problems using EFGM is described in section 2.4.

#### **4.2 Short Description of Implementation Procedure for Galerkin Meshfree Methods**

The application of Galerkin meshfree methods can be divided into four steps. These steps are representation of the problem domain, interpolation of field variables, formulation of system equations, and solution of system equations for field variables. The representation of problem and its boundary are carried out using arbitrary scattered nodes which don't have any predefined relation. This is the main difference between the discretization of FEM and meshfree methods. Shape functions (interpolation functions) are constructed to interpolate field variables at any point within the problem domain. To construct shape functions, a local domain of a point of interest is formed by the selection of any number of neighbour nodes. The formation of local domain is different from the element structure of FEM. It is carried out without using any predefined relation, and the selection of nodes only depends on closeness of nodes to

point of interest. Meshfree methods formulate the system equations for local domains and then combine them to obtain global system equations. The formation of system equations for a local domain can be different for different meshfree methods. Some meshfree methods use strong form system equations and some use weak form system equations. The solution of system equations is similar to that for FEM. However, it must be considered that system equations of meshfree methods can be asymmetric.

#### **4.2.1 Basic Definitions for Meshfree Methods**

The local domain and the background cell are terms that are always encountered in the application of meshfree methods. Short explanations of these terms are given in the below.

##### **4.2.1.1 Local Domains (Support and Influence Domains)**

A local domain determines the nodes used for the approximation of field variables. It is similar to element structure of FEM and BEM. However, three important differences found between the elements of FEM and BEM, and the local domain phenomena. First of all, elements are used for interpolation and integration purposes, but local domains are only used for interpolation. Secondly, elements have to be predefined regular shapes but this is not a condition for the local domains. Lastly, the local domains don't have any predefined nodes as the elements.

The size of a local domain is determined by

$$r_s = \alpha_s \times r_c \quad (4.1)$$

where  $r_c$  is the average nodal spacing and  $\alpha_s$  is the dimensionless size of support domain.

##### **4.2.1.2 Background cells**

In Galerkin meshfree methods, the global problem domain is discretized into cells to carry out numerical integration. Generally, the background cell term is used instead of cell. The background cells can be rectangular or triangular for a two-dimensional domain. By looking at the appearance of background cells and elements, it may be considered that they are analogous. However, they are not same. The background cells are only used for integration purpose. The background cells and local domains are shown in Fig. 4.1.

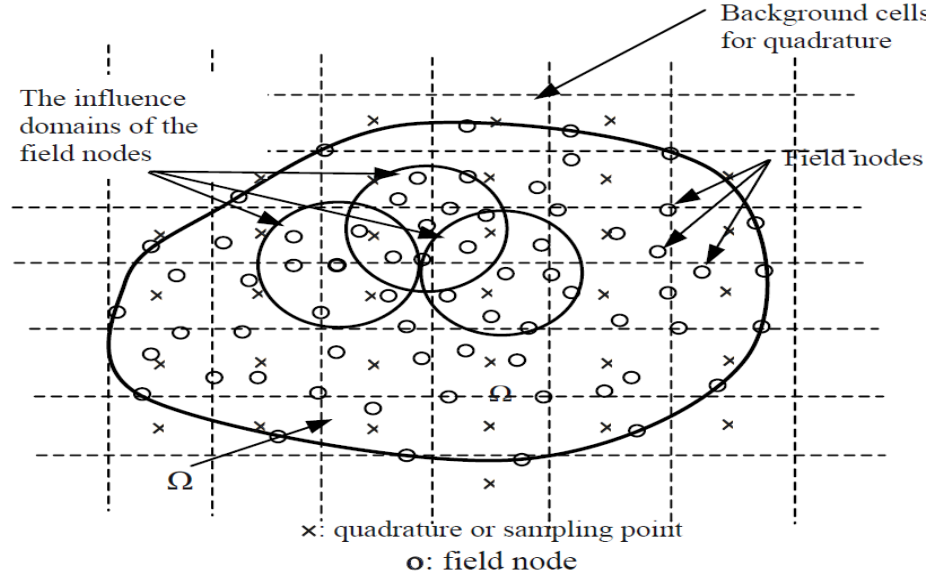


**Figure.4.1.**Support Domain; the centre is a quadrature point

### 4.3 Formulation of Moving Least-Squares (MLS) Shape Functions

The MLS approximation for the function of a field variable  $u(\mathbf{x})$  in a local domain  $\Omega$  is defined at a point  $\mathbf{x}$  as

$$u^h(\mathbf{x}) = \sum_{i=1}^m p_i(\mathbf{x})a_i(\mathbf{x}) = \mathbf{p}^T(\mathbf{x})\mathbf{a}(\mathbf{x}) \quad (4.2)$$

where  $m$  is the number of basis terms,  $\mathbf{p}^T(\mathbf{x}) = \{p_1(\mathbf{x}), p_2(\mathbf{x}), p_3(\mathbf{x}), \dots, p_m(\mathbf{x})\}$  is the vector of monomial basis functions,  $\mathbf{a}^T(\mathbf{x}) = \{a_1(\mathbf{x}), a_2(\mathbf{x}), a_3(\mathbf{x}), \dots, a_m(\mathbf{x})\}$  is the vector of coefficients to be determined, and  $\mathbf{x}^T = [x, y]$  is the position vector for 2D problems. The monomials providing minimum completeness are selected from the Pascal triangle to build the basis function  $\mathbf{p}^T(\mathbf{x})$ . For example, the linear and quadratic basis functions in 2D problems can be given by

$$\mathbf{p}^T(\mathbf{x}) = [1, x, y], \quad m = 3 \quad (4.3)$$

$$\mathbf{p}^T(\mathbf{x}) = [1, x, y, x^2, xy, y^2], \quad m = 6 \quad (4.4)$$

The difference between the function  $u(\mathbf{x})$  and its local approximation  $u^h(\mathbf{x})$  must be minimized by weighted discrete  $L_2$  norm to obtain the vector of coefficients  $\mathbf{a}(\mathbf{x})$ .

$$J = \sum_{i=1}^n w(\mathbf{x} - \mathbf{x}_i) [\mathbf{p}^T(\mathbf{x}_i)\mathbf{a}(\mathbf{x}) - u_i]^2 \quad (4.5)$$



where  $n$  is the number of nodes in the support domain of point  $\mathbf{x}$ ,  $u_i$  is the nodal value of  $u$  at  $\mathbf{x} = \mathbf{x}_i$ ,  $w(\mathbf{x} - \mathbf{x}_i)$  is the weight function associated with the influence domain of node  $i$ . The weight function must be greater than zero for all nodes in the support domain of point  $\mathbf{x}$ .

The minimization of weighted residual with respect to  $\mathbf{a}(\mathbf{x})$  at any arbitrary point  $\mathbf{x}$  gives

$$\frac{\partial J}{\partial \mathbf{a}} = 0 \quad (4.6)$$

which can be written as a set of linear equations.

$$\mathbf{A}(\mathbf{x})\mathbf{a}(\mathbf{x}) = \mathbf{B}(\mathbf{x})\mathbf{U}_s \quad (4.7)$$

where  $\mathbf{U}_s = \{u_1, u_2, u_3, \dots, u_n\}^T$  is the vector of nodal values of field function for the nodes of support domain. The matrices  $\mathbf{A}$  and  $\mathbf{B}$  have the following forms

$$\mathbf{A}(\mathbf{x}) = \sum_{i=1}^n w_i(\mathbf{x})p(x_i)p^T(x_i), \quad w_i(\mathbf{x}) = w(\mathbf{x} - \mathbf{x}_i) \quad (4.8)$$

$$\mathbf{B}(\mathbf{x}) = [w_1(\mathbf{x})p(x_1) \quad w_2(\mathbf{x})p(x_2) \quad \dots \quad w_n(\mathbf{x})p(x_n)] \quad (4.9)$$

The matrix  $\mathbf{A}$  is called as weighted moment matrix of MLS and if it is non-singular  $\mathbf{a}(\mathbf{x})$  can be written as

$$\mathbf{a}(\mathbf{x}) = \mathbf{A}^{-1}(\mathbf{x})\mathbf{B}(\mathbf{x})\mathbf{U}_s \quad (4.10)$$

The local approximation  $u^h(\mathbf{x})$  can be rewritten by substituting Eq. (3.10) into Eq. (2)

$$u^h(\mathbf{x}) = \sum_{i=1}^n \phi_i(\mathbf{x})u_i = \Phi^T(\mathbf{x})\mathbf{U}_s \quad (4.11)$$

where  $\Phi^T$  is the vector of MLS shape functions and it can be expressed as

$$\Phi^T(\mathbf{x}) = \{\phi_1(\mathbf{x}) \quad \phi_2(\mathbf{x}) \quad \dots \quad \phi_n(\mathbf{x})\} = \mathbf{p}^T(\mathbf{x})\mathbf{A}^{-1}(\mathbf{x})\mathbf{B}(\mathbf{x}) \quad (4.12)$$

The partial derivatives of shape function can be achieved by the following equation.

$$\Phi_{,i} = (\mathbf{p}^T\mathbf{A}^{-1}\mathbf{B})_{,i} = \mathbf{p}_{,i}^T\mathbf{A}^{-1}\mathbf{B} + \mathbf{p}^T\mathbf{A}_{,i}^{-1}\mathbf{B} + \mathbf{p}^T\mathbf{A}^{-1}\mathbf{B}_{,i} \quad (4.13)$$

where

$$\mathbf{A}_{,i}^{-1} = -\mathbf{A}^{-1}\mathbf{A}_{,i}\mathbf{A}^{-1} \quad (4.14)$$

The spatial derivative are designated with index  $i$  following a comma. The derivation procedure of MLS shape functions indicates that weight functions are one of key points of the MLS approximation. The continuity and locality features of the MLS approximation are mainly based on weight functions. The basic features of the MLS approximation such as continuity and locality, are mainly based on weight functions [10]. Weight functions characterize the basic features of the MLS approximation such as continuity and locality. The weight function must be positive inside the support domain by taking its maximum value at the centre of support domain and must be zero outside the support domain using a monotonically decrease. There are various weight functions in literature [10]. The cubic spline and quartic spline weight functions are used in this work and are given by

$$w_i(\mathbf{x} - x_i) = w(\bar{r}_i) = \begin{cases} 2/3 - 4\bar{r}_i^2 + 4\bar{r}_i^3 & \bar{r}_i \leq 0.5 \\ 4/3 - 4\bar{r}_i + 4\bar{r}_i^2 - 4/3\bar{r}_i^3 & 0.5 < \bar{r}_i \leq 1 \\ 0 & \bar{r}_i > 1 \end{cases} \quad (4.15)$$

$$w_i(\mathbf{x} - x_i) = w(\bar{r}_i) = \begin{cases} 1 - 6\bar{r}_i^2 + 8\bar{r}_i^3 - 3\bar{r}_i^4 & \bar{r}_i \leq 1 \\ 0 & \bar{r}_i > 1 \end{cases} \quad (4.16)$$

For rectangular influence domain in 2-D problems, weight functions can be obtained by

$$w(\bar{r}_i) = w(r_x)w(r_y) = w_x w_y \quad (4.17)$$

$$r_x = \frac{|x - x_i|}{r_{wx}} \text{ and } r_y = \frac{|y - y_i|}{r_{wy}} \quad (4.18)$$

where  $r_{wx}$  and  $r_{wy}$  are the size of support domain in the  $x$  and  $y$  direction.

#### 4.4 Governing equations and weak form

A typical Mindlin-Reissner plate with mid-plane lying in the  $x$ - $y$  plane of Cartesian coordinate system is depicted in Fig. 3.2. The displacement field of a point at a distance  $z$  to the mid-plane can be written as

$$u = z\theta_x \text{ and } v = z\theta_y \quad (4.19)$$

where  $u$  and  $v$  are the displacements of the plate in  $x$  and  $y$  directions, respectively.  $\theta_x$  and  $\theta_y$  are the rotations of cross-section of the plate about  $y$  and  $x$  axes,

respectively. The lateral deflection of mid-plane is indicated by  $w$ . The vector of displacements can be denoted as

$$\begin{Bmatrix} u \\ v \\ w \end{Bmatrix} = \begin{bmatrix} 0 & z & 0 \\ 0 & 0 & z \\ 1 & 0 & 0 \end{bmatrix} \begin{Bmatrix} w \\ \theta_x \\ \theta_y \end{Bmatrix} = \mathbf{L}_d \mathbf{u} \quad (4.20)$$

where  $\mathbf{u} = \{w \ \theta_x \ \theta_y\}^T$  is the vector of independent field variables. The linear strains in the Mindlin-Reissner plate are as follows

$$\begin{Bmatrix} \varepsilon_{xx} \\ \varepsilon_{yy} \\ \varepsilon_{xy} \\ \gamma_{xz} \\ \gamma_{yz} \end{Bmatrix} = \begin{Bmatrix} z \frac{\partial \theta_x}{\partial x} \\ z \frac{\partial \theta_y}{\partial y} \\ z \frac{\partial \theta_x}{\partial y} + z \frac{\partial \theta_y}{\partial x} \\ \theta_x + \frac{\partial w}{\partial x} \\ \theta_y + \frac{\partial w}{\partial y} \end{Bmatrix} = \mathbf{L}_d \mathbf{u} \quad (4.21)$$

where

$$\mathbf{L}_d = \begin{bmatrix} 0 & 0 & 0 & \frac{\partial}{\partial x} & \frac{\partial}{\partial y} \\ z \frac{\partial}{\partial x} & 0 & z \frac{\partial}{\partial y} & 1 & 0 \\ 0 & z \frac{\partial}{\partial y} & z \frac{\partial}{\partial x} & 0 & 1 \end{bmatrix}^T \quad (4.22)$$

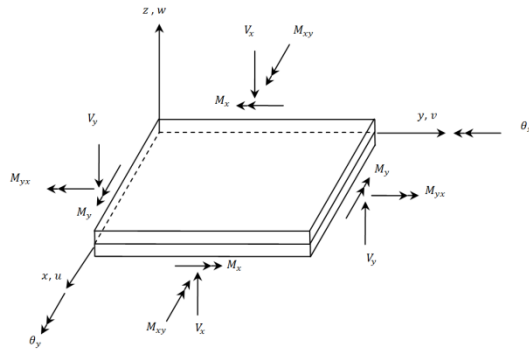


**Figure 4.2.** A typical Mindlin-Reissner plate

The stresses using the Generalized Hooke's law for isotropic linear elastic materials is obtained with  $\sigma = D\varepsilon$ .

$$\begin{Bmatrix} \sigma_{xx} \\ \sigma_{yy} \\ \sigma_{xy} \\ \sigma_{xz} \\ \sigma_{yz} \end{Bmatrix} = \begin{bmatrix} \frac{E}{1-\nu^2} & \frac{E\nu}{1-\nu^2} & 0 & 0 & 0 \\ \frac{E\nu}{1-\nu^2} & \frac{E}{1-\nu^2} & 0 & 0 & 0 \\ 0 & 0 & G & 0 & 0 \\ 0 & 0 & 0 & k_{sh}G & 0 \\ 0 & 0 & 0 & 0 & k_{sh}G \end{bmatrix} \begin{Bmatrix} \varepsilon_{xx} \\ \varepsilon_{yy} \\ \varepsilon_{xy} \\ \gamma_{xz} \\ \gamma_{yz} \end{Bmatrix} \quad (4.23)$$

where  $E$  is Young's modulus,  $\nu$  is Poisson's ratio,  $G = E/(2(1 + \nu))$  is shear modulus,  $k_{sh}$  is shear correction factor often  $5/6$  is used for Mindlin-Reissner plates.

The stress resultants, moments and shears per unit of length, can be obtained using the stresses as

$$\mathbf{M} = \int_{-h/2}^{h/2} z \begin{bmatrix} \sigma_{xx} \\ \sigma_{yy} \\ \sigma_{xy} \end{bmatrix} dz \quad (4.24)$$

$$\mathbf{V} = \int_{-h/2}^{h/2} \begin{bmatrix} \sigma_{xz} \\ \sigma_{yz} \end{bmatrix} dz \quad (4.25)$$

where  $h$  is the thickness of the plate.

The Galerkin weak form for Mindlin-Reissner plates can be written as

$$\int_{\Omega} \delta(\mathbf{L}_d u)^T \mathbf{D} \mathbf{L}_d u d\Omega - \int_{\Omega} \delta(\mathbf{L}_u u)^T b d\Omega - \int_{\Gamma_t} \delta(\mathbf{L}_u u)^T t_{\Gamma} dS = 0 \quad (4.26)$$

where  $\Gamma_t$  is the edge surface of the plate where natural boundary condition is specified,  $b$  is the body force vector and  $t_{\Gamma}$  is traction on the edge of the plate. By considering only transverse load, the body force vector can be defined as  $b = \{0 \quad 0 \quad b_z\}^T$ . The external traction on the edge of the plate  $t_{\Gamma}$  can be expressed in terms of stresses on the surface of the edge:

$$t_{\Gamma} = \begin{bmatrix} n_x & 0 & 0 & n_y & 0 \\ 0 & n_y & n_x & 0 & 0 \\ 0 & 0 & 0 & n_x & n_y \end{bmatrix} \begin{Bmatrix} \sigma_{xx} \\ \sigma_{yy} \\ \sigma_{xy} \\ \sigma_{xz} \\ \sigma_{yz} \end{Bmatrix} = \begin{Bmatrix} \sigma_{xx}n_x + \sigma_{xz}n_y \\ \sigma_{xy}n_x + \sigma_{yy}n_y \\ \sigma_{xz}n_x + \sigma_{yz}n_y \end{Bmatrix} \quad (4.27)$$

The penalty method is used to implement the essential boundary conditions and is applied to the EFGM by the addition of following term to Galerkin weak form.

$$\delta \int_{\Gamma_u} \frac{1}{2} (u_b - u_\Gamma)^T \alpha (u_b - u_\Gamma) d\Gamma \quad (4.28)$$

where  $u_b$  is the prescribed essential boundary conditions,  $u_\Gamma$  is the approximation function of the prescribed essential boundary conditions,  $\Gamma_u$  is the domain of nodes in the essential boundary,  $\alpha$  is a diagonal matrix of penalty factors with dimensions equal to the number of DOF per node. The penalty factors are constant values for the whole problem domain.

Inserting Eq. (4.28) into Eq. (4.26) leads to the following the Galerkin weak form

$$\begin{aligned} \int_{\Omega} \delta (\mathbf{L}_d u)^T D L_d u d\Omega - \int_{\Omega} \delta (\mathbf{L}_u u)^T b d\Omega - \int_{\Gamma_t} \delta (\mathbf{L}_u u)^T t_\Gamma dS \\ + \delta \int_{\Gamma_u} \frac{1}{2} (u_b - u_\Gamma)^T \alpha (u_b - u_\Gamma) d\Gamma = 0 \end{aligned} \quad (4.29)$$

The discrete system equation can be written as

$$(\mathbf{K} + \mathbf{K}^\alpha) \mathbf{U} = (\mathbf{F} + \mathbf{F}^\alpha) \quad (4.30)$$

where  $\mathbf{K}$  is the global stiffness matrix and is obtained by assembling the point stiffness matrices

$$K_{ij} = \int_{\Omega} \mathbf{B}_i^T \mathbf{D} \mathbf{B}_j d\Omega \quad (4.31)$$

in which

$$\mathbf{B}_i = \begin{bmatrix} 0 & 0 & 0 & \frac{\partial \phi_i}{\partial x} & \frac{\partial \phi_i}{\partial y} \\ \frac{\partial \phi_i}{\partial x} & 0 & \frac{\partial \phi_i}{\partial y} & \phi_i & 0 \\ 0 & \frac{\partial \phi_i}{\partial y} & \frac{\partial \phi_i}{\partial x} & 0 & \phi_i \end{bmatrix}^T \quad (4.32)$$

and

$$\mathbf{D} = \begin{bmatrix} \frac{Et^3}{12(1-\nu^2)} & \nu \frac{Et^3}{12(1-\nu^2)} & 0 & 0 & 0 \\ \nu \frac{Et^3}{12(1-\nu^2)} & \frac{Et^3}{12(1-\nu^2)} & 0 & 0 & 0 \\ 0 & 0 & \frac{1-\nu}{2} & 0 & 0 \\ 0 & 0 & 0 & k_{sh}G & 0 \\ 0 & 0 & 0 & 0 & k_{sh}G \end{bmatrix} \quad (4.33)$$

The  $\mathbf{K}^\alpha$  is the matrix of penalty factors defined by

$$(\mathbf{K}^\alpha)_{ij} = \int_{\Gamma_u} \varphi_i^T \boldsymbol{\alpha} \varphi_j d\Gamma \quad (4.34)$$

where  $\varphi_i$  is a diagonal matrix. If the relevant DOF is free, the diagonal elements of  $\varphi_i$  are equal to 0, otherwise equal to 1.

The force vector  $\mathbf{F}$  in Eq. (4.30) is the global force vector assembled using the nodal force vector of

$$F_i = \int_{\Omega} (\mathbf{L}_u \Phi_i)^T b d\Omega + \int_{\Omega} (\mathbf{L}_u \Phi_i)^T t_\Gamma dS \quad (4.35)$$

where  $\Phi_i$  is a diagonal matrix of shape functions.

The  $\mathbf{F}^\alpha$  vector shows the forces obtained by the implementation of essential boundary conditions and can be obtained as follows

$$F_i^\alpha = \int_{\Gamma_u} \varphi_i^T \boldsymbol{\alpha} u_\Gamma d\Gamma \quad (4.36)$$

## CHAPTER 5

### NUMERICAL EXPERIMENTS AND DISCUSSIONS

#### 5.1 Introduction

In order to investigate the effects of selectable parameters of the EFG method on the solution accuracy of the Reissner-Mindlin plate bending problems, three numerical examples have been performed. The numerical examples are simply supported square plate under transverse centric point load, simply supported square plate under uniform transverse load, clamped circular plate under uniform transverse load. Analytical solutions and solutions of EFG method are compared to determine the effects of different values of parameters on the accuracy of EFG method.

The results of the numerical examples are given in the table form, however, some of the results found in these tables are beyond being wrong. Also, these results are invalid results. Several figures are given after the tables to increase readability of the effects of selectable parameters. The invalid/unacceptable results are not introduced into figures because they obstruct to follow the variations of displacements/moments against the values of selectable parameters on the figures. The value of penalty coefficient is presented in the form of  $10^{\alpha p}$ . The number of gauss points in a background cell, central deflections and moments of plates are symbolized with  $n_g$ ,  $w_c$ , and  $M_c$  respectively.

#### 5.2 Simply supported square plate under transverse centric point load

The simply supported square plate is loaded with transverse centric point load as shown in Fig.5.1. The material properties are as follows; Young's modulus  $E$  of material is 10920 Pa and Poisson's ratio is  $\nu = 0.3$ . The thickness and length of the plate are given by  $h = 0.01$  m and  $L = 1$  m, respectively. The value of applied transverse load  $P$  is 16.3527 N. Due to symmetry, only one quarter of the plate can be used in EFGM solutions. The EFGM models used in the solutions are shown in Fig. 5.2. In the model of quarter square plate, 1089 field nodes and 1024 background cells

are used for regular and irregular node distributions. The normalized deflection values at the centre of square plate are used as the critical value for the evaluation of accuracy.

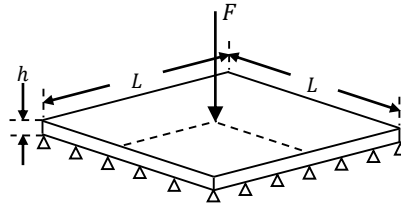


**Figure 5.1.** Simply supported square plate under transverse centric point load

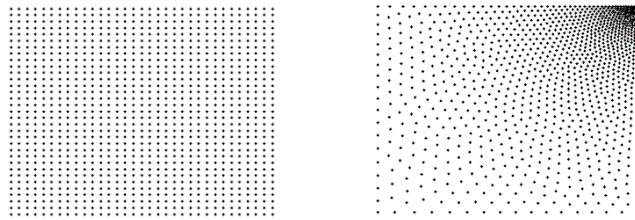


**Figure 5.2.** The EFGM models for **a)** regular node distributions, **b)** irregular node distributions

The results obtained using the selectable parameters with different values are presented in Table 5.1 to Table 5.8. Since, the simply supported square plate under transverse centric point load has stress singularity problem at the centre of plate, only displacement results are used for accuracy performance investigations. The variations of displacement against the number of gauss points in a background cell are given in Table 5.1, Table 5.2, Table 5.5 and Table 5.6. The effect of value of penalty coefficient on the displacement is given in Table 5.3, Table 5.4, Table 5.7 and Table 5.8. Table 5.1 to Table 5.4 is achieved by the utilization of cubic spline weight function and Table 5.5 to Table 5.8 is provided using quartic spline weight function.

According to Fig. 5.3, there are some fluctuations found in results for the value of  $\alpha_s = 3.5$ ,  $\alpha_s = 4$  and  $\alpha_s = 4$ . However, it is not shown for value of  $\alpha_s = 2.5$  and  $\alpha_s = 3.0$ . In Fig. 5.4, several variations are observed in the accuracy of displacement results for the different values of  $\alpha_s$  at number of gauss points in a background equals to 4 except  $\alpha_s = 2.5$  and  $\alpha_s = 3.0$ . However, if the number of gauss points is selected between 5 and 8, no variation is observed for different values of  $\alpha_s$  at the same figure. From Fig. 5.5 and Fig. 5.6, the value of penalty coefficient between  $1 \times 10^6$  and  $1 \times 10^{10}$  does not cause any variation in results. But, the value of penalty coefficient



greater than 10 shows a deviation in results. The solutions obtained using cubic spline weight function are given in Fig. 5.3, Fig. 5.4, Fig. 5.5 and Fig. 5.6. The same configurations of these figures are given for the quartic spline weight function in Fig. 5.7 to Fig. 5.10. The results obtained using quartic spline weight function show less variation comparing to the results obtained using cubic spline weight functions. The increase in number of monomials cause accuracy loss in results.

**Table 5.1.** Normalized central deflections  $w_c / \left( \frac{pL^4}{100D} \right)$  of simply supported square plate under transverse centric point load for regular node distribution using cubic spline weight function with  $\alpha_p = 6$ .

Number of monomials	Number of gauss points	Dimensionless size of support domain ( $\alpha_s$ )					Exact
		2.5	3.0	3.5	4.0	4.5	
<b>3</b>	4×4	0.011608	0.011631	0.011648	0.011609	0.011711	0.011600
	5×5	0.011608	0.011630	0.011666	0.011651	0.011576	
	6×6	0.011608	0.011630	0.011641	0.011639	0.011652	
	7×7	0.011608	0.011630	0.011628	0.011613	0.011639	
	8×8	0.011609	0.011630	0.011651	0.011656	0.011664	
<b>6</b>	4×4	0.011626	0.011628	0.011647	0.011700	0.011678	
	5×5	0.011625	0.011628	0.011647	0.011677	0.011654	
	6×6	0.011625	0.011628	0.011646	0.011673	0.011682	
	7×7	0.011625	0.011628	0.011647	0.011658	0.011691	
	8×8	0.011625	0.011629	0.011647	0.011737	0.011638	
<b>10</b>	4×4	0.000104	0.011630	0.011648	0.011703	0.011712	
	5×5	0.000123	0.011631	0.011647	0.011696	0.011708	
	6×6	0.000320	0.011630	0.011647	0.011722	0.011706	
	7×7	0.000088	0.011630	0.011647	0.011704	0.011707	
	8×8	0.000003	0.011631	0.011648	0.011707	0.011707	

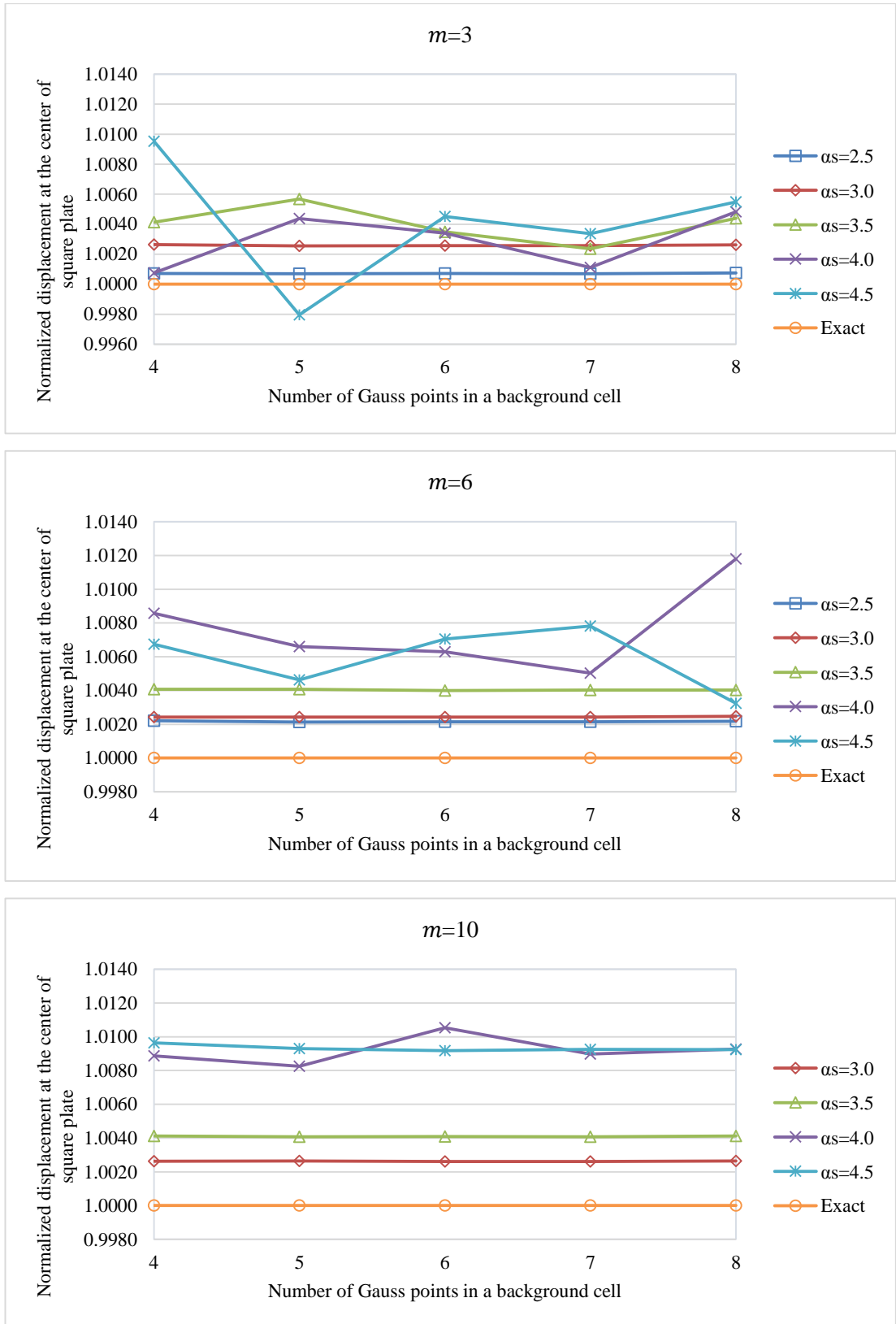


**Figure 5.3.** Variations of normalized central deflections  $w_c/\left(\frac{\rho L^4}{100D}\right)$  against  $n_g$  for simply supported square plate under transverse centric point load using cubic spline weight functions and regular node distribution with  $\alpha_p = 6$ .

**Table 5.2.** Normalized central deflections  $w_c / \left( \frac{pL^4}{100D} \right)$  of simply supported square plate under transverse centric point load for irregular node distribution using cubic spline weight function with  $\alpha_p = 6$ .

Number of monomials	Number of gauss points	Dimensionless size of support domain ( $\alpha_s$ )					Exact
		2.5	3.0	3.5	4.0	4.5	
<b>3</b>	4×4	0.011659	0.011708	0.012028	0.012305	0.012560	0.011600
	5×5	0.011634	0.011656	0.011734	0.011866	0.011797	
	6×6	0.011631	0.011646	0.011665	0.011717	0.011708	
	7×7	0.011629	0.011638	0.011644	0.011671	0.011678	
	8×8	0.011630	0.011633	0.011640	0.011648	0.011648	
<b>6</b>	4×4	0.011686	0.011685	0.011709	0.011809	0.011973	
	5×5	0.011636	0.011636	0.011643	0.011658	0.011687	
	6×6	0.011635	0.011636	0.011639	0.011645	0.011657	
	7×7	0.011635	0.011635	0.011637	0.011640	0.011646	
	8×8	0.011635	0.011636	0.011637	0.011639	0.011642	
<b>10</b>	4×4	0.000721	0.011756	0.011768	0.011835	0.011951	
	5×5	0.000045	0.011641	0.011642	0.011656	0.011673	
	6×6	0.000108	0.011640	0.011639	0.011647	0.011654	
	7×7	0.000438	0.011637	0.011638	0.011640	0.011645	
	8×8	0.002536	0.011637	0.011638	0.011639	0.011643	

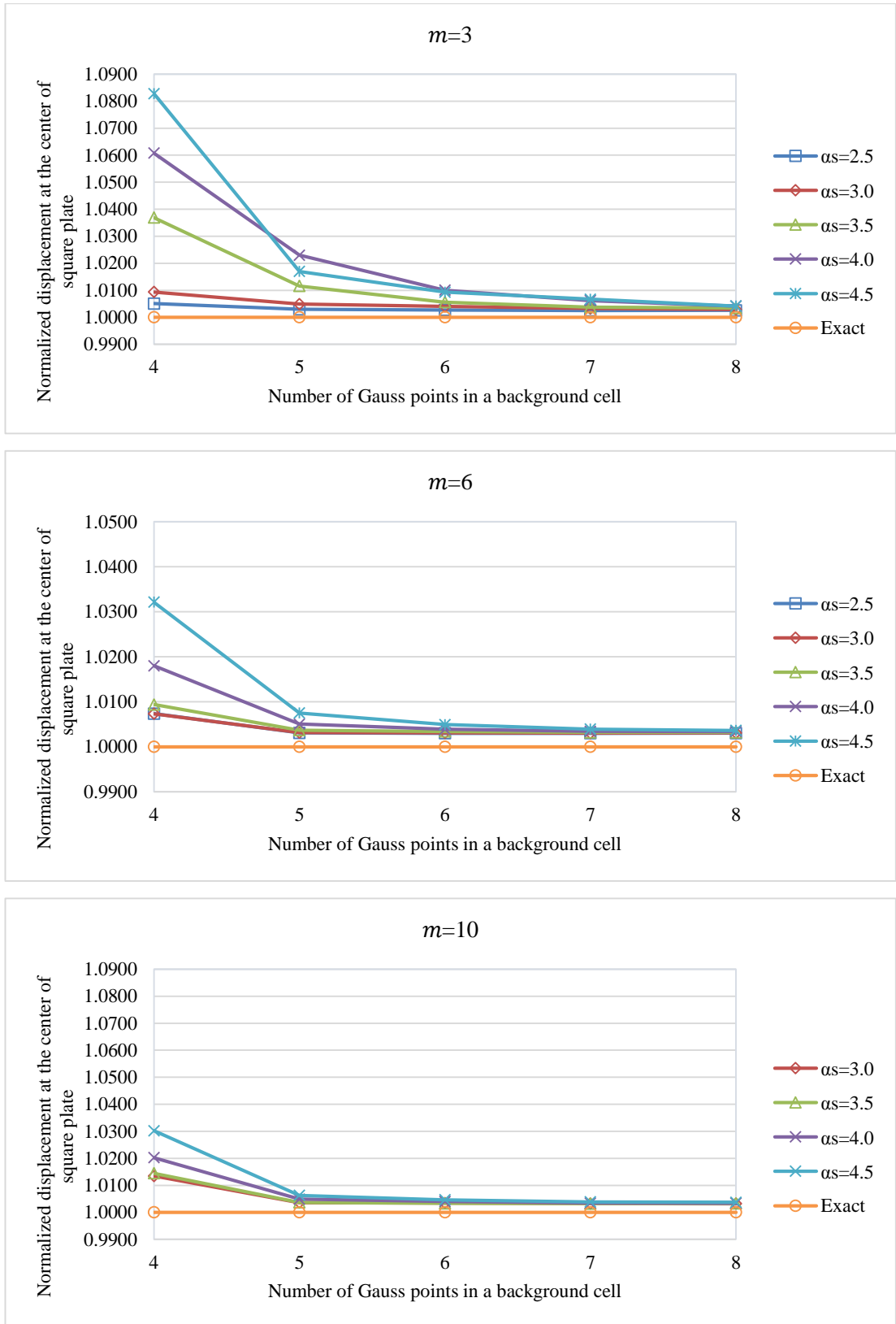


**Figure 5.4.** Variations of normalized central deflections  $w_c/\left(\frac{\rho L^4}{100D}\right)$  against  $n_g$  for simply supported square plate under transverse centric point load using cubic spline weight functions and irregular node distribution with  $\alpha_p = 6$ .

**Table 5.3.** Variations of normalized central deflections  $w_c / \left( \frac{pL^4}{100D} \right)$  of simply supported square plate under transverse centric point load using regular node distribution using cubic spline weight function with  $n_g = 5$ .

Number of monomials	Value of penalty coefficient	Dimensionless size of support domain ( $\alpha_s$ )					Exact
		2.5	3.0	3.5	4.0	4.5	
<b>3</b>	6	0.011608	0.011630	0.011666	0.011651	0.011576	0.011600
	7	0.011608	0.011630	0.011621	0.011639	0.011634	
	8	0.011608	0.011630	0.011618	0.011628	0.011654	
	9	0.011608	0.011629	0.011651	0.011657	0.011630	
	10	0.011609	0.011620	0.011669	0.011520	0.011249	
	11	0.011596	0.011757	-0.005365	0.011210	0.010949	
<b>6</b>	6	0.011625	0.011628	0.011647	0.011677	0.011654	
	7	0.011625	0.011628	0.011650	0.011616	0.011698	
	8	0.011624	0.011628	0.011630	0.011609	0.011675	
	9	0.011623	0.011627	0.012068	0.011639	0.011512	
	10	0.011602	0.011615	0.011900	0.010187	0.011287	
	11	0.011751	0.011082	0.011605	0.046484	0.011575	
<b>10</b>	6	-0.000209	0.011631	0.011647	0.011696	0.011708	
	7	-0.001322	0.011631	0.011648	0.011697	0.011708	
	8	0.000390	0.011631	0.011644	0.011784	0.011686	
	9	0.000190	0.011632	0.011723	0.011661	0.011708	
	10	0.000140	0.011648	0.012131	0.011501	0.011365	
	11	-0.000332	0.011686	0.009992	0.012668	0.013610	

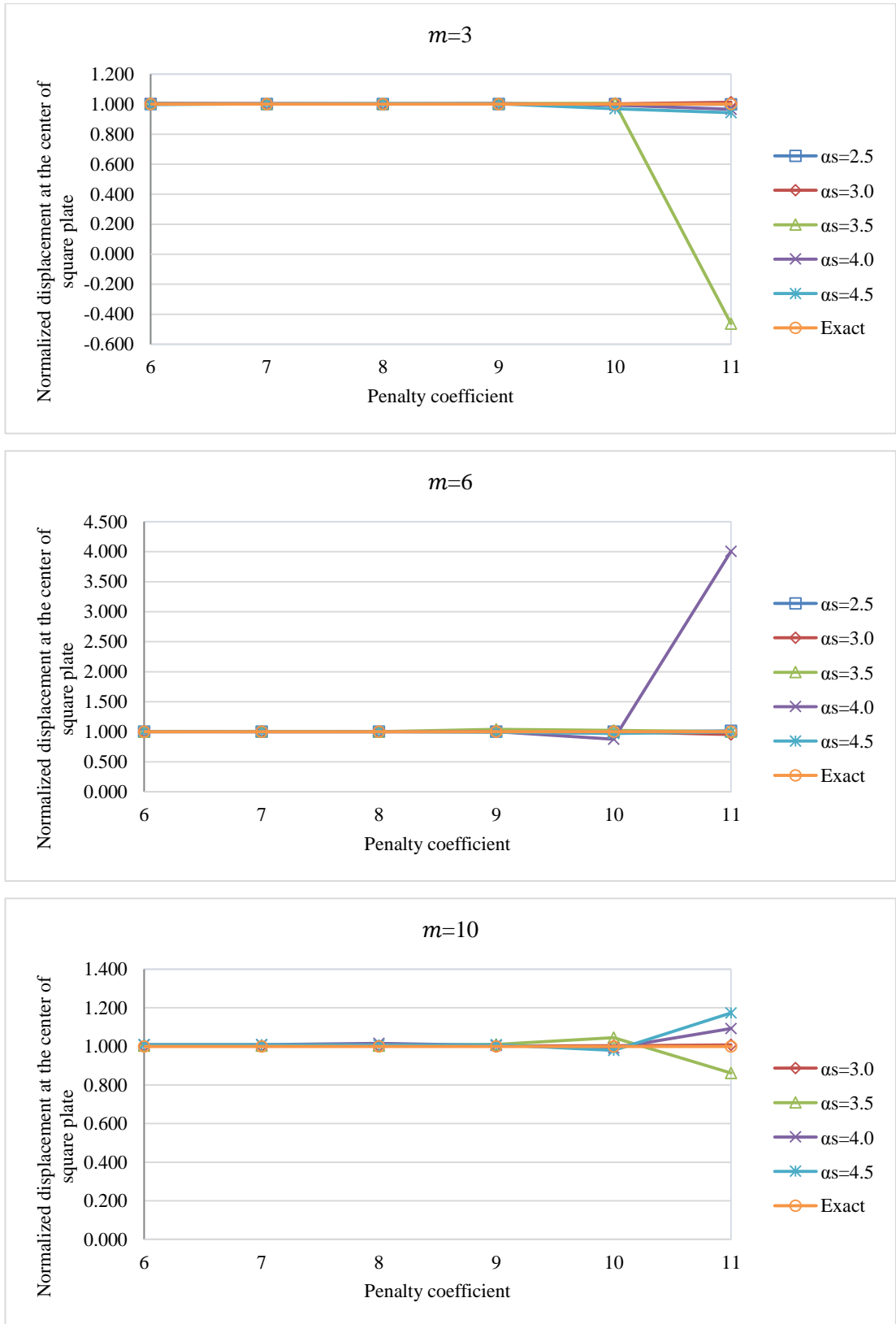


**Figure 5.5.** Variations of normalized central deflections  $w_c/\left(\frac{pL^4}{100D}\right)$  against  $\alpha_p$  for simply supported square plate under transverse centric point load using cubic spline weight functions and regular node distribution with  $n_g = 5$ .

**Table 5.4.** Variations of normalized central deflections  $w_c / \left( \frac{pL^4}{100D} \right)$  of simply supported square plate under transverse centric point load using irregular node distribution using cubic spline weight function with  $n_g = 5$ .

Number of monomials	Value of penalty coefficient	Dimensionless size of support domain ( $\alpha_s$ )					Exact
		2.5	3.0	3.5	4.0	4.5	
<b>3</b>	6	0.011634	0.011656	0.011734	0.011866	0.011797	0.011600
	7	0.011634	0.011656	0.011735	0.011867	0.011791	
	8	0.011634	0.011656	0.011732	0.011838	0.011796	
	9	0.011635	0.011657	0.011721	0.011819	0.011582	
	10	0.011629	0.011673	0.011850	0.011781	0.011813	
	11	0.011555	0.028047	0.011431	0.009145	0.011257	
<b>6</b>	6	0.011636	0.011636	0.011643	0.011658	0.011687	
	7	0.011636	0.011636	0.011643	0.011659	0.011686	
	8	0.011636	0.011636	0.011643	0.011657	0.011661	
	9	0.011633	0.011635	0.011643	0.011621	0.011661	
	10	0.011665	0.011639	0.011782	0.012890	0.011496	
	11	0.011791	0.011721	0.009100	-0.005537	-0.002784	
<b>10</b>	6	0.002575	0.011641	0.011642	0.011656	0.011673	
	7	-0.000099	0.011641	0.011642	0.011656	0.011672	
	8	-0.000081	0.011641	0.011642	0.011655	0.011673	
	9	0.000094	0.011651	0.011643	0.011661	0.011693	
	10	0.000706	0.011696	0.011624	0.010894	0.011369	
	11	0.000165	0.012081	0.006998	0.009700	0.005584	



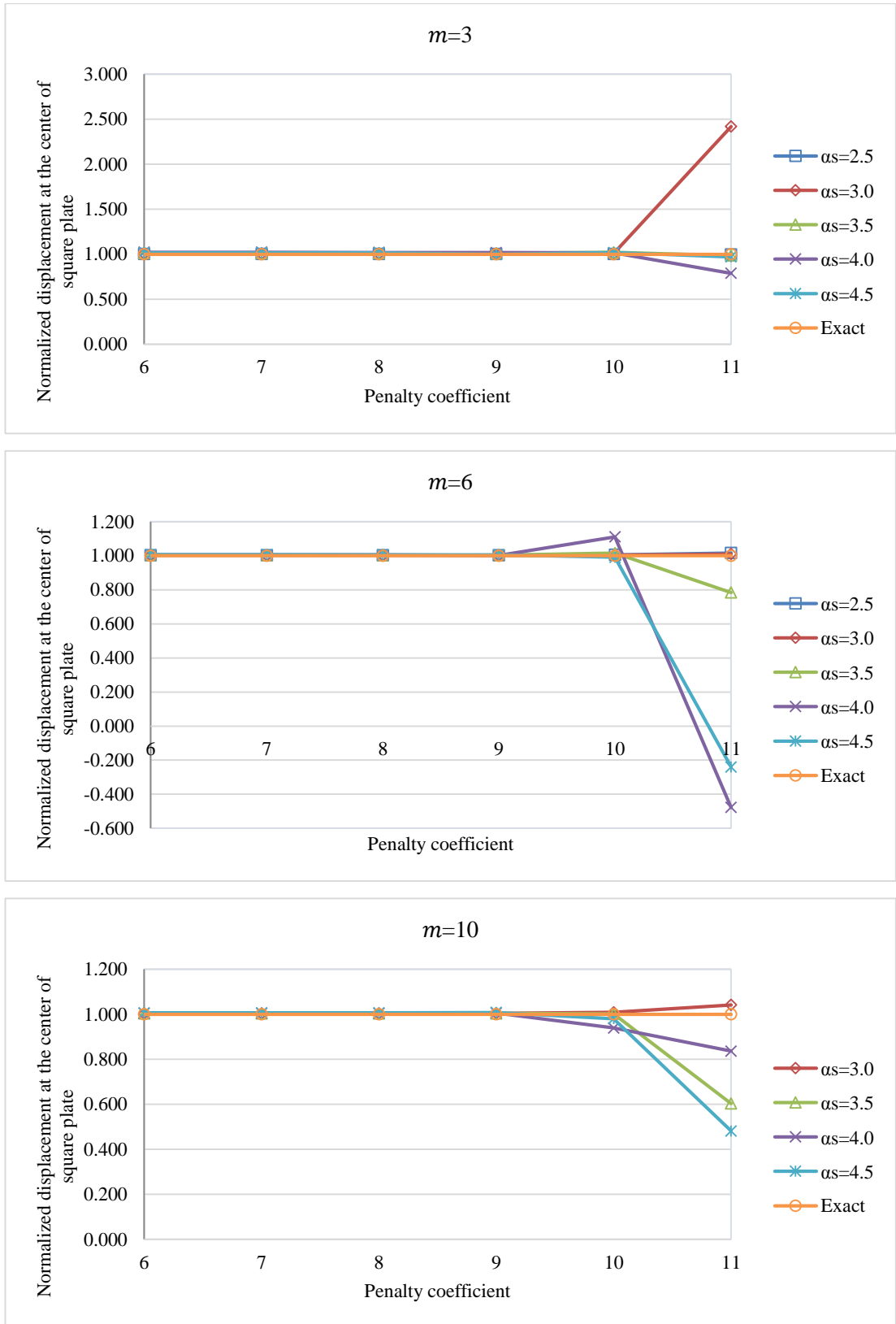


**Figure 5.6.** Variations of normalized central deflections  $w_c / \left( \frac{\rho L^4}{100D} \right)$  against  $\alpha_p$  for simply supported square plate under transverse centric point load using cubic spline weight functions and irregular node distribution with  $n_g = 5$ .

**Table 5.5.** Variations of normalized central deflections  $w_c / \left( \frac{pL^4}{100D} \right)$  of simply supported square plate under transverse centric point load using regular node distribution using quartic spline weight function with  $\alpha_p = 6$ .

Number of monomials	Number of gauss points	Dimensionless size of support domain ( $\alpha_s$ )					Exact
		2.5	3.0	3.5	4.0	4.5	
<b>3</b>	4×4	0.011613	0.011624	0.011631	0.011632	0.011639	0.011600
	5×5	0.011600	0.011624	0.011628	0.011632	0.011637	
	6×6	0.011604	0.011624	0.011629	0.011632	0.011640	
	7×7	0.011603	0.011624	0.011628	0.011632	0.011639	
	8×8	0.011603	0.011624	0.011629	0.011633	0.011639	
<b>6</b>	4×4	0.011626	0.011629	0.011662	0.011639	0.011658	
	5×5	0.011625	0.011630	0.011662	0.011639	0.011657	
	6×6	0.011625	0.011630	0.011660	0.011639	0.011657	
	7×7	0.011625	0.011630	0.011661	0.011639	0.011657	
	8×8	0.011625	0.011630	0.011661	0.011639	0.011658	
<b>10</b>	4×4	-	0.011631	0.011665	0.011671	0.011685	
	5×5	0.000062	0.011631	0.011666	0.011670	0.011682	
	6×6	0.000132	0.011631	0.011665	0.011670	0.011681	
	7×7	0.000097	0.011630	0.011665	0.011670	0.011681	
	8×8	0.000262	0.011631	0.011666	0.011670	0.011682	

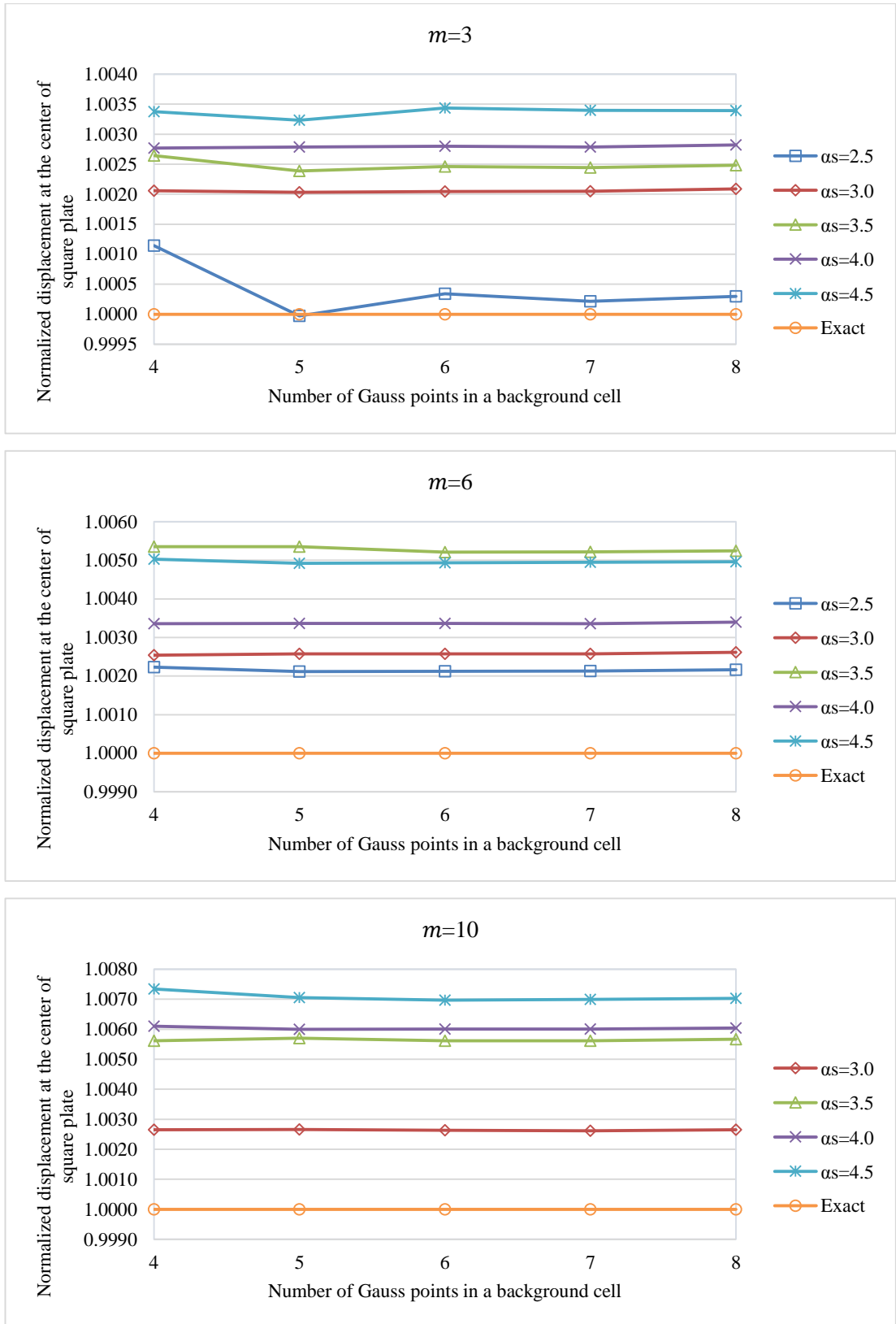


**Figure 5.7.** Variations of normalized central deflections  $w_c/\left(\frac{\rho L^4}{100D}\right)$  against  $n_g$  for simply supported square plate under transverse centric point load using quartic spline weight functions and regular node distribution with  $\alpha_p = 6$ .

**Table 5.6.** Variations of normalized central deflections  $w_c / \left( \frac{pL^4}{100D} \right)$  of simply supported square plate under transverse centric point load using irregular node distribution using quartic spline weight function with  $\alpha_p = 6$ .

Number of monomials	Number of gauss points	Dimensionless size of support domain ( $\alpha_s$ )					Exact
		2.5	3.0	3.5	4.0	4.5	
<b>3</b>	4×4	0.011692	0.011759	0.011773	0.011866	0.012094	0.011600
	5×5	0.011632	0.011652	0.011662	0.011682	0.011742	
	6×6	0.011628	0.011637	0.011641	0.011646	0.011663	
	7×7	0.011625	0.011633	0.011637	0.011638	0.011641	
	8×8	0.011625	0.011632	0.011636	0.011637	0.011639	
<b>6</b>	4×4	0.011691	0.011713	0.011812	0.011820	0.011885	
	5×5	0.011639	0.011640	0.011652	0.011660	0.011675	
	6×6	0.011636	0.011638	0.011641	0.011645	0.011653	
	7×7	0.011635	0.011636	0.011638	0.011639	0.011642	
	8×8	0.011635	0.011636	0.011637	0.011639	0.011639	
<b>10</b>	4×4	0.011963	0.011822	0.011963	0.012021	0.011947	
	5×5	0.000049	0.011654	0.011657	0.011664	0.011669	
	6×6	-	0.011647	0.011644	0.011650	0.011648	
	7×7	0.011727	0.011639	0.011641	0.011642	0.011643	
	8×8	0.007144	0.011638	0.011639	0.011640	0.011642	

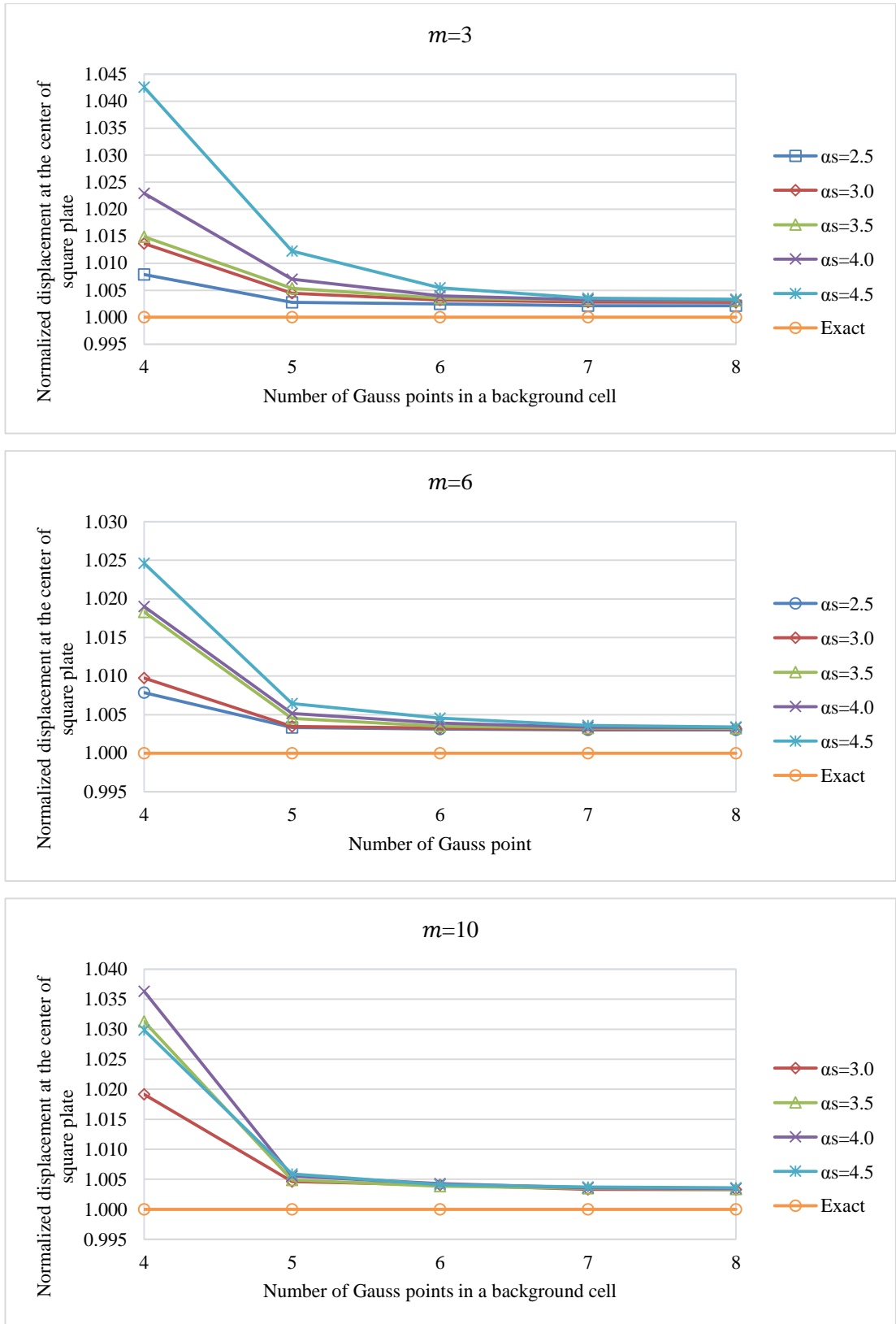


**Figure 5.8.** Variations of normalized central deflections  $w_c / \left( \frac{\rho L^4}{100D} \right)$  against  $n_g$  for simply supported square plate under transverse centric point load using quartic spline weight functions and irregular node distribution with  $\alpha_p = 6$ .

**Table 5.7.** Variations of normalized central deflections  $w_c / \left( \frac{pL^4}{100D} \right)$  of simply supported square plate under transverse centric point load using regular node distribution using quartic spline weight function with  $n_g = 5$ .

Number of monomials	Value of penalty coefficient	Dimensionless size of support domain ( $\alpha_s$ )					Exact
		2.5	3.0	3.5	4.0	4.5	
<b>3</b>	6	0.011508	0.011529	0.011532	0.011536	0.011539	0.011600
	7	0.011508	0.011529	0.011532	0.011536	0.011533	
	8	0.011508	0.011529	0.011521	0.011534	0.011533	
	9	0.011508	0.011529	0.011533	0.011537	0.011540	
	10	0.011506	0.011496	0.011566	0.011501	0.011682	
	11	0.010910	0.011573	0.011898	0.012166	0.011505	
<b>6</b>	6	0.011533	0.011534	0.011551	0.011539	0.011549	
	7	0.011533	0.011534	0.011551	0.011539	0.011550	
	8	0.011533	0.011534	0.011549	0.011535	0.011536	
	9	0.011534	0.011535	0.011249	0.011531	0.011553	
	10	0.011551	0.011560	0.011440	0.011593	0.011654	
	11	0.011092	0.011046	0.011636	0.001501	0.010940	
<b>10</b>	6	0.001816	0.011535	0.011556	0.011558	0.011565	
	7	0.000162	0.011535	0.011556	0.011558	0.011564	
	8	0.001090	0.011536	0.011564	0.011558	0.011383	
	9	0.000014	0.011540	0.011528	0.011557	0.011540	
	10	0.001959	0.011533	0.011156	0.011426	0.011345	
	11	0.000434	0.010755	0.007045	0.010245	0.012292	

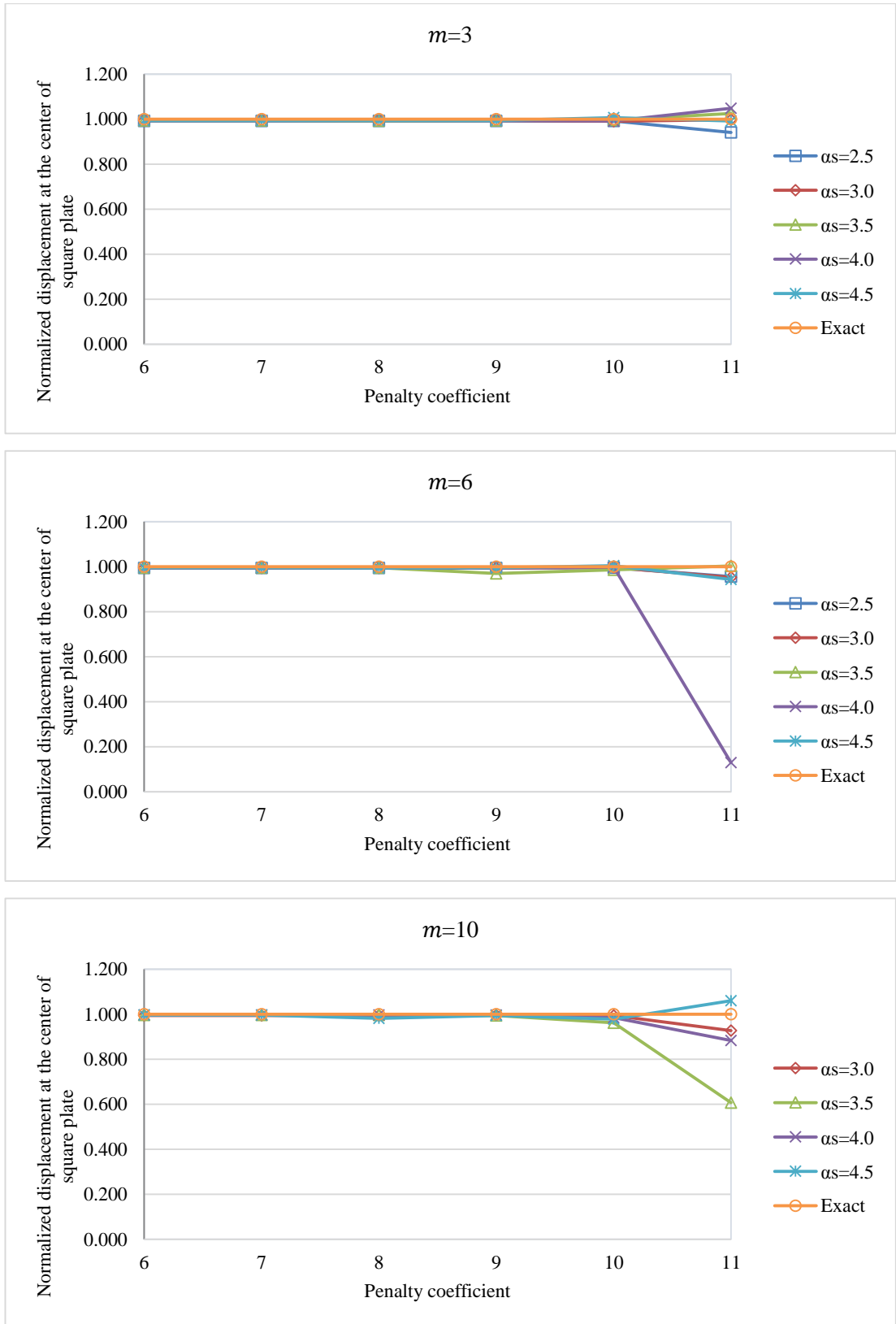


**Figure 5.9.** Variations of normalized central deflections  $w_c/\left(\frac{pL^4}{100D}\right)$  against  $\alpha_p$  for simply supported square plate under transverse centric point load using quartic spline weight functions and regular node distribution with  $n_g = 5$ .

**Table 5.8.** Variations of normalized central deflections  $w_c / \left( \frac{pL^4}{100D} \right)$  of simply supported square plate under transverse centric point load using irregular node distribution using quartic spline weight function with  $n_g = 5$ .

Number of monomials	Value of penalty coefficient	Dimensionless size of support domain ( $\alpha_s$ )					Exact
		2.5	3.0	3.5	4.0	4.5	
<b>3</b>	6	0.011634	0.011656	0.011734	0.011866	0.011797	0.011600
	7	0.011634	0.011656	0.011735	0.011867	0.011791	
	8	0.011634	0.011656	0.011732	0.011838	0.011796	
	9	0.011635	0.011657	0.011721	0.011819	0.011582	
	10	0.011629	0.011673	0.011850	0.011781	0.011813	
	11	0.011555	0.028047	0.011431	0.009145	0.011257	
<b>6</b>	6	0.011636	0.011636	0.011643	0.011658	0.011687	
	7	0.011636	0.011636	0.011643	0.011659	0.011686	
	8	0.011636	0.011636	0.011643	0.011657	0.011661	
	9	0.011633	0.011635	0.011643	0.011621	0.011661	
	10	0.011665	0.011639	0.011782	0.012890	0.011496	
	11	0.011791	0.011721	0.009100	-0.005537	-0.002784	
<b>10</b>	6	0.002575	0.011641	0.011642	0.011656	0.011673	
	7	-0.000099	0.011641	0.011642	0.011656	0.011672	
	8	-0.000081	0.011641	0.011642	0.011655	0.011673	
	9	0.000094	0.011651	0.011643	0.011661	0.011693	
	10	0.000706	0.011696	0.011624	0.010894	0.011369	
	11	0.000165	0.012081	0.006998	0.009700	0.005584	



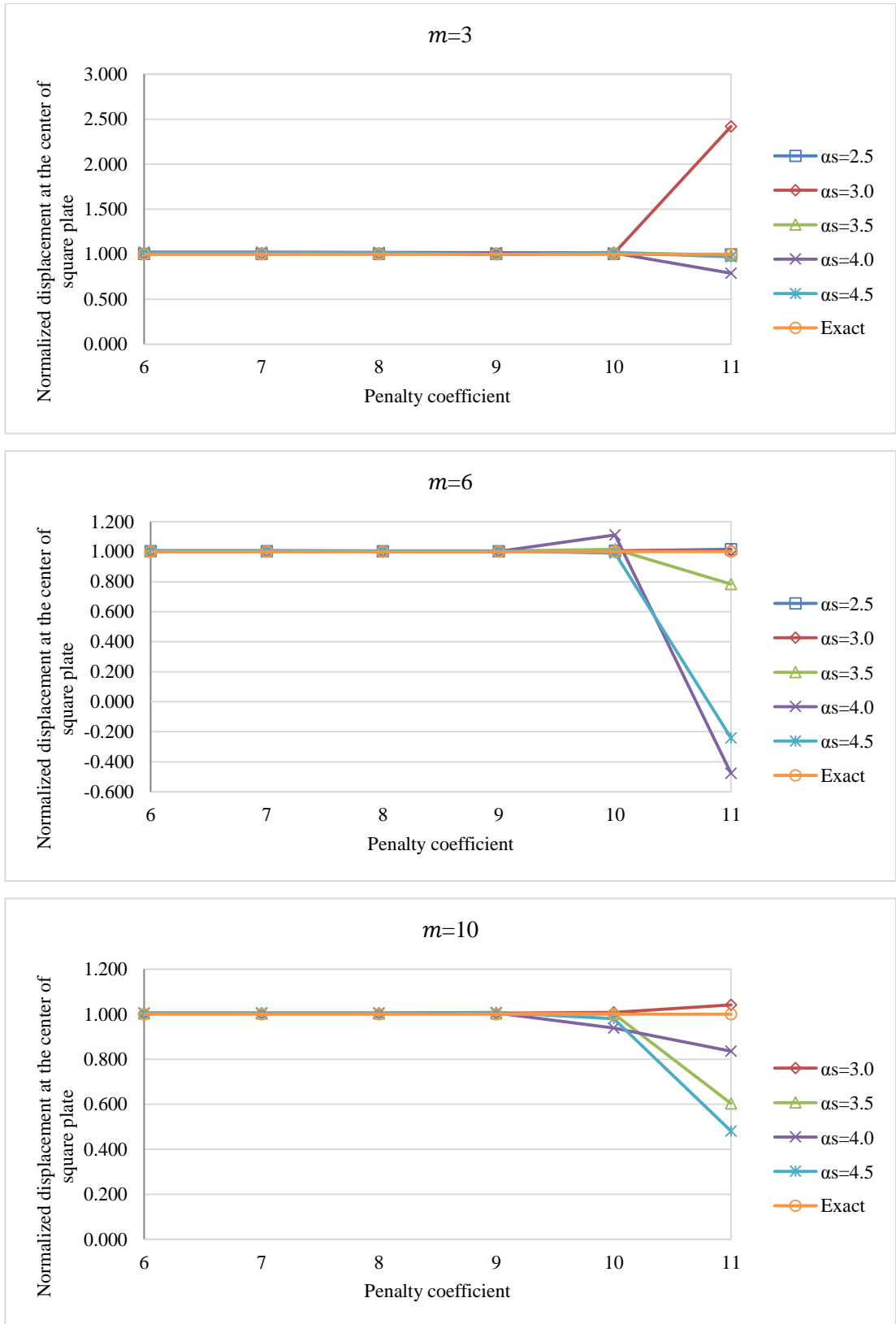


**Figure 5.10.** Variations of normalized central deflections  $w_c / \left( \frac{pL^4}{100D} \right)$  against  $\alpha_p$  for simply supported square plate under transverse centric point load using quartic spline weight functions and irregular node distribution with  $n_g = 5$ .

### 5.3 Simply supported square plate under uniform transverse load.

Simply supported square plate under transverse uniform distributed load is shown in Fig.5.11. It is analysed by using different values for the selectable parameters. The thickness and length of the plate are given by  $h = 0.01$  m and  $L = 1$  m, respectively. The Young's modulus  $E$  of material is 10920 Pa and Poisson's ratio is  $\nu = 0.3$ . Due to symmetry, only one quarter of the plate, shown in Fig. 5.12, is used in EFGM solutions. In the model of quarter square plate, 1089 field nodes and 1024 background cells were used for regular and irregular node distributions. The value of applied load  $P$  is 1.0 Pa. The normalized deflection and normalized moment values at the centre of square plate were taken as the critical value for assessment of accuracy. The results obtained using different values for the selectable parameters are presented in Table 5.9 to Table 5.24. Table 5.9 to Table 5.16 is obtained by the usage of cubic spline weight function and Table 5.17 to Table 5.24 is provided with the use of quartic spline weight function.

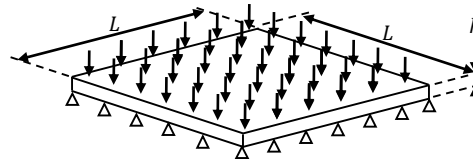


**Figure 5.11.** Simply supported square plate under uniform load.

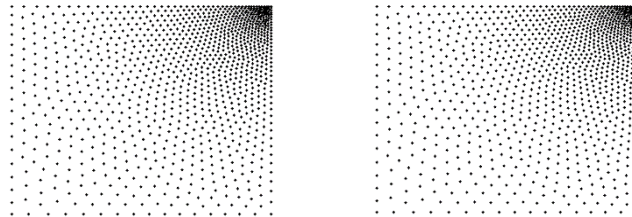


**Figure 5.12.** The EFGM models for a) regular node distributions, b) irregular node distributions

From Fig. 5.13, Fig. 5.15, Fig. 5.21 and Fig. 5.23, the variations in displacement results against number of gauss points in a background cell are less than 0.2% of exact result. However, it is not possible to say same thing for moment. The variations in moment results are important and the number of gauss points in a background cell equals 5 is suitable to decrease variations with a reasonable computation cost. The variations in

displacement and moment results are observed for different values of penalty coefficient. The variations in displacements and moments are shown for the values of penalty coefficient greater than  $1 \times 10^8$  and  $1 \times 10^6$ , respectively. The value of penalty coefficient is selected as  $1 \times 10^6$  to reduce fluctuations in results. By comparing the results for regular and irregular node distributions, it can be pointed that the results of irregular node distributions are smoother. It is shown that an increase in number of monomials cannot guaranteed any increase in results. The review of results for cubic and quartic spline weight functions indicate that the results of quartic spline weight function are smoother than results of cubic weight function. The accuracy of solutions for  $\alpha_s = 3$  are higher than the other ones.

**Table 5.9.** Normalized central deflections  $w_c / \left( \frac{pL^4}{100D} \right)$  of simply supported square plate subjected to uniform load for regular node distribution using cubic spline weight function with  $\alpha_p = 6$ .

Number of monomials	Number of gauss points	Dimensionless size of support domain ( $\alpha_s$ )					Exact
		2.5	3.0	3.5	4.0	4.5	
<b>3</b>	4×4	0.406125	0.406447	0.406393	0.406216	0.407077	0.4064
	5×5	0.406124	0.406419	0.406544	0.406286	0.405935	
	6×6	0.406127	0.406427	0.406370	0.406575	0.406616	
	7×7	0.406122	0.406425	0.406139	0.406295	0.406523	
	8×8	0.406126	0.406426	0.406452	0.406633	0.406710	
<b>6</b>	4×4	0.406448	0.406441	0.406593	0.407067	0.406862	
	5×5	0.406436	0.406442	0.406593	0.406840	0.406661	
	6×6	0.406440	0.406442	0.406587	0.406799	0.406981	
	7×7	0.406438	0.406442	0.406590	0.406669	0.407065	
	8×8	0.406439	0.406442	0.406584	0.407450	0.406604	
<b>10</b>	4×4	0.000504	0.406456	0.406602	0.407074	0.407162	
	5×5	-	0.406454	0.406591	0.407029	0.407138	
	6×6	-	0.406453	0.406594	0.407265	0.407121	
	7×7	0.000094	0.406453	0.406592	0.407110	0.407134	
	8×8	0.002630	0.406453	0.406592	0.407127	0.407127	

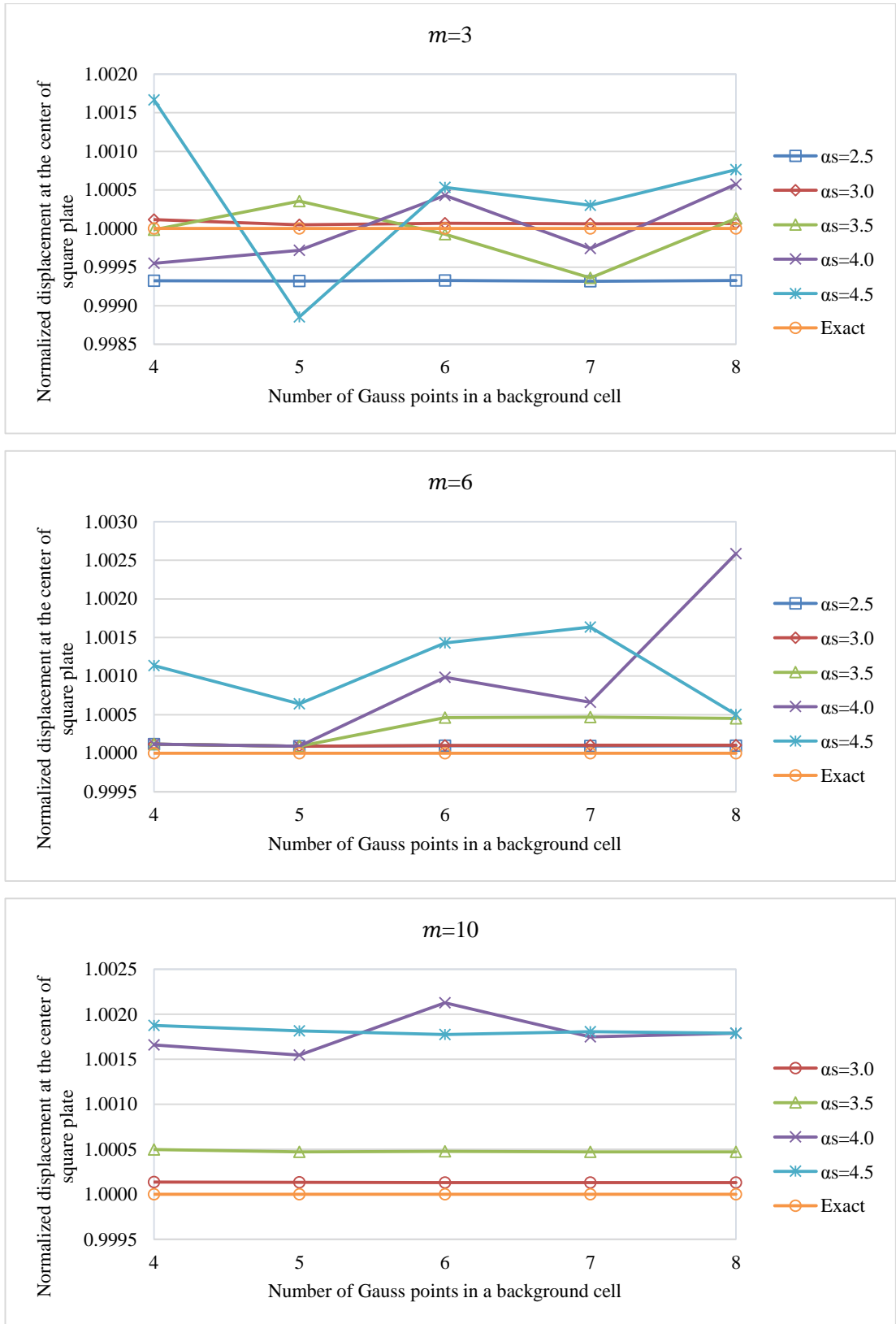


**Figure 5.13.** Variations of normalized central deflections  $w_c / \left( \frac{pL^4}{100D} \right)$  against  $n_g$  for simply supported square plate subjected to uniform load using cubic spline weight functions and regular node distribution with  $\alpha_p = 6$ .

**Table 5.10.** Normalized central moments  $M_c / \left(\frac{pL^2}{10}\right)$  of simply supported square plate subjected to uniform load for regular node distribution using cubic spline weight function with  $\alpha_p = 6$

Number of monomials	Number of gauss points	Dimensionless size of support domain ( $\alpha_s$ )					Exact
		2.5	3.0	3.5	4.0	4.5	
<b>3</b>	4×4	0.465908	0.477236	0.478844	0.468530	0.492989	0.4789
	5×5	0.465861	0.477124	0.490604	0.476325	0.474944	
	6×6	0.465962	0.477132	0.481406	0.479368	0.481487	
	7×7	0.465868	0.477156	0.466563	0.475205	0.479422	
	8×8	0.465916	0.477134	0.486288	0.486924	0.485117	
<b>6</b>	4×4	0.478715	0.475355	0.476658	0.533247	0.473470	
	5×5	0.476724	0.475148	0.476658	0.508265	0.490959	
	6×6	0.477565	0.475239	0.476750	0.509770	0.508166	
	7×7	0.477247	0.475199	0.476842	0.492523	0.512757	
	8×8	0.477316	0.475208	0.476471	0.567429	0.485658	
<b>10</b>	4×4	0.047502	0.473487	0.464784	0.553512	0.551347	
	5×5	-	0.473020	0.467739	0.567587	0.560778	
	6×6	-	0.472050	0.466511	0.551792	0.553217	
	7×7	0.009211	0.471502	0.467141	0.557828	0.558613	
	8×8	0.440787	0.471477	0.467166	0.528077	0.556545	

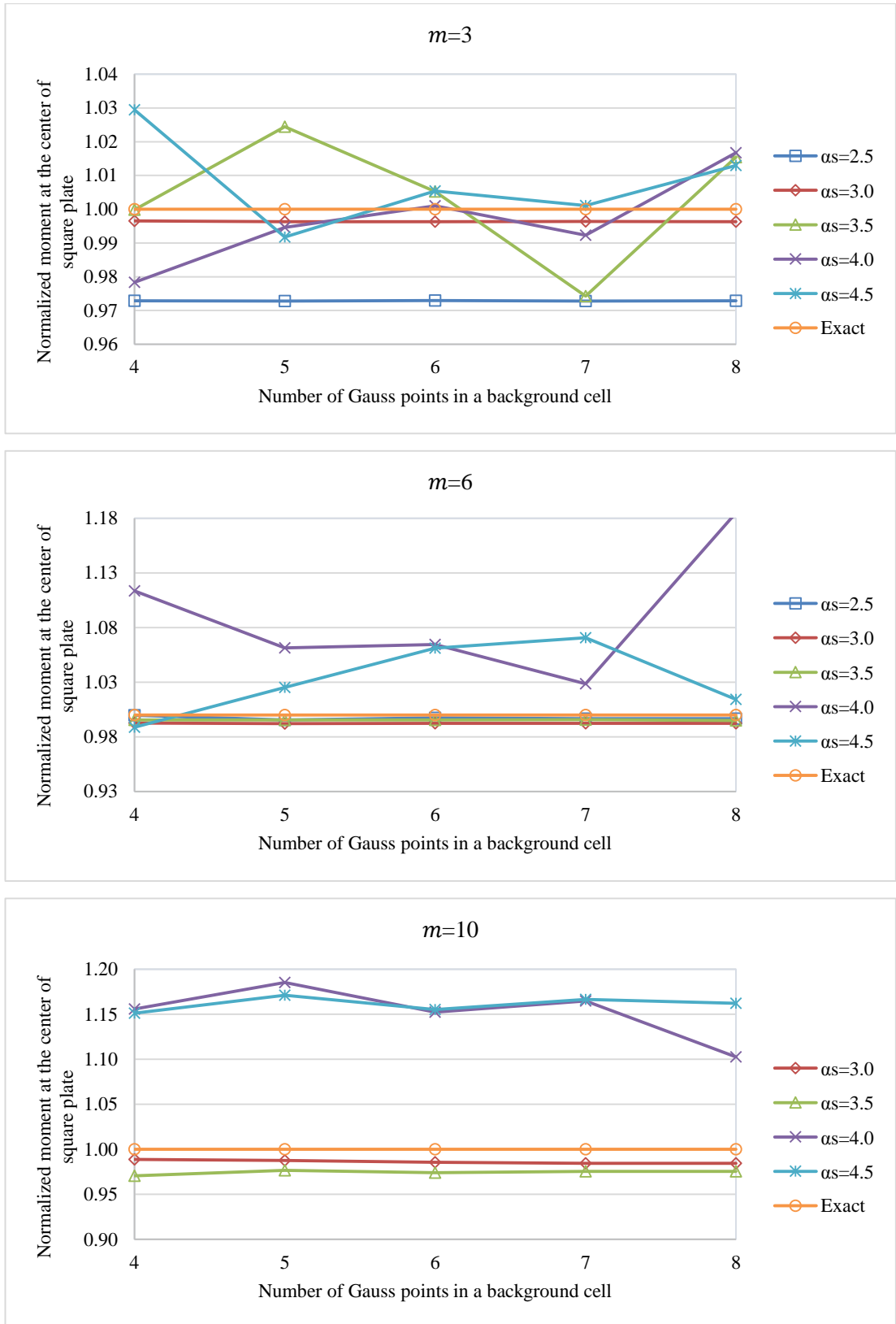


**Figure 5.14.** Variations of normalized central moments  $M_c / \left( \frac{pL^2}{10} \right)$  against  $n_g$  for simply supported square plate subjected to uniform load using cubic spline weight functions and regular node distribution with  $\alpha_p = 6$ .

**Table 5.11.** Normalized central deflections  $w_c / \left( \frac{pL^4}{100D} \right)$  of simply supported square plate subjected to uniform load for irregular node distribution using cubic spline weight function with  $\alpha_p = 6$ .

Number of monomials	Number of gauss points	Dimensionless size of support domain ( $\alpha_s$ )					Exact
		2.5	3.0	3.5	4.0	4.5	
<b>3</b>	4×4	0.406510	0.407413	0.413576	0.419243	0.421976	0.4064
	5×5	0.406339	0.406818	0.408303	0.410831	0.409785	
	6×6	0.406282	0.406572	0.407042	0.407971	0.407881	
	7×7	0.406255	0.406415	0.406627	0.407131	0.407222	
	8×8	0.406254	0.406331	0.406529	0.406676	0.406721	
<b>6</b>	4×4	0.406542	0.406556	0.406977	0.408746	0.411523	
	5×5	0.406459	0.406471	0.406580	0.406896	0.407403	
	6×6	0.406445	0.406455	0.406511	0.406620	0.406828	
	7×7	0.406440	0.406447	0.406477	0.406533	0.406631	
	8×8	0.406437	0.406447	0.406465	0.406515	0.406567	
<b>10</b>	4×4	0.099456	0.406742	0.406980	0.407986	0.409514	
	5×5	0.008230	0.406526	0.406542	0.406790	0.407075	
	6×6	0.002251	0.406511	0.406491	0.406622	0.406756	
	7×7	0.486834	0.406470	0.406477	0.406520	0.406616	
	8×8	0.003929	0.406463	0.406471	0.406501	0.406573	



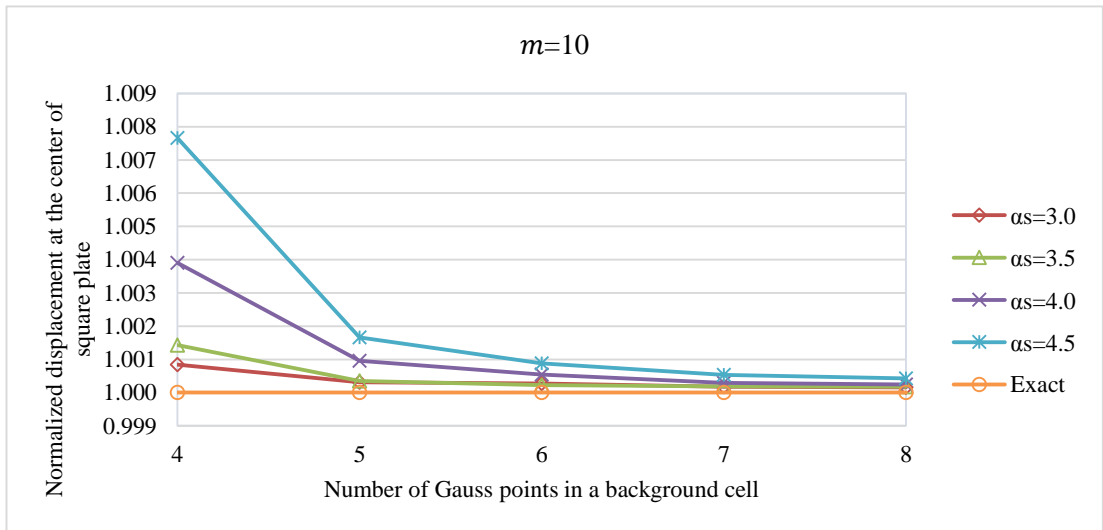
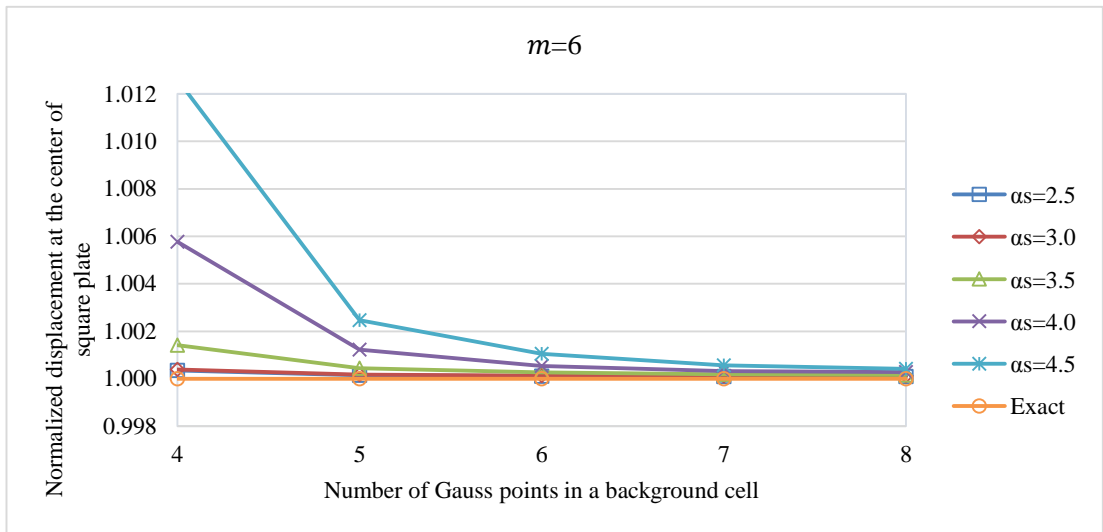
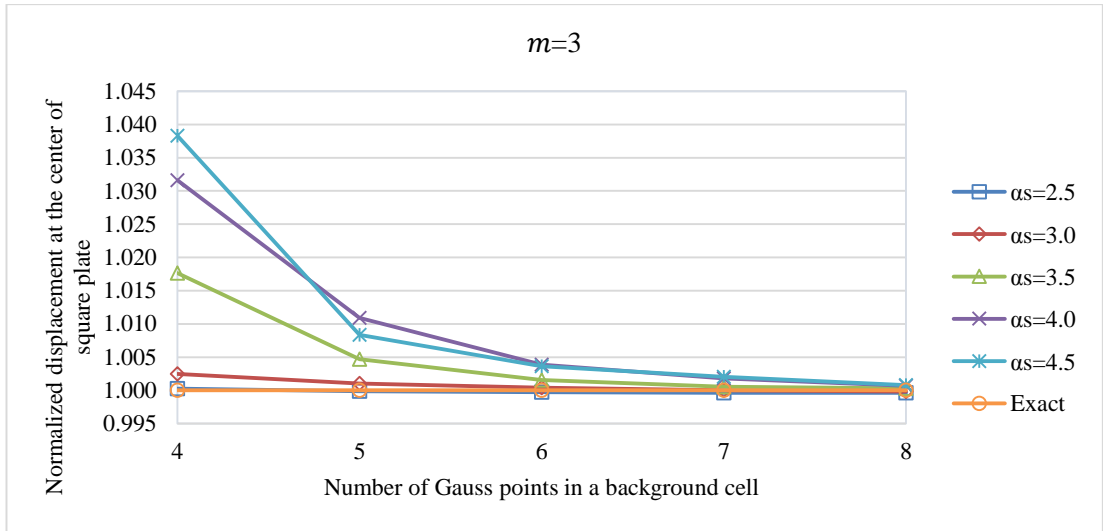


**Figure 5.15.** Variations of normalized central deflections  $w_c / \left( \frac{pL^4}{100D} \right)$  against  $n_g$  for simply supported square plate subjected to uniform load using cubic spline weight functions and irregular node distribution with  $\alpha_p = 6$ .

**Table 5.12.** Normalized central moments  $M_c / \left(\frac{pL^2}{10}\right)$  of simply supported square plate subjected to uniform load for irregular node distribution using cubic spline weight function with  $\alpha_p = 6$ .

Number of monomials	Number of gauss points	Dimensionless size of support domain ( $\alpha_s$ )					Exact
		2.5	3.0	3.5	4.0	4.5	
<b>3</b>	4×4	0.462163	0.452059	0.586793	0.788000	1.233154	0.4789
	5×5	0.484287	0.491661	0.549301	0.485057	0.541503	
	6×6	0.469131	0.479985	0.468504	0.486260	0.480093	
	7×7	0.476790	0.477586	0.477429	0.484557	0.495301	
	8×8	0.473940	0.479066	0.476112	0.483704	0.480869	
<b>6</b>	4×4	0.454368	0.485642	0.402171	0.335533	0.899370	
	5×5	0.488675	0.485269	0.484494	0.492242	0.528780	
	6×6	0.454355	0.470597	0.479163	0.467722	0.479242	
	7×7	0.488484	0.480897	0.473508	0.485336	0.486683	
	8×8	0.468165	0.475295	0.480348	0.477380	0.482623	
<b>10</b>	4×4	133.3553	0.379987	0.456289	0.577763	0.618072	
	5×5	1.898563	0.509234	0.487986	0.510251	0.390230	
	6×6	0.549946	0.427753	0.460868	0.468436	0.500102	
	7×7	18.72356	0.472461	0.468415	0.487375	0.467321	
	8×8	2.391880	0.457493	0.485846	0.468485	0.472815	

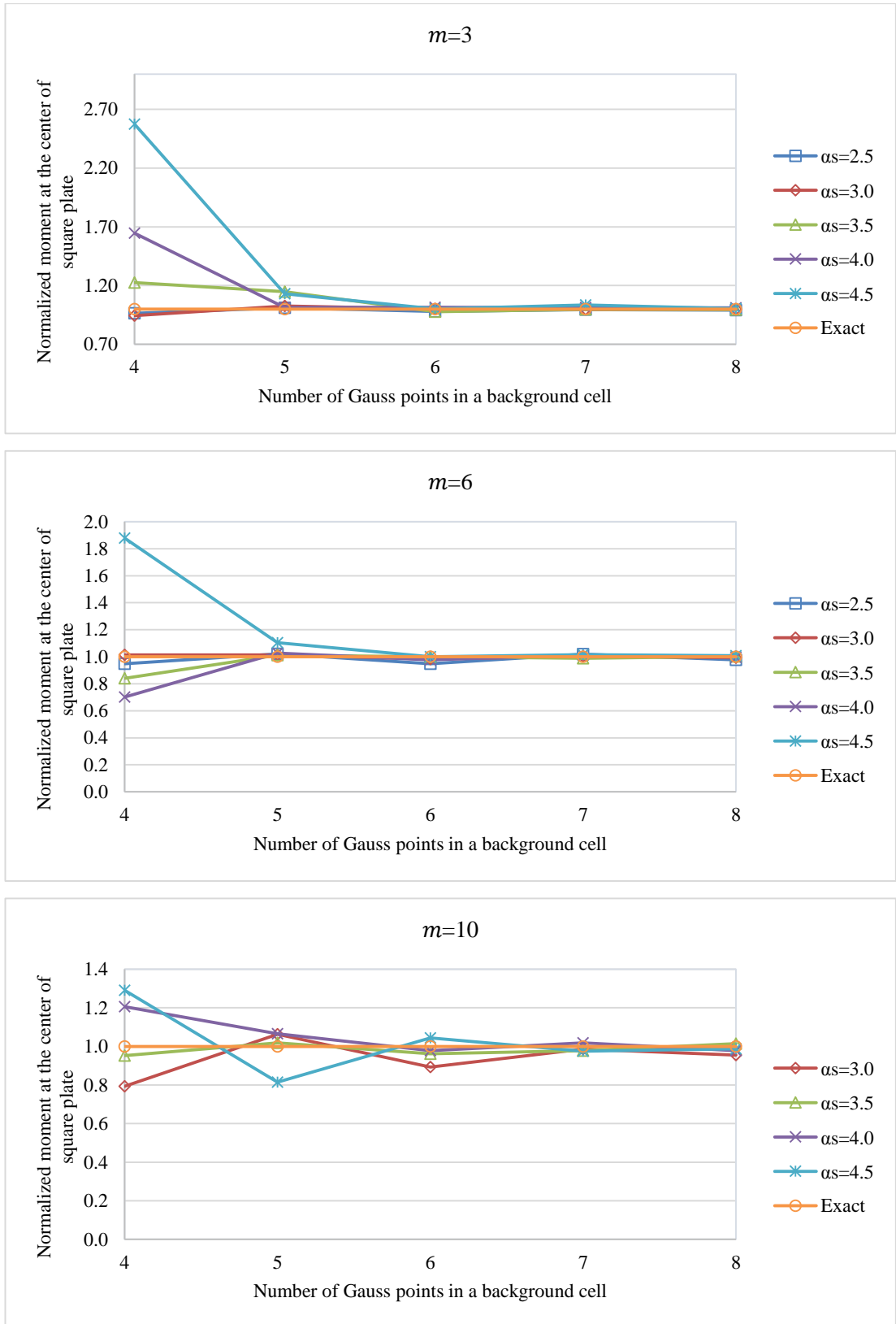


**Figure 5.16.** Variations of normalized central moments  $M_c / \left( \frac{pL^2}{10} \right)$  against  $n_g$  for simply supported square plate subjected to uniform load using cubic spline weight functions and irregular node distribution with  $\alpha_p = 6$ .

**Table 5.13.** Variations of normalized central deflections  $w_c / \left( \frac{pL^4}{100D} \right)$  of simply supported square plate subjected to uniform load using regular node distribution using cubic spline weight function with  $n_g = 5$ .

Number of monomials	Value of penalty coefficient	Dimensionless size of support domain ( $\alpha_s$ )					Exact
		2.5	3.0	3.5	4.0	4.5	
<b>3</b>	6	0.406124	0.406419	0.406544	0.406286	0.405935	0.4064
	7	0.406124	0.406419	0.406173	0.406511	0.406447	
	8	0.406125	0.406424	0.406136	0.406379	0.406661	
	9	0.406135	0.406396	0.406556	0.407010	0.406176	
	10	0.406156	0.406113	0.408414	0.405107	0.403696	
	11	0.405627	0.413570	0.303081	0.385763	0.386330	
<b>6</b>	6	0.406436	0.406442	0.406587	0.406840	0.406661	
	7	0.406436	0.406443	0.406665	0.406507	0.407531	
	8	0.406426	0.406436	0.406445	0.406323	0.407429	
	9	0.406383	0.406372	0.426644	0.406621	0.401259	
	10	0.405441	0.405901	0.425925	0.347944	0.395093	
	11	0.411339	0.398761	0.407843	1.161832	0.406219	
<b>10</b>	6	0.005101	0.406454	0.406591	0.407029	0.407138	
	7	-0.006104	0.406454	0.406618	0.407070	0.407220	
	8	0.008291	0.406455	0.406467	0.407763	0.407196	
	9	0.004782	0.406530	0.409589	0.408196	0.408115	
	10	0.007121	0.407200	0.427764	0.402099	0.393411	
	11	-0.004692	0.409140	0.336089	0.418981	0.507675	

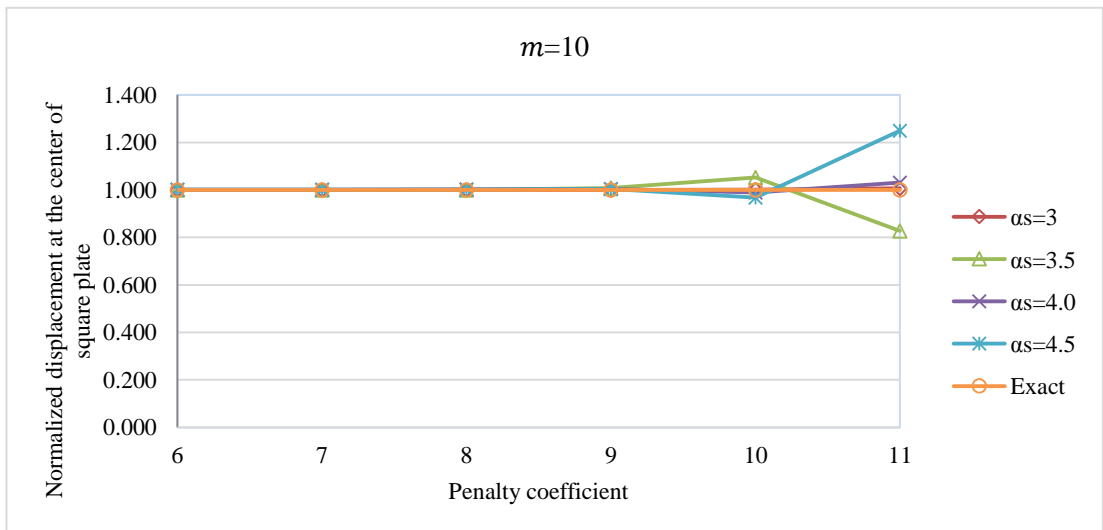
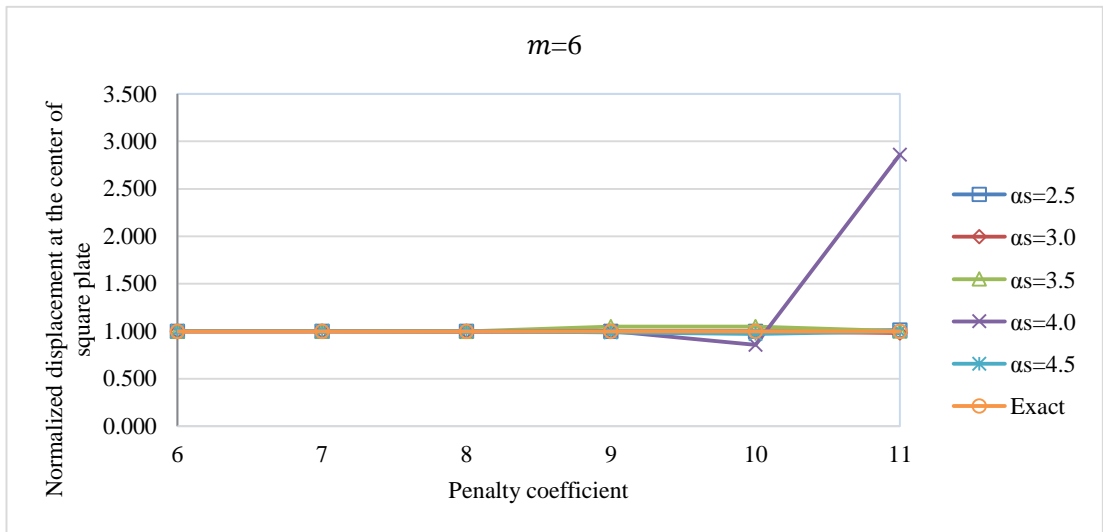
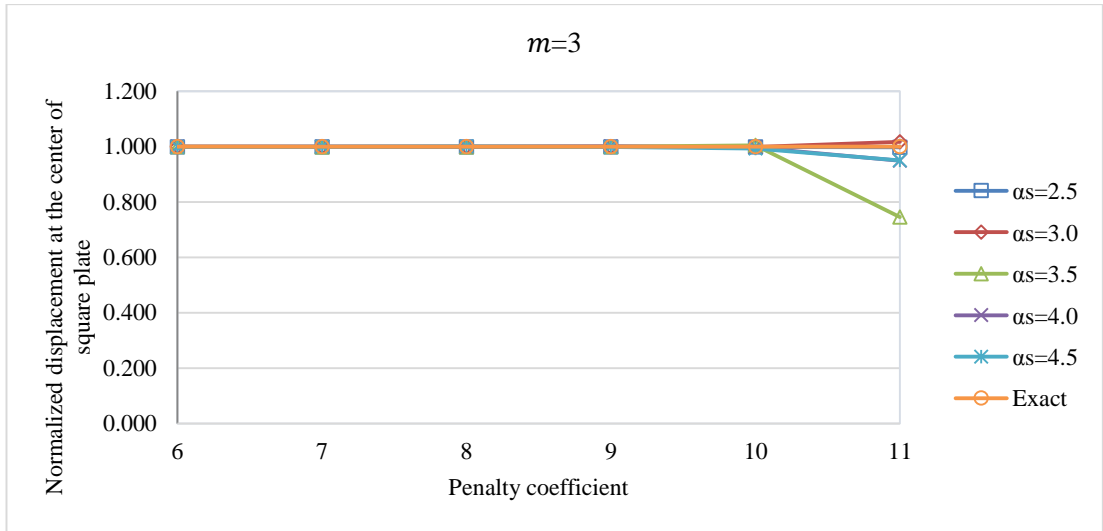


**Figure 5.17.** Variations of normalized central deflections  $w_c / \left( \frac{pL^4}{100D} \right)$  against  $\alpha_p$  for simply supported square plate subjected to uniform load using quartic spline weight functions and regular node distribution with  $n_g = 5$ .

**Table 5.14.** Variations of normalized central moments  $M_c/\left(\frac{pL^2}{10}\right)$  of simply supported square plate subjected to uniform load using regular node distribution using cubic spline weight function with  $n_g = 5$ .

Number of monomials	Value of penalty coefficient	Dimensionless size of support domain ( $\alpha_s$ )					Exact
		2.5	3.0	3.5	4.0	4.5	
<b>3</b>	6	0.465861	0.477124	0.490604	0.476325	0.474944	0.4789
	7	0.465861	0.477131	0.476854	0.484699	0.477998	
	8	0.465862	0.477274	0.476025	0.480848	0.480860	
	9	0.465898	0.476066	0.475138	0.488999	0.487681	
	10	0.466449	0.542014	0.482575	0.470388	0.464470	
	11	0.465259	0.593314	0.099355	0.208429	0.477018	
<b>6</b>	6	0.476724	0.475148	0.476696	0.508265	0.490959	
	7	0.476719	0.475145	0.480891	0.479825	0.541073	
	8	0.476706	0.475232	0.477623	0.464833	0.481892	
	9	0.476676	0.476350	0.702373	0.516292	0.771494	
	10	0.477879	0.177135	0.080488	1.396184	0.658199	
	11	0.473519	7.118890	1.535408	18.904350	0.265464	
<b>10</b>	6	-1.898563	0.473020	0.467739	0.567587	0.560778	
	7	-0.779907	0.473035	0.466115	0.499341	0.552515	
	8	-1.355116	0.472708	0.464424	0.554111	0.763799	
	9	-0.965741	0.475136	0.689665	0.457188	1.310356	
	10	-0.061856	0.474889	0.809296	1.500415	20.92811	
	11	-0.220529	0.537894	2.098230	3.548006	6.556247	

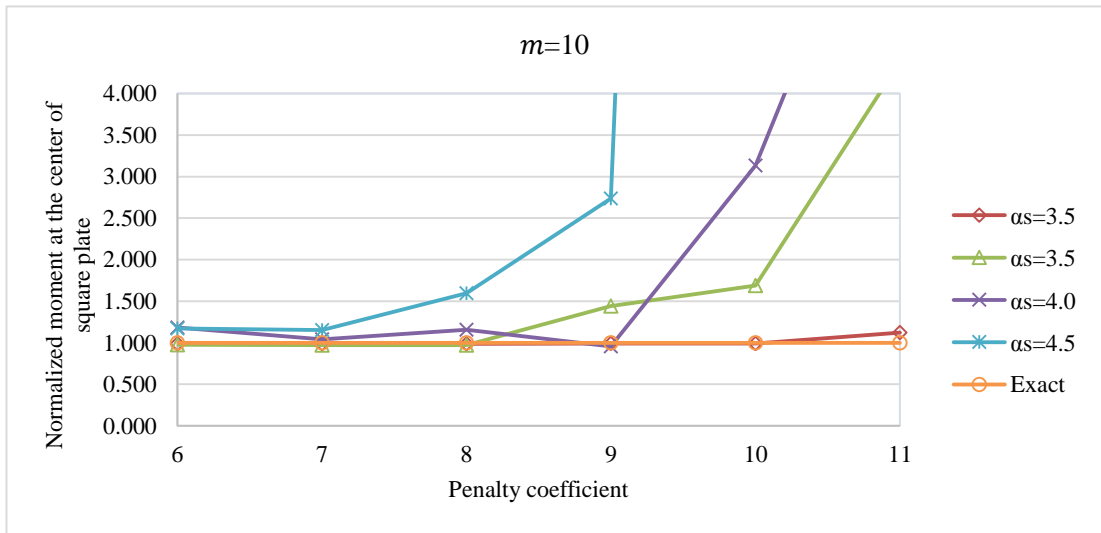
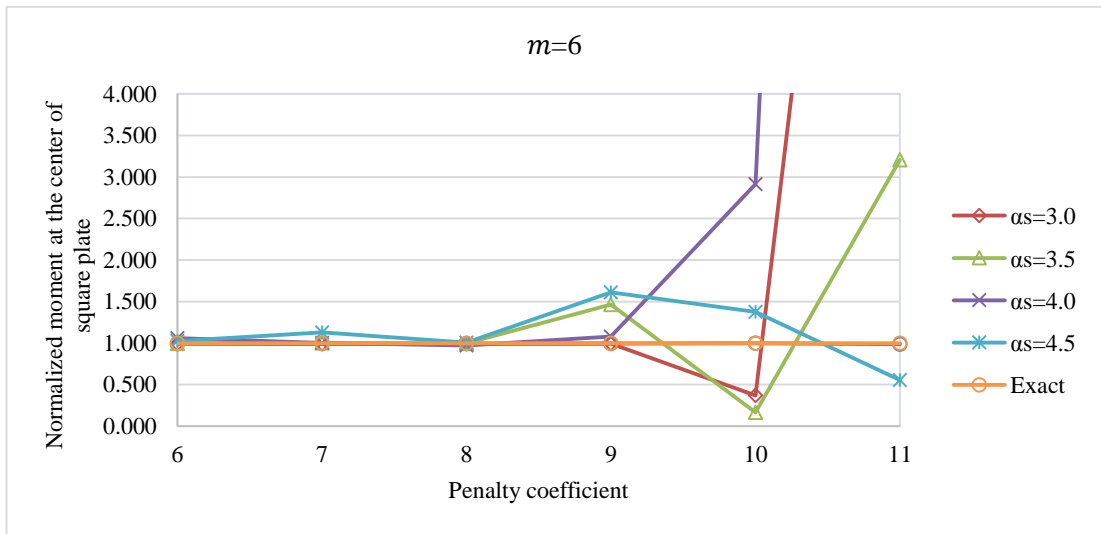
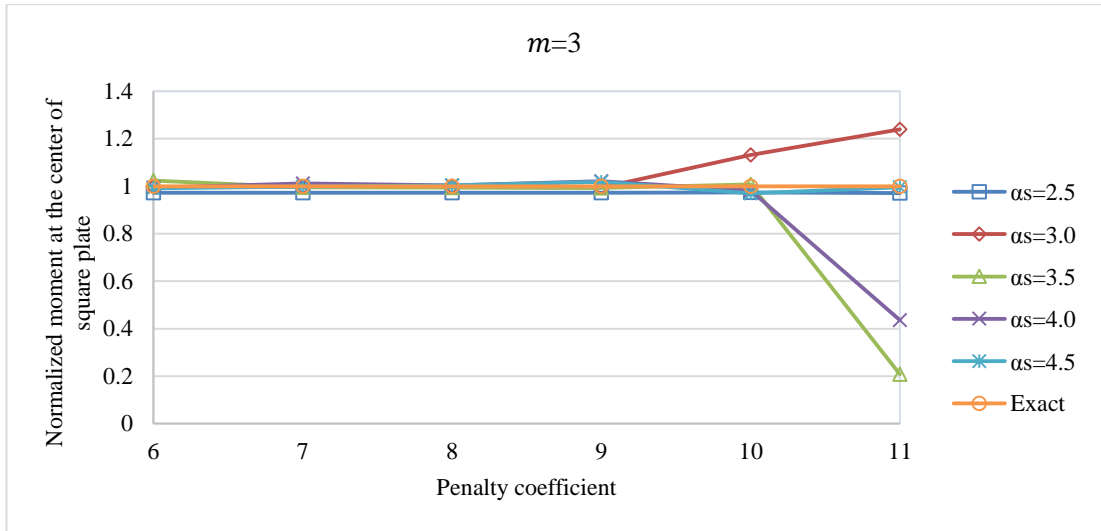


**Figure 5.18.** Variations of normalized central moments  $M_c / \left( \frac{pL^2}{10} \right)$  against  $\alpha_p$  for simply supported square plate subjected to uniform load using quartic spline weight functions and regular node distribution with  $n_g = 5$ .

**Table 5.15.** Variations of normalized central deflections  $w_c / \left( \frac{pL^4}{100D} \right)$  of simply supported square plate subjected to uniform load using irregular node distribution using cubic spline weight function with  $n_g = 5$ .

Number of monomials	Value of penalty coefficient	Dimensionless size of support domain ( $\alpha_s$ )					Exact
		2.5	3.0	3.5	4.0	4.5	
<b>3</b>	6	0.406339	0.406818	0.408304	0.410834	0.409786	0.4064
	7	0.406339	0.406818	0.408303	0.410790	0.409024	
	8	0.406342	0.406820	0.408486	0.410406	0.408707	
	9	0.406362	0.406769	0.407661	0.409504	0.408980	
	10	0.406363	0.409116	0.407741	0.411189	0.406833	
	11	0.407814	0.226611	0.408141	0.381858	0.399561	
<b>6</b>	6	0.406459	0.406471	0.406580	0.406897	0.407401	
	7	0.406459	0.406472	0.406579	0.406896	0.407530	
	8	0.406434	0.406468	0.406577	0.407816	0.408537	
	9	0.406579	0.406583	0.406600	0.406350	0.423195	
	10	0.405013	0.408022	0.426530	0.425535	0.609899	
	11	0.387544	0.416706	0.227181	0.911252	0.521799	
<b>10</b>	6	0.008230	0.406527	0.406542	0.406790	0.407074	
	7	0.010900	0.406527	0.406545	0.406790	0.407082	
	8	0.016128	0.406570	0.406529	0.407110	0.406912	
	9	0.001619	0.406568	0.406714	0.406545	0.400725	
	10	0.005487	0.404763	0.409905	0.399975	0.435560	
	11	0.000430	0.386955	0.374940	11.074030	0.441067	



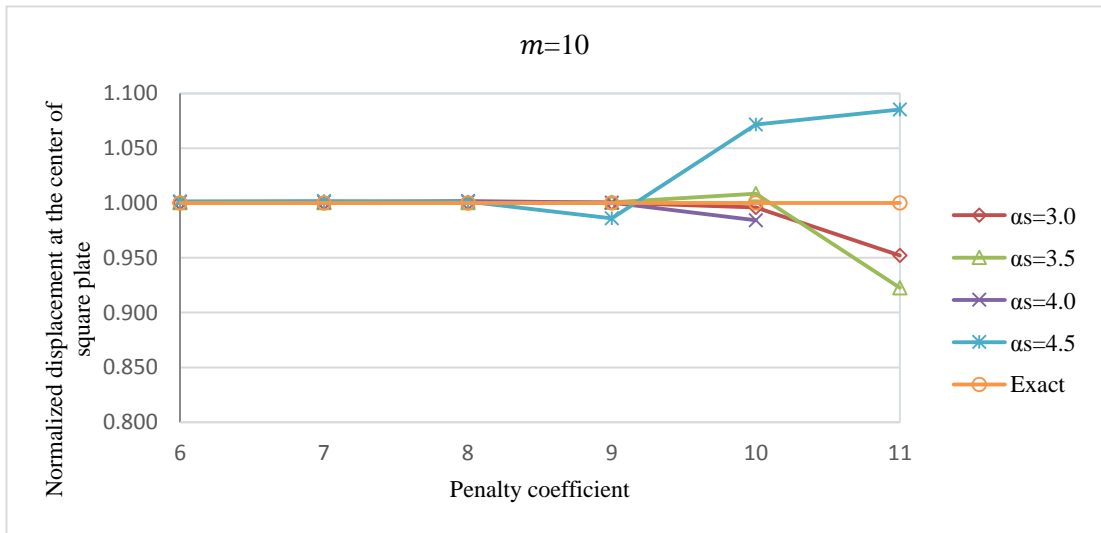
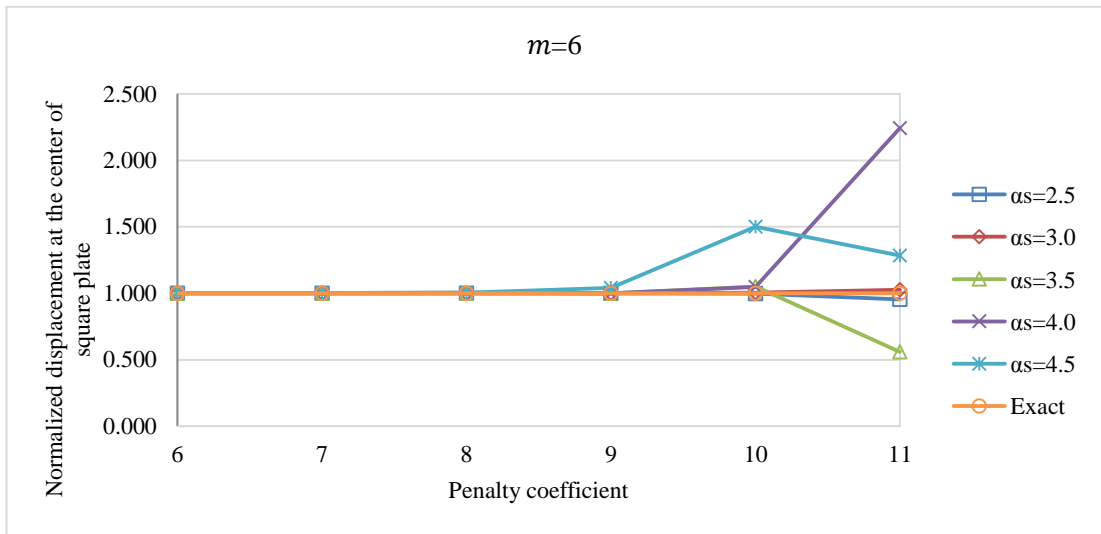
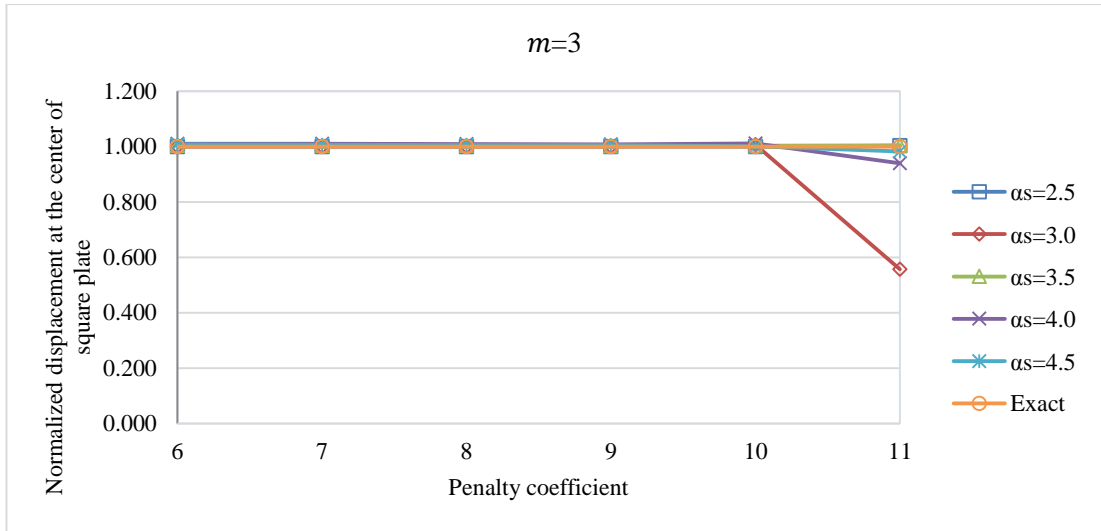


**Figure 5.19.** Variations of normalized central deflections  $w_c / \left( \frac{pL^4}{100D} \right)$  against  $\alpha_p$  for simply supported square plate subjected to uniform load using quartic spline weight functions and irregular node distribution with  $n_g = 5$ .

**Table 5.16.** Variations of normalized central moments  $M_c / \left( \frac{pL^2}{10} \right)$  of simply supported square plate subjected to uniform load using irregular node distribution using cubic spline weight function with  $n_g = 5$ .

Number of monomials	Value of penalty coefficient	Dimensionless size of support domain ( $\alpha_s$ )					Exact
		2.5	3.0	3.5	4.0	4.5	
<b>3</b>	6	0.484287	0.491661	0.549301	0.485057	0.541503	0.4789
	7	0.484206	0.491508	0.549034	0.484946	0.528225	
	8	0.484303	0.491721	0.550993	0.484046	0.474842	
	9	0.481672	0.501556	0.470179	0.428830	0.492756	
	10	0.485118	1.032503	0.753860	0.518583	0.414814	
	11	0.938223	8.490625	0.204448	0.410389	0.406419	
<b>6</b>	6	0.488675	0.485269	0.484494	0.492242	0.528780	
	7	0.488475	0.485232	0.484243	0.491473	0.582196	
	8	0.489361	0.483544	0.474901	0.506475	1.535594	
	9	0.485903	0.483757	0.421949	0.468657	0.742513	
	10	0.659297	0.470658	62.297360	0.880942	3.077730	
	11	0.032074	0.047749	6.969470	206.150000	4.105061	
<b>10</b>	6	-	0.473020	0.467739	0.567587	0.560778	
	7	-	0.473035	0.466115	0.499341	0.552515	
	8	-	0.472708	0.464424	0.554111	0.763799	
	9	-	0.475136	0.689665	0.457188	1.310356	
	10	-	0.474889	0.809296	1.500415	20.92811	
	11	-	0.537894	2.098230	3.548006	6.556247	

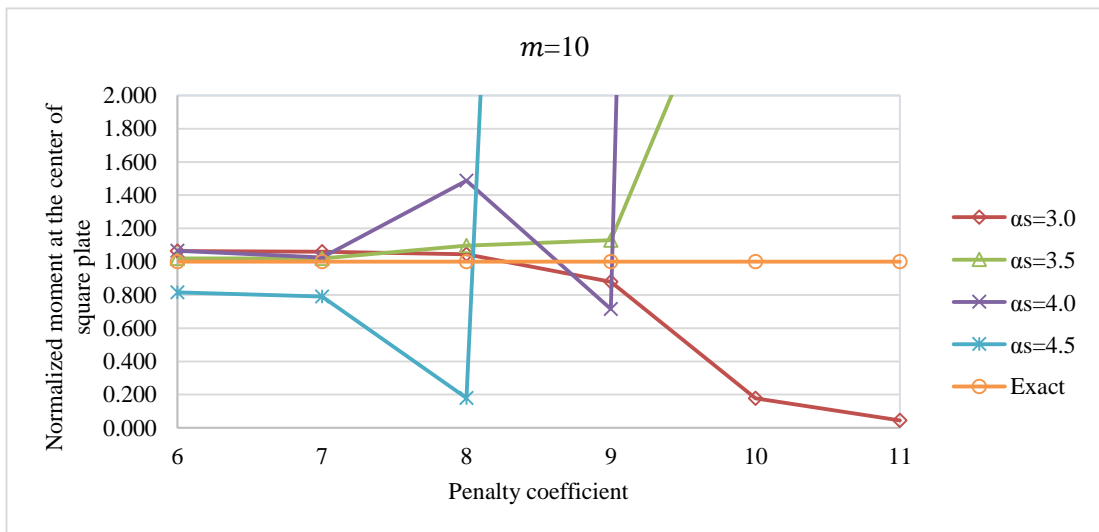
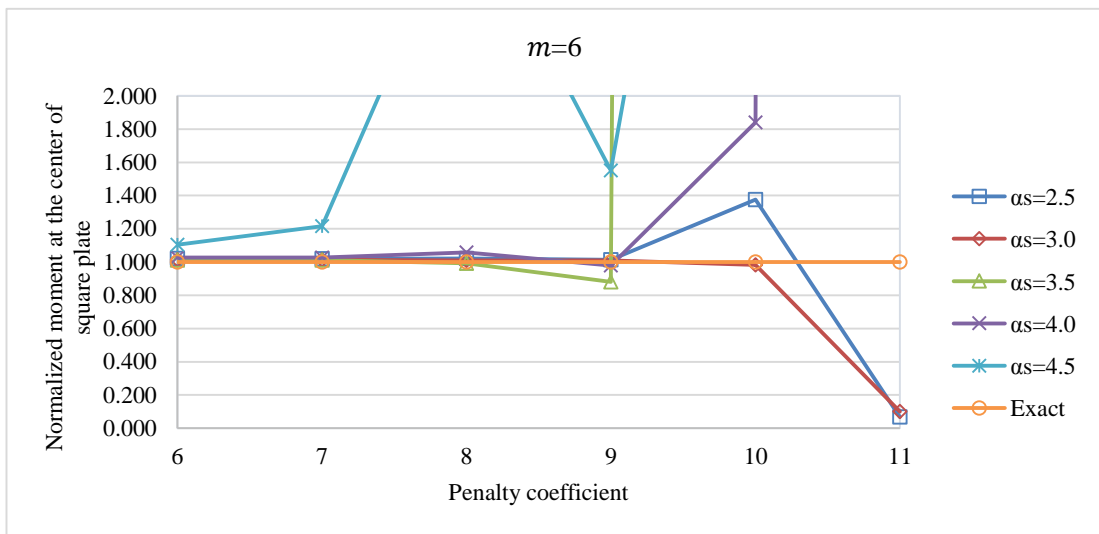
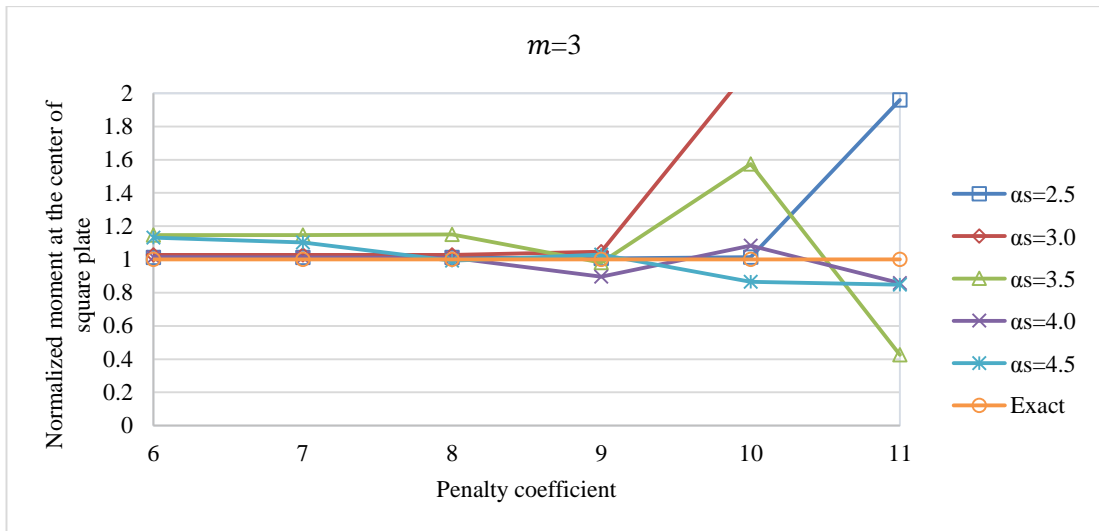


**Figure 5.20.** Variations of normalized central moments  $M_c/\left(\frac{pL^2}{10}\right)$  against  $\alpha_p$  for simply supported square plate subjected to uniform load using quartic spline weight functions and irregular node distribution with  $n_g = 5$ .

**Table 5.17.** Variations of normalized central deflections  $w_c / \left( \frac{pL^4}{100D} \right)$  of simply supported square plate subjected to uniform load using regular node distribution using quartic spline weight function with  $\alpha_p = 6$ .

Number of monomials	Number of gauss points	Dimensionless size of support domain ( $\alpha_s$ )					Exact
		2.5	3.0	3.5	4.0	4.5	
<b>3</b>	4×4	0.406038	0.406323	0.406388	0.406437	0.406506	0.4064
	5×5	0.405621	0.406313	0.406303	0.406437	0.406479	
	6×6	0.405753	0.406315	0.406325	0.406439	0.406499	
	7×7	0.405711	0.406316	0.406323	0.406439	0.406498	
	8×8	0.405723	0.406316	0.406320	0.406438	0.406489	
<b>6</b>	4×4	0.406453	0.406456	0.406734	0.406529	0.406700	
	5×5	0.406432	0.406458	0.406734	0.406529	0.406683	
	6×6	0.406437	0.406458	0.406720	0.406528	0.406686	
	7×7	0.406435	0.406457	0.406720	0.406527	0.406687	
	8×8	0.406436	0.406457	0.406719	0.406528	0.406687	
<b>10</b>	4×4	-	0.406458	0.406771	0.406800	0.406933	
	5×5	0.002882	0.406454	0.406775	0.406794	0.406913	
	6×6	0.003296	0.406453	0.406759	0.406794	0.406891	
	7×7	0.004063	0.406452	0.406754	0.406794	0.406899	
	8×8	0.000251	0.406452	0.406759	0.406794	0.406893	

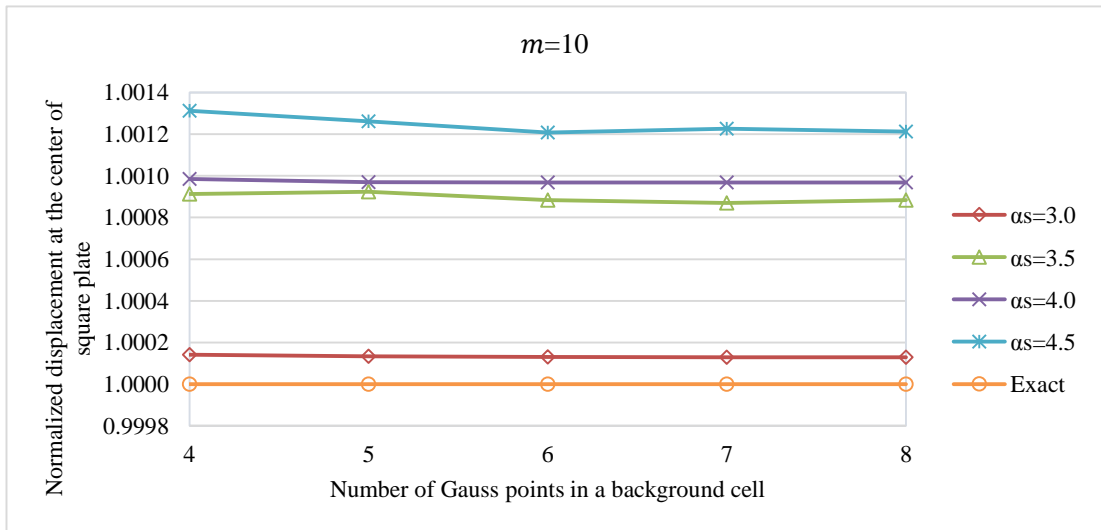
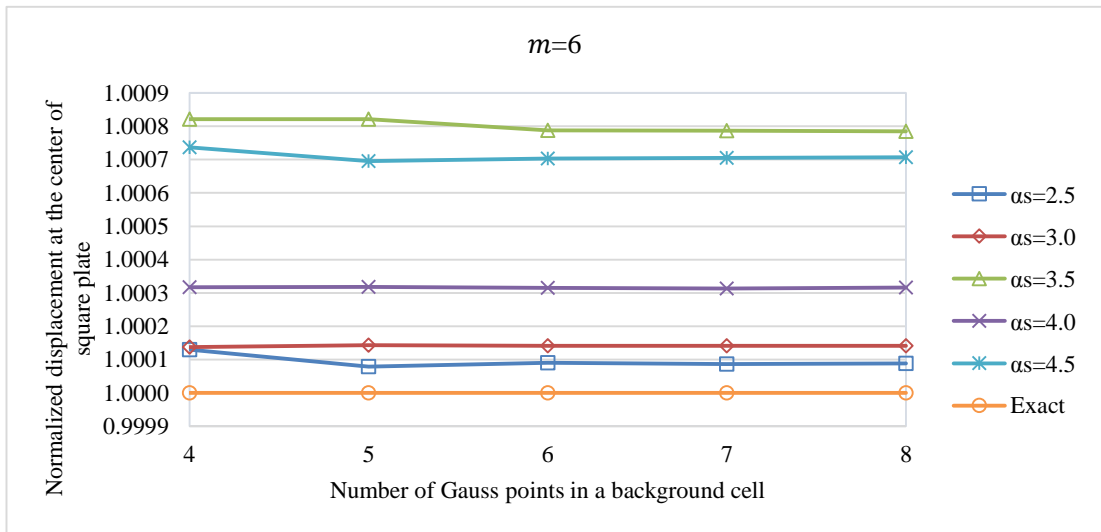
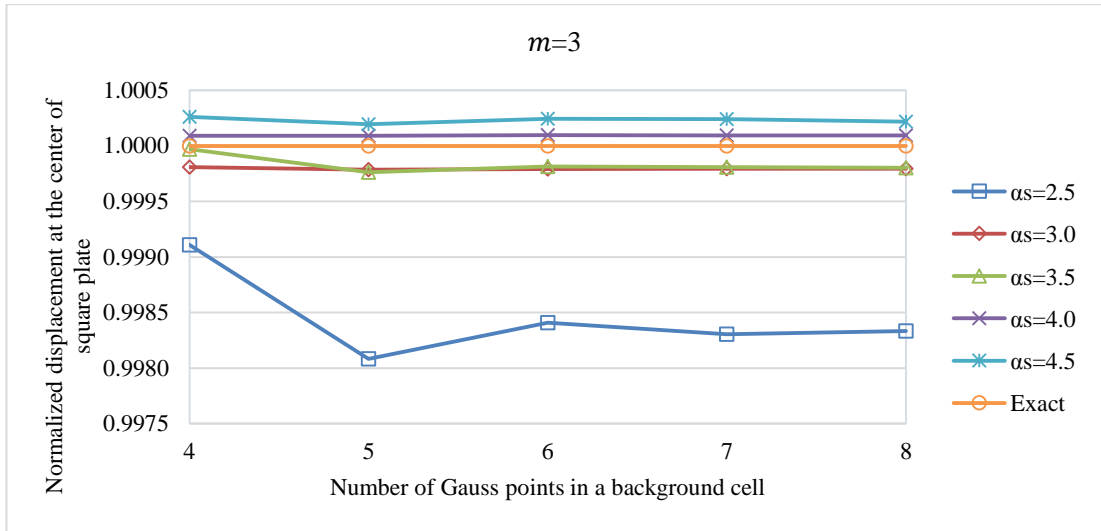


**Figure 5.21.** Variations of normalized central deflections  $w_c / \left( \frac{pL^4}{100D} \right)$  against  $n_g$  for simply supported square plate subjected to uniform load using quartic spline weight functions and regular node distribution with  $\alpha_p = 6$ .

**Table 5.18.** Variations of normalized central moments  $M_c / \left( \frac{pL^2}{10} \right)$  of simply supported square plate subjected to uniform load using regular node distribution using quartic spline weight function with  $\alpha_p = 6$ .

Number of monomials	Number of gauss points	Dimensionless size of support domain ( $\alpha_s$ )					Exact
		2.5	3.0	3.5	4.0	4.5	
<b>3</b>	4×4	0.474955	0.475765	0.478047	0.478991	0.480130	0.4789
	5×5	0.474722	0.475776	0.478018	0.478998	0.480092	
	6×6	0.474776	0.475814	0.478044	0.478993	0.480687	
	7×7	0.474744	0.475815	0.478010	0.479012	0.480405	
	8×8	0.474770	0.475813	0.478042	0.478990	0.480379	
<b>6</b>	4×4	0.479195	0.471815	0.480843	0.475026	0.480291	
	5×5	0.475777	0.471669	0.480843	0.475361	0.479640	
	6×6	0.477068	0.471664	0.480491	0.475338	0.480184	
	7×7	0.476537	0.471658	0.480443	0.475282	0.479814	
	8×8	0.476699	0.471635	0.480289	0.475294	0.479645	
<b>10</b>	4×4	-	0.476271	0.500018	0.483480	0.501804	
	5×5	0.244558	0.475173	0.508968	0.489483	0.504555	
	6×6	0.011884	0.474485	0.505329	0.489959	0.502493	
	7×7	0.611912	0.474033	0.506119	0.489406	0.504481	
	8×8	0.028622	0.473952	0.507093	0.489326	0.503133	

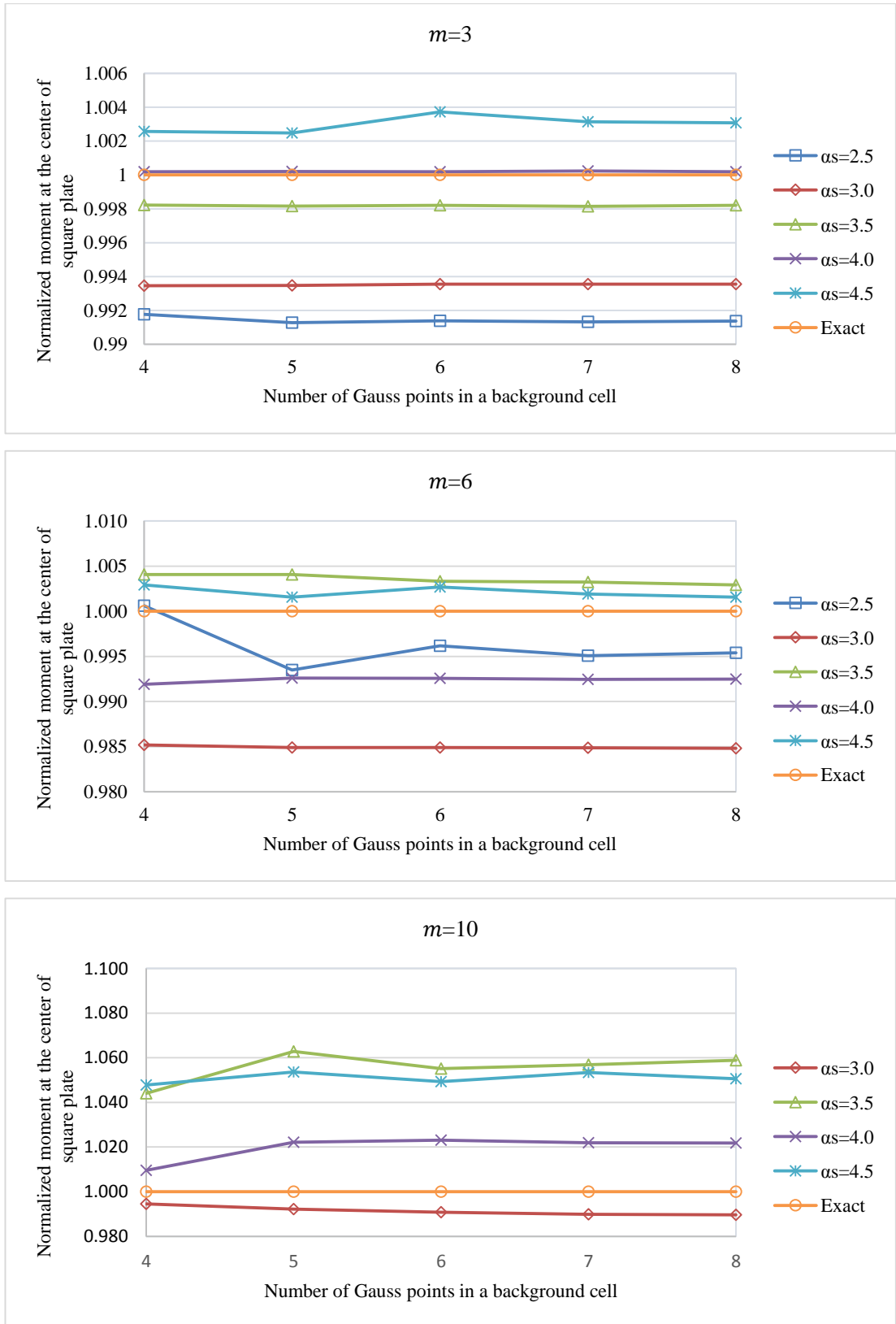


**Figure 5.22.** Variations of normalized central moments  $M_c/\left(\frac{pL^2}{10}\right)$  against  $n_g$  for simply supported square plate subjected to uniform load using quartic spline weight functions and regular node distribution with  $\alpha_p = 6$ .

**Table 5.19.** Variations of normalized central deflections  $w_c / \left( \frac{pL^4}{100D} \right)$  of simply supported square plate subjected to uniform load using irregular node distribution using quartic spline weight function with  $\alpha_p = 6$ .

Number of monomials	Number of gauss points	Dimensionless size of support domain ( $\alpha_s$ )					Exact
		2.5	3.0	3.5	4.0	4.5	
<b>3</b>	4×4	0.406926	0.407955	0.408515	0.410224	0.413500	0.4064
	5×5	0.406160	0.406663	0.406884	0.407259	0.408343	
	6×6	0.406066	0.406404	0.406538	0.406642	0.406964	
	7×7	0.406018	0.406341	0.406466	0.406493	0.406574	
	8×8	0.406004	0.406319	0.406434	0.406458	0.406514	
<b>6</b>	4×4	0.406667	0.407029	0.408037	0.408138	0.409672	
	5×5	0.406496	0.406541	0.406724	0.406888	0.407140	
	6×6	0.406461	0.406482	0.406531	0.406613	0.406739	
	7×7	0.406438	0.406456	0.406489	0.406516	0.406560	
	8×8	0.406427	0.406452	0.406472	0.406503	0.406510	
<b>10</b>	4×4	0.411965	0.407610	0.409147	0.408592	0.409139	
	5×5	0.001206	0.406740	0.406761	0.406908	0.406985	
	6×6	0.001237	0.406625	0.406581	0.406672	0.406657	
	7×7	0.285492	0.406498	0.406520	0.406550	0.406579	
	8×8	0.269857	0.406484	0.406493	0.406518	0.406546	



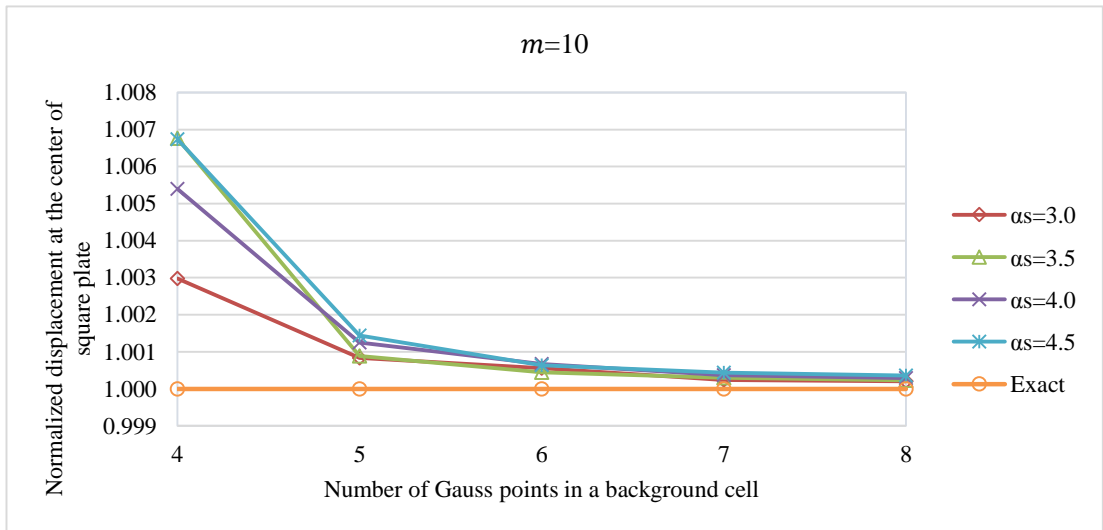
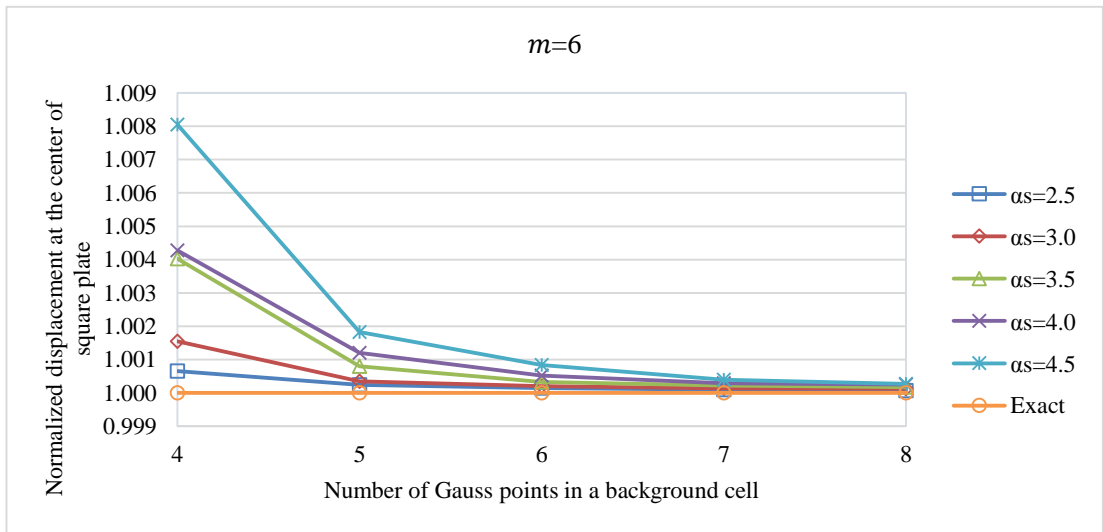
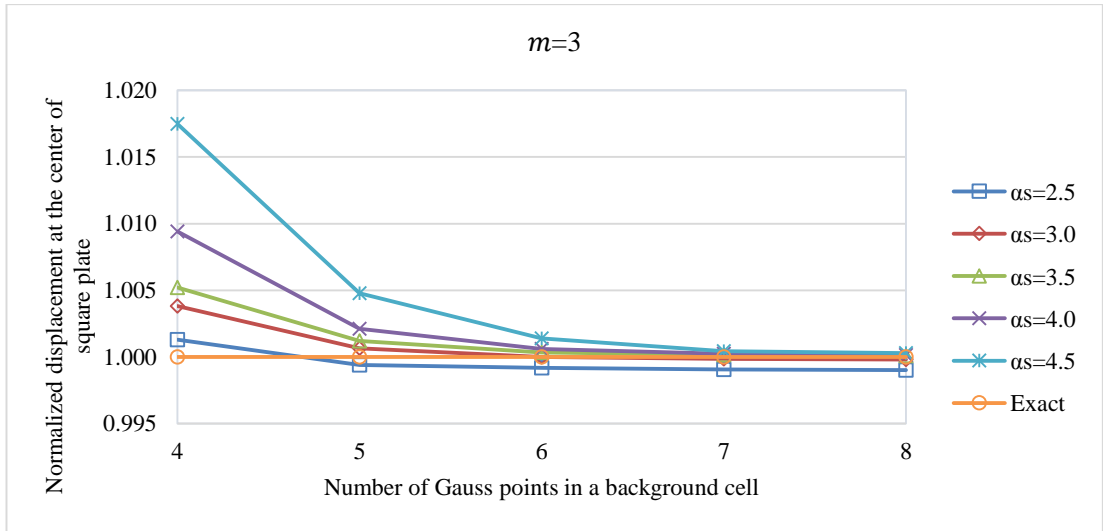


**Figure 5.23.** Variations of normalized central deflections  $w_c / \left( \frac{pL^4}{100D} \right)$  against  $n_g$  for simply supported square plate subjected to uniform load using quartic spline weight functions and irregular node distribution with  $\alpha_p = 6$ .

**Table 5.20.** Variations of normalized central moments  $M_c / \left(\frac{pL^2}{10}\right)$  of simply supported square plate subjected to uniform load using irregular node distribution using quartic spline weight function with  $\alpha_p = 6$ .

Number of monomials	Number of gauss points	Dimensionless size of support domain ( $\alpha_s$ )					Exact
		2.5	3.0	3.5	4.0	4.5	
<b>3</b>	4×4	0.500941	0.510744	0.519388	0.633194	0.772233	0.4789
	5×5	0.487774	0.498832	0.510473	0.497286	0.535530	
	6×6	0.474766	0.478865	0.479829	0.489514	0.502671	
	7×7	0.476700	0.476526	0.479432	0.478829	0.480024	
	8×8	0.477039	0.477445	0.479317	0.479033	0.479634	
<b>6</b>	4×4	0.436144	0.525295	0.191414	0.233889	0.624271	
	5×5	0.488024	0.470448	0.470466	0.502900	0.510002	
	6×6	0.448284	0.474818	0.471619	0.473901	0.478424	
	7×7	0.494882	0.479647	0.472074	0.473989	0.480477	
	8×8	0.468516	0.473432	0.473805	0.477381	0.478062	
<b>10</b>	4×4	4.252219	0.518256	0.763737	0.497792	0.758090	
	5×5	0.443840	0.455181	0.568449	0.497086	0.498329	
	6×6	0.133912	0.473568	0.436037	0.447018	0.465614	
	7×7	21.898450	0.456527	0.472774	0.487005	0.487260	
	8×8	98.188270	0.474986	0.491722	0.466110	0.469057	

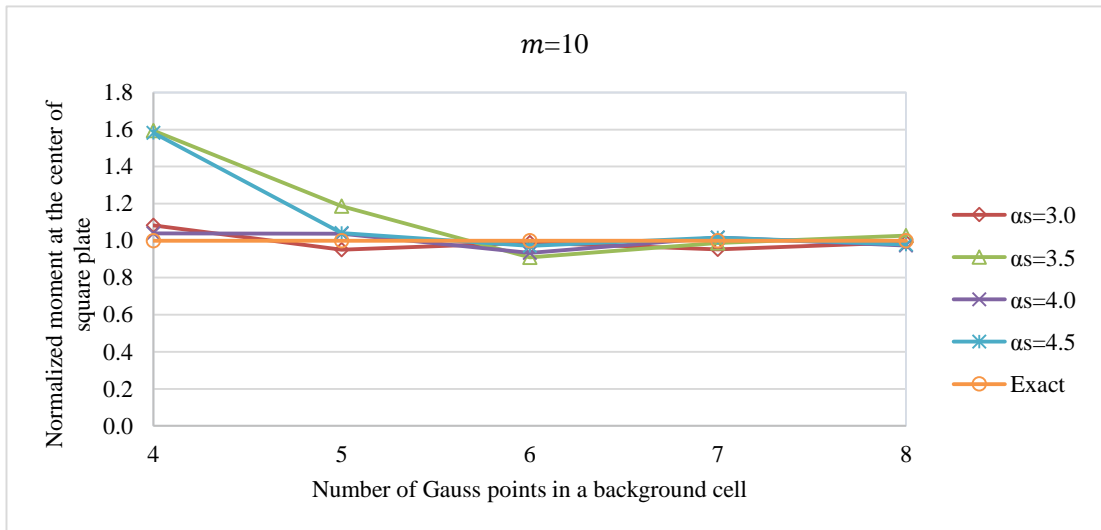
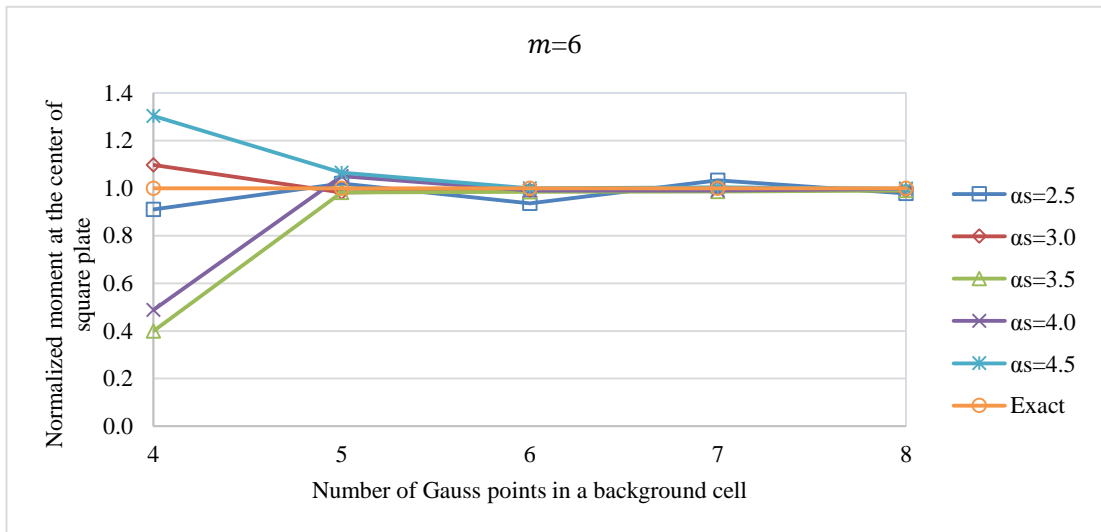
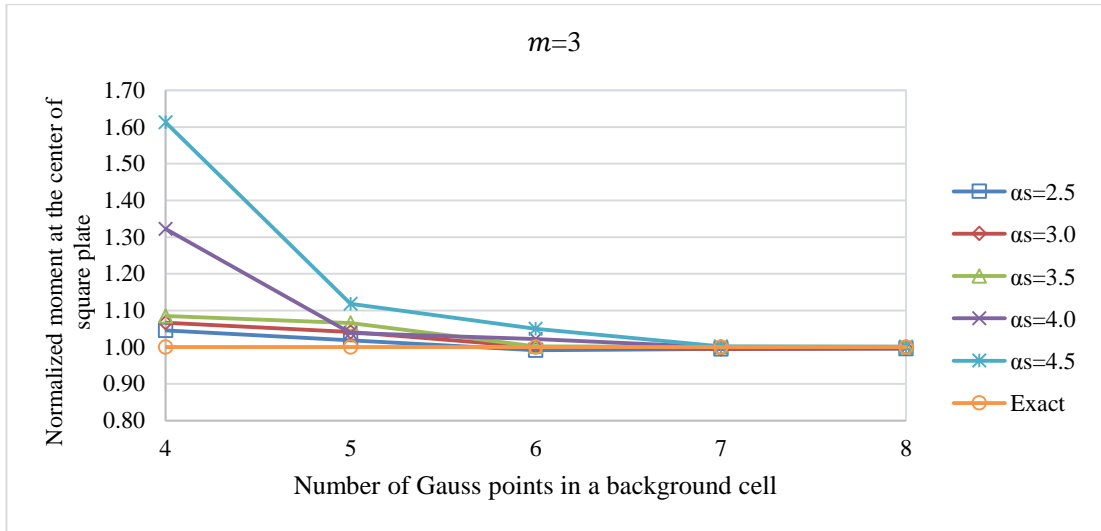


**Figure 5.24.** Variations of normalized central moments  $M_c / \left( \frac{pL^2}{10} \right)$  against  $n_g$  for simply supported square plate subjected to uniform load using quartic spline weight functions and irregular node distribution with  $\alpha_p = 6$ .

**Table 5.21.** Variations of normalized central deflections  $w_c / \left( \frac{pL^4}{100D} \right)$  of simply supported square plate subjected to uniform load using regular node distribution using quartic spline weight function with  $n_g = 5$ .

Number of monomials	Value of penalty coefficient	Dimensionless size of support domain ( $\alpha_s$ )					Exact
		2.5	3.0	3.5	4.0	4.5	
<b>3</b>	6	0.405069	0.406245	0.406169	0.406428	0.406472	0.4064
	7	0.405069	0.406245	0.406169	0.406429	0.406464	
	8	0.405069	0.406244	0.406168	0.406421	0.406425	
	9	0.405082	0.406230	0.406052	0.406420	0.406370	
	10	0.405021	0.406222	0.406125	0.406529	0.407933	
	11	0.405595	0.399518	0.402957	0.402484	0.407624	
<b>6</b>	6	0.406432	0.406439	0.406658	0.406555	0.406716	
	7	0.406432	0.406438	0.406656	0.406553	0.406716	
	8	0.406425	0.406438	0.406650	0.406559	0.407218	
	9	0.406454	0.406518	0.406438	0.407196	0.406922	
	10	0.407387	0.406121	0.410978	0.407688	0.406072	
	11	0.420549	0.350452	0.394587	0.139971	0.378275	
<b>10</b>	6	0.000090	0.406461	0.406651	0.406782	0.406989	
	7	0.003644	0.406462	0.406647	0.406784	0.406983	
	8	0.001025	0.406462	0.406663	0.406782	0.406988	
	9	0.000149	0.406575	0.416249	0.406858	0.405604	
	10	0.000565	0.406438	0.404399	0.406543	0.407764	
	11	0.010702	0.368051	0.587419	0.417085	0.439110	

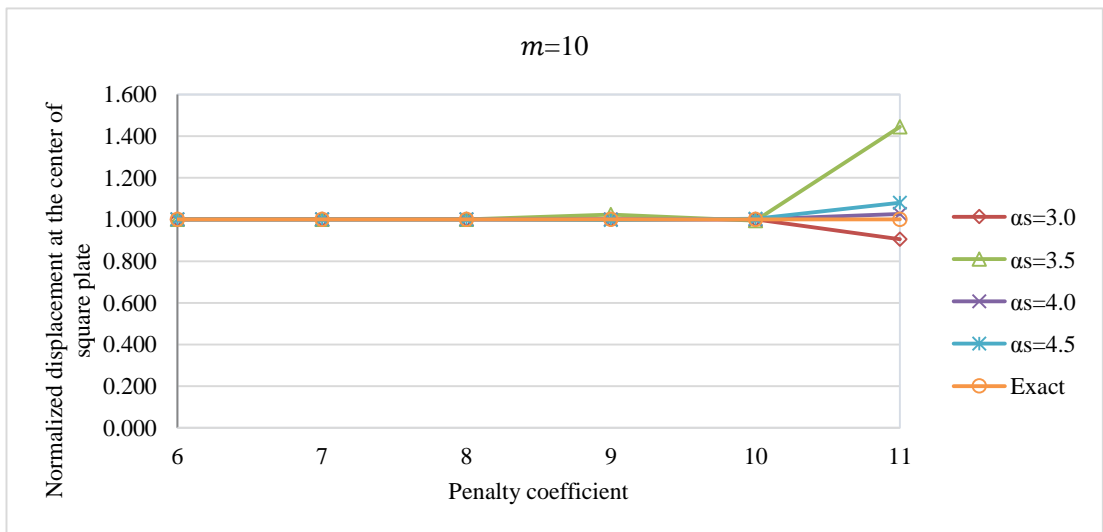
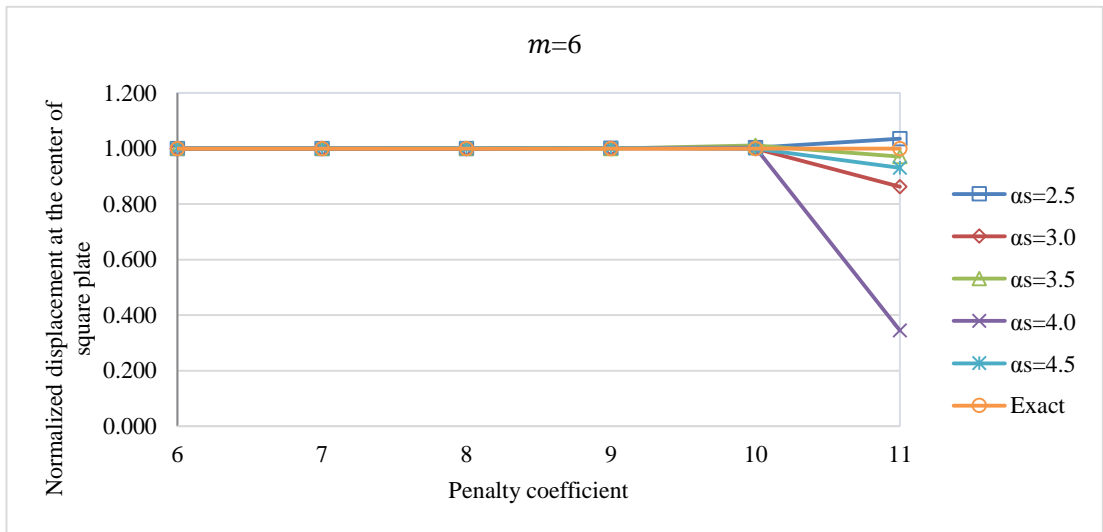
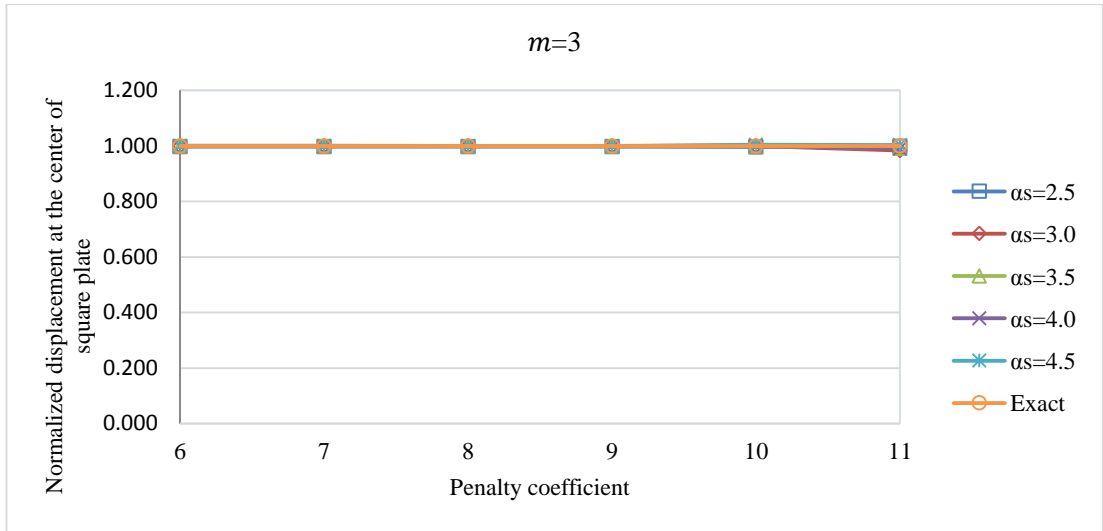


**Figure 5.25.** Variations of normalized central deflections  $w_c / \left( \frac{pL^4}{100D} \right)$  against  $\alpha_p$  for simply supported square plate subjected to uniform load using quartic spline weight functions and regular node distribution with  $n_g = 5$ .

**Table 5.22.** Variations of normalized central moments  $M_c / \left( \frac{pL^2}{10} \right)$  of simply supported square plate subjected to uniform load using regular node distribution using quartic spline weight function with  $n_g = 5$ .

Number of monomials	Value of penalty coefficient	Dimensionless size of support domain ( $\alpha_s$ )					Exact
		2.5	3.0	3.5	4.0	4.5	
<b>3</b>	6	0.474406	0.475655	0.477373	0.478328	0.479166	0.4789
	7	0.474406	0.475654	0.477363	0.478215	0.478602	
	8	0.474404	0.475604	0.477390	0.478737	0.476812	
	9	0.474435	0.475605	0.506951	0.478845	0.476696	
	10	0.474279	0.476157	0.477331	0.479676	0.462304	
	11	0.469205	0.497267	0.440079	0.442223	0.522211	
<b>6</b>	6	0.476007	0.474167	0.479295	0.476484	0.478854	
	7	0.476008	0.474170	0.479186	0.476505	0.478825	
	8	0.475991	0.474140	0.478270	0.476312	0.569628	
	9	0.475796	0.473611	0.465516	0.505158	0.478359	
	10	0.478325	0.465400	0.811708	0.732157	0.474307	
	11	0.495293	0.994706	4.080440	15.008180	1.097208	
<b>10</b>	6	-0.010357	0.476495	0.481383	0.490768	0.495233	
	7	0.129741	0.476508	0.480983	0.490931	0.494938	
	8	0.014068	0.476452	0.483248	0.491120	0.495976	
	9	0.032385	0.476181	2.337011	0.493356	0.504126	
	10	0.024393	0.477495	0.335882	0.542988	0.559046	
	11	-0.207908	0.545043	19.189340	1.045473	3.320348	

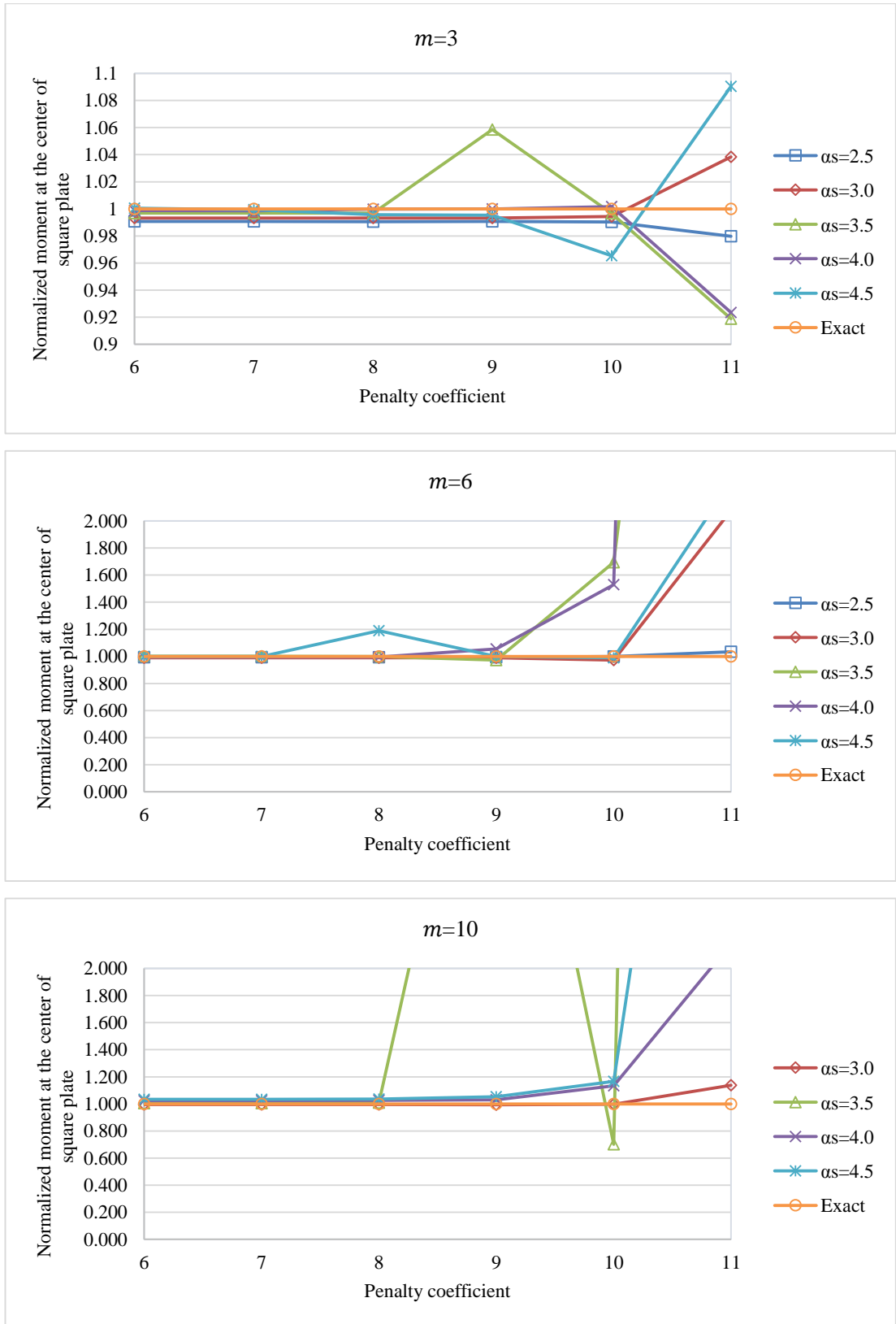


**Figure 5.26.** Variations of normalized central moments  $M_c / \left( \frac{pL^2}{10} \right)$  against  $\alpha_p$  for simply supported square plate subjected to uniform load using quartic spline weight functions and regular node distribution with  $n_g = 5$ .

**Table 5.23.** Variations of normalized central deflections  $w_c / \left( \frac{pL^4}{100D} \right)$  of simply supported square plate subjected to uniform load using irregular node distribution using quartic spline weight function with  $n_g = 5$ .

Number of monomials	Value of penalty coefficient	Dimensionless size of support domain ( $\alpha_s$ )					Exact
		2.5	3.0	3.5	4.0	4.5	
<b>3</b>	6	0.406160	0.406663	0.406884	0.407259	0.408340	0.4064
	7	0.406160	0.406663	0.406884	0.407259	0.408367	
	8	0.406154	0.406661	0.406878	0.407271	0.408532	
	9	0.406140	0.406653	0.407263	0.407275	0.408434	
	10	0.406406	0.407082	0.403233	0.406768	0.408135	
	11	0.410263	0.390615	0.397850	0.408035	0.376149	
<b>6</b>	6	0.406496	0.406541	0.406724	0.406887	0.407140	
	7	0.406496	0.406541	0.406723	0.406889	0.407141	
	8	0.406493	0.406552	0.406715	0.406859	0.407144	
	9	0.406589	0.406340	0.406732	0.406868	0.412941	
	10	0.405775	0.405738	0.406930	0.406493	0.401575	
	11	0.410250	0.797125	0.418938	0.158991	0.372854	
<b>10</b>	6	0.000164	0.406740	0.406761	0.406908	0.406984	
	7	0.000027	0.406743	0.406758	0.406903	0.406982	
	8	0.002892	0.406701	0.406772	0.406917	0.406967	
	9	0.000824	0.406369	0.406219	0.406655	0.406810	
	10	0.001105	0.399881	0.402341	0.401290	0.392903	
	11	0.000832	0.408988	2.046256	0.386997	1.485735	



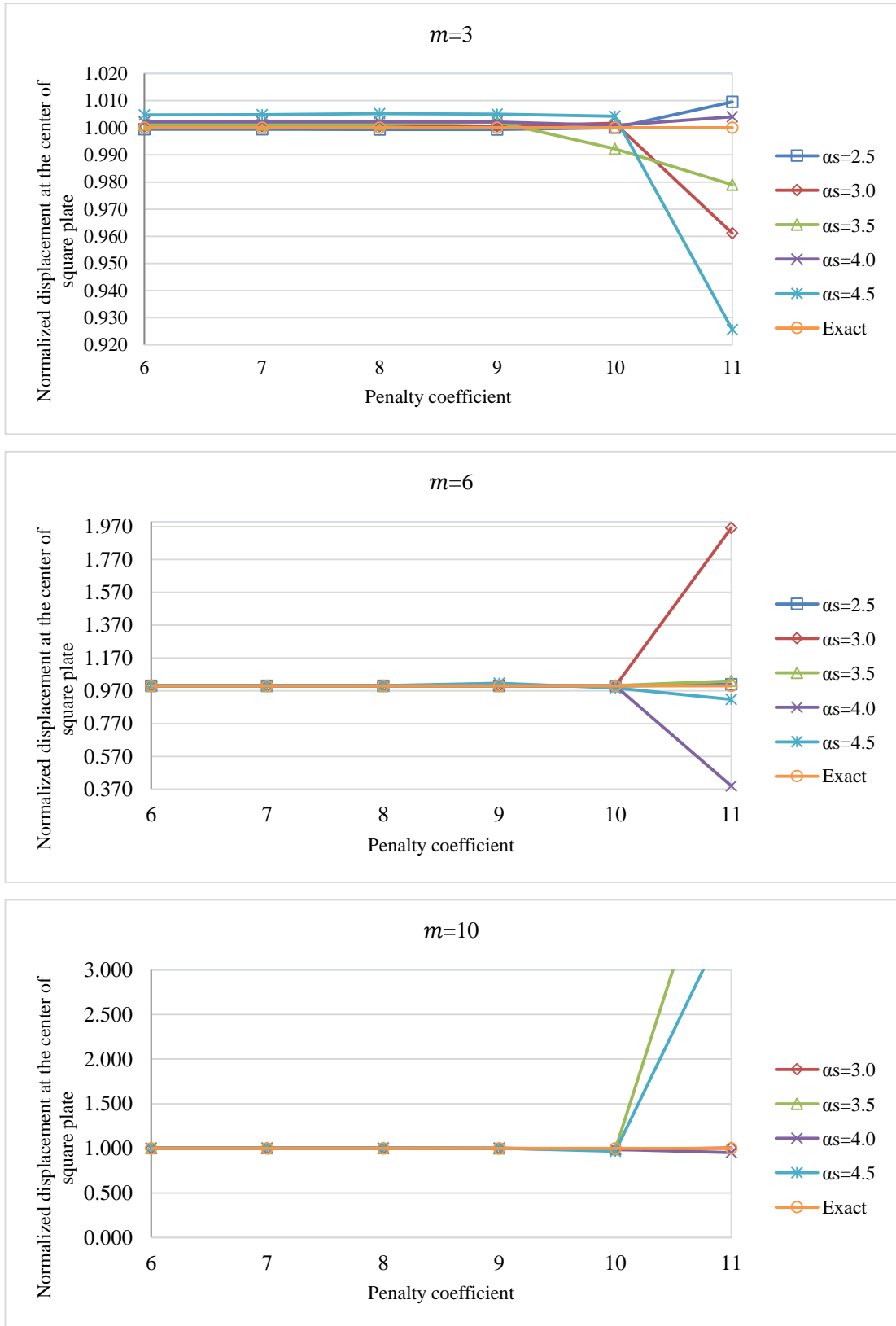


**Figure 5.27.** Variations of normalized central deflections  $w_c / \left( \frac{pL^4}{100D} \right)$  against  $\alpha_p$  for simply supported square plate subjected to uniform load using quartic spline weight functions and irregular node distribution with  $n_g = 5$ .

**Table 5.24.** Variations of normalized central moments  $M_c / \left( \frac{pL^2}{10} \right)$  of simply supported square plate subjected to uniform load using irregular node distribution using quartic spline weight function with  $n_g = 5$ .

Number of monomials	Value of penalty coefficient	Dimensionless size of support domain ( $\alpha_s$ )					Exact
		2.5	3.0	3.5	4.0	4.5	
<b>3</b>	6	0.487777	0.498836	0.510496	0.497278	0.535784	0.4789
	7	0.487719	0.498959	0.510468	0.497331	0.539101	
	8	0.487386	0.498971	0.512029	0.495936	0.521160	
	9	0.480718	0.485348	0.632008	0.512237	0.563054	
	10	0.463171	0.099233	0.834846	0.128121	0.390597	
	11	1.609723	0.006072	0.224897	0.268324	0.592333	
<b>6</b>	6	0.488044	0.470402	0.470146	0.502782	0.509977	
	7	0.488293	0.470451	0.469549	0.503575	0.509719	
	8	0.488077	0.471394	0.481768	0.494887	0.518118	
	9	0.484345	0.454101	0.480443	0.453891	0.176384	
	10	0.450247	0.543436	0.007022	0.428636	1.516732	
	11	0.555949	0.994598	3.813639	2.254813	2.125904	
<b>10</b>	6	-0.028252	0.454212	0.568492	0.495713	0.498427	
	7	-0.104334	0.453278	0.574682	0.492612	0.505043	
	8	-0.048502	0.447237	0.514597	0.491597	0.539705	
	9	0.555588	0.125224	1.352816	0.779891	0.381794	
	10	0.443912	1.683166	11.354310	0.856711	5.488006	
	11	1.133775	7.702520	5346.3000	64.356670	86.438590	

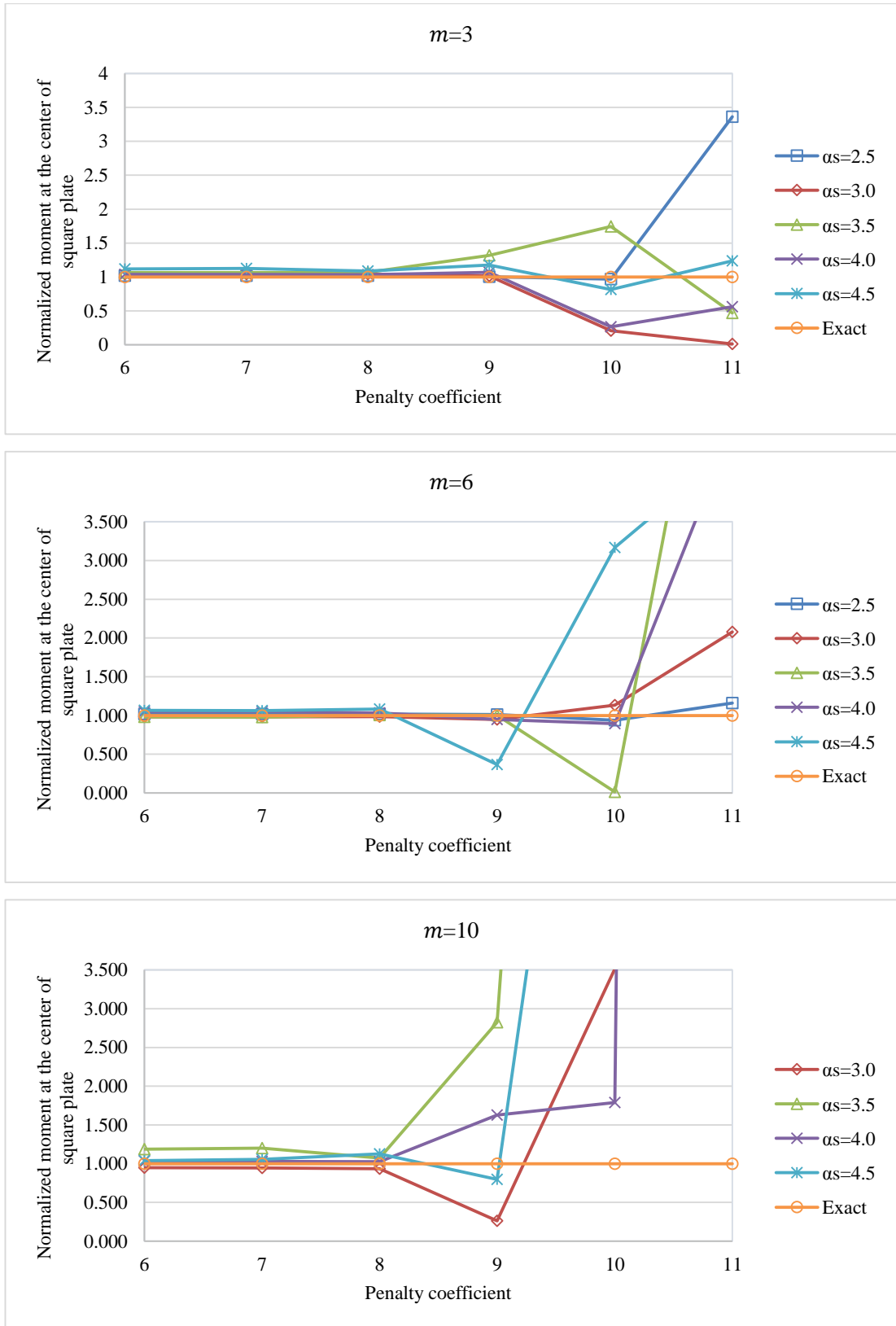


**Figure 5.28.** Variations of normalized central moments  $M_c/\left(\frac{pL^2}{10}\right)$  against  $\alpha_p$  for simply supported square plate subjected to uniform load using quartic spline weight functions and irregular node distribution with  $n_g = 5$ .

#### 5.4 Clamped circular plate under uniform load

A clamped circular plate is subjected to uniform transverse load as shown in Fig. 5.29. The thickness, radius, Young's modulus and Poisson's ratio of the problem are  $h = 1$ ,  $R = 5$ ,  $10.92$  and  $\nu = 0.3$ , respectively. Due to the symmetry, one quarter of the circular plate is modelled. In the models of quarter circular plate, 817 field nodes and 768 background cells were used for regular and irregular node distributions. The value of applied uniform transverse load  $P$  is  $1 \text{ Pa}$ . The normalized deflection and normalized moment values for the use of cubic spline weight function are provided from Table 5.25 to Table 5.32. Also, the utilization of quartic spline weight function is presented from Table 5.33 to Table 5.40.

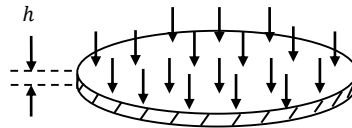


**Figure 5.29.** Clamped circular plate under uniform load.

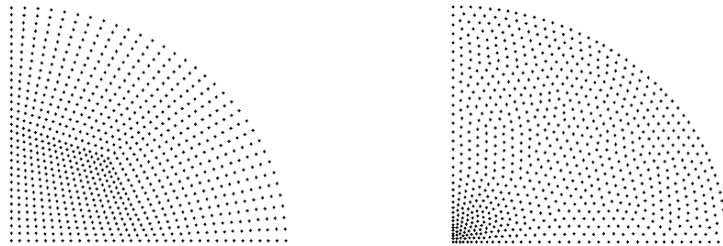


**Figure 5.30.** The EFGM models for **a)** regular node distributions, **b)** irregular node distributions

Fig. 5.31 to Fig. 5.46 are used to depict the results of displacements and moments. The survey of results show that displacements and moments do not exhibit any fluctuations, except the moment values obtained using  $\alpha_p = 1 \times 10^{10}$  for regular node distribution, shown in Fig. 5.36 and Fig.5.44. Also, it is shown that the accuracy of  $\alpha_s = 3$  is higher than the other values of  $\alpha_s$ . The variations of displacements/moments against number of gauss points in a background cell are small so the variations can be neglected and any values between 4 and 8 can be used for number of gauss points in a background cell. The number of gauss points in a background cell is selected as 5 to increase the accuracy of the results.

**Table 5.25.** Normalized central deflections  $w_c / \left( \frac{pL^4}{100D} \right)$  of clamped circular plate subjected to uniform load for regular node distribution using cubic spline weight function with  $\alpha_p = 6$ .

Number of monomials	Number of gauss points	Dimensionless size of support domain ( $\alpha_s$ )					Exact
		2.5	3.0	3.5	4.0	4.5	
<b>3</b>	4×4	0.184962	0.185032	0.185283	0.185462	0.185478	0.184821
	5×5	0.184963	0.185033	0.185283	0.185453	0.185486	
	6×6	0.184963	0.185033	0.185288	0.185460	0.185478	
	7×7	0.184963	0.185033	0.185281	0.185460	0.185483	
	8×8	0.184962	0.185032	0.185285	0.185459	0.185524	
<b>6</b>	4×4	0.184969	0.184976	0.185094	0.185484	0.185553	
	5×5	0.184968	0.184976	0.185087	0.185487	0.185551	
	6×6	0.184969	0.184976	0.185092	0.185485	0.185555	
	7×7	0.184969	0.184976	0.185089	0.185485	0.185550	
	8×8	0.184968	0.184975	0.185089	0.185484	0.185552	
<b>10</b>	4×4	0.014055	0.171670	0.185078	0.185561	0.185747	
	5×5	0.012204	0.016623	0.185084	0.185548	0.185726	
	6×6	0.014806	0.033808	0.185075	0.185549	0.185731	
	7×7	0.000114	0.016053	0.185079	0.185550	0.185729	
	8×8	0.001214	0.817412	0.185076	0.185549	0.185726	

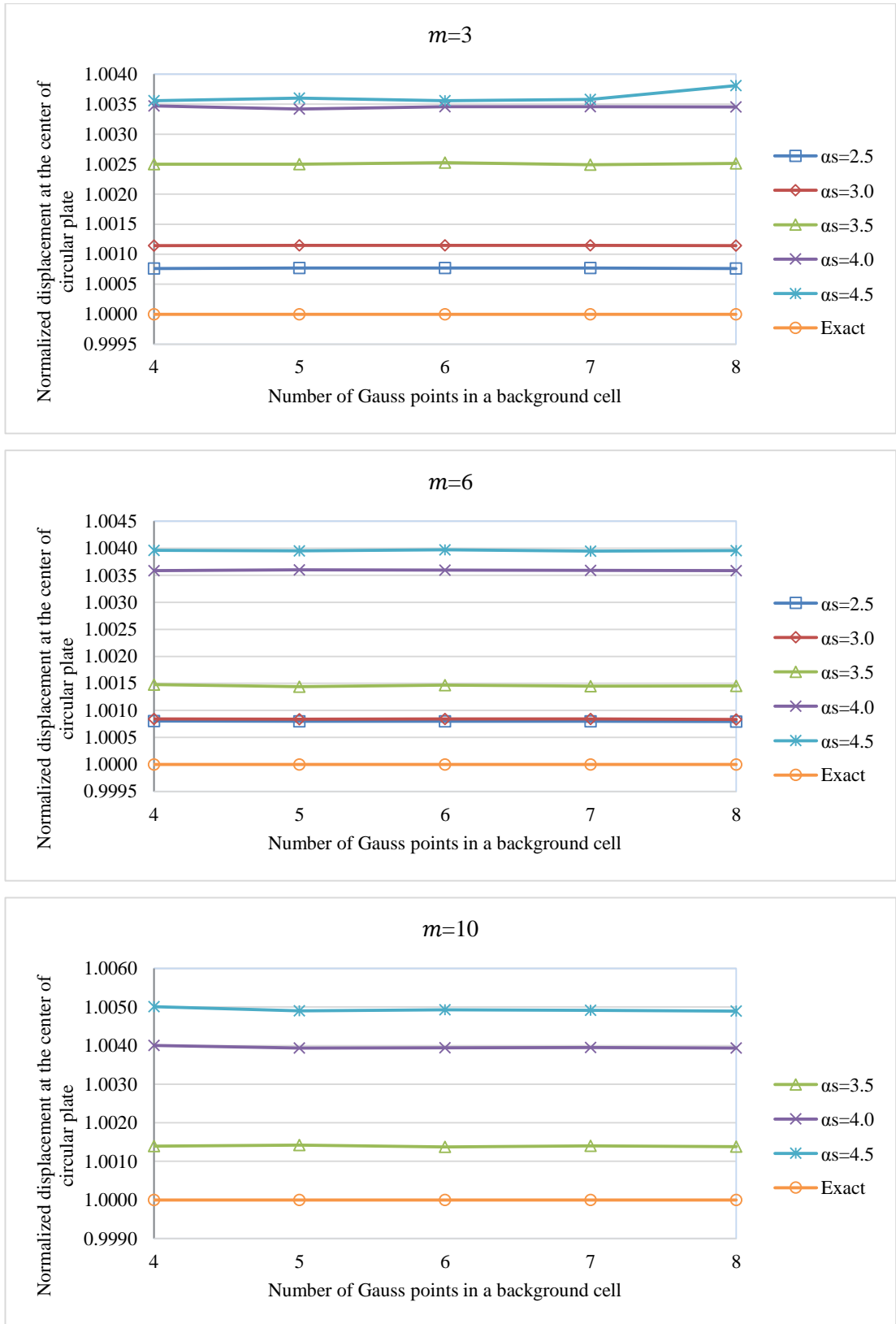


**Figure 5.31.** Variations of normalized central deflections  $w_c / \left( \frac{pL^4}{100D} \right)$  against  $n_g$  for clamped circular plate subjected to uniform load using cubic spline weight functions and regular node distribution with  $\alpha_p = 6$ .

**Table 5.26.** Normalized central moments  $M_c / \left( \frac{pL^2}{10} \right)$  of clamped circular plate subjected to uniform load for regular node distribution using cubic spline weight function with  $\alpha_p = 6$ .

Number of monomials	Number of gauss points	Dimensionless size of support domain ( $\alpha_s$ )					Exact
		2.5	3.0	3.5	4.0	4.5	
<b>3</b>	4×4	0.803680	0.806758	0.830426	0.846829	0.835969	0.812520
	5×5	0.803677	0.806782	0.830392	0.847048	0.836797	
	6×6	0.803752	0.806785	0.830788	0.847678	0.836002	
	7×7	0.803742	0.806785	0.830156	0.847701	0.836552	
	8×8	0.803733	0.806755	0.830739	0.847640	0.837486	
<b>6</b>	4×4	0.808700	0.796474	0.793807	0.883111	0.909413	
	5×5	0.806172	0.796241	0.792974	0.884294	0.915492	
	6×6	0.807652	0.796330	0.793558	0.883861	0.913206	
	7×7	0.806739	0.796369	0.793311	0.883997	0.913641	
	8×8	0.807389	0.796252	0.793320	0.884050	0.913174	
<b>10</b>	4×4	96.711680	397.45560	0.754975	0.962686	1.003314	
	5×5	159.87640	113.93760	0.749735	0.956152	0.984276	
	6×6	231.55416	68.746000	0.751476	0.955871	0.993536	
	7×7	40.369640	26.492380	0.750867	0.957365	0.986871	
	8×8	3.2632990	1643.1324	0.751800	0.957184	0.988544	

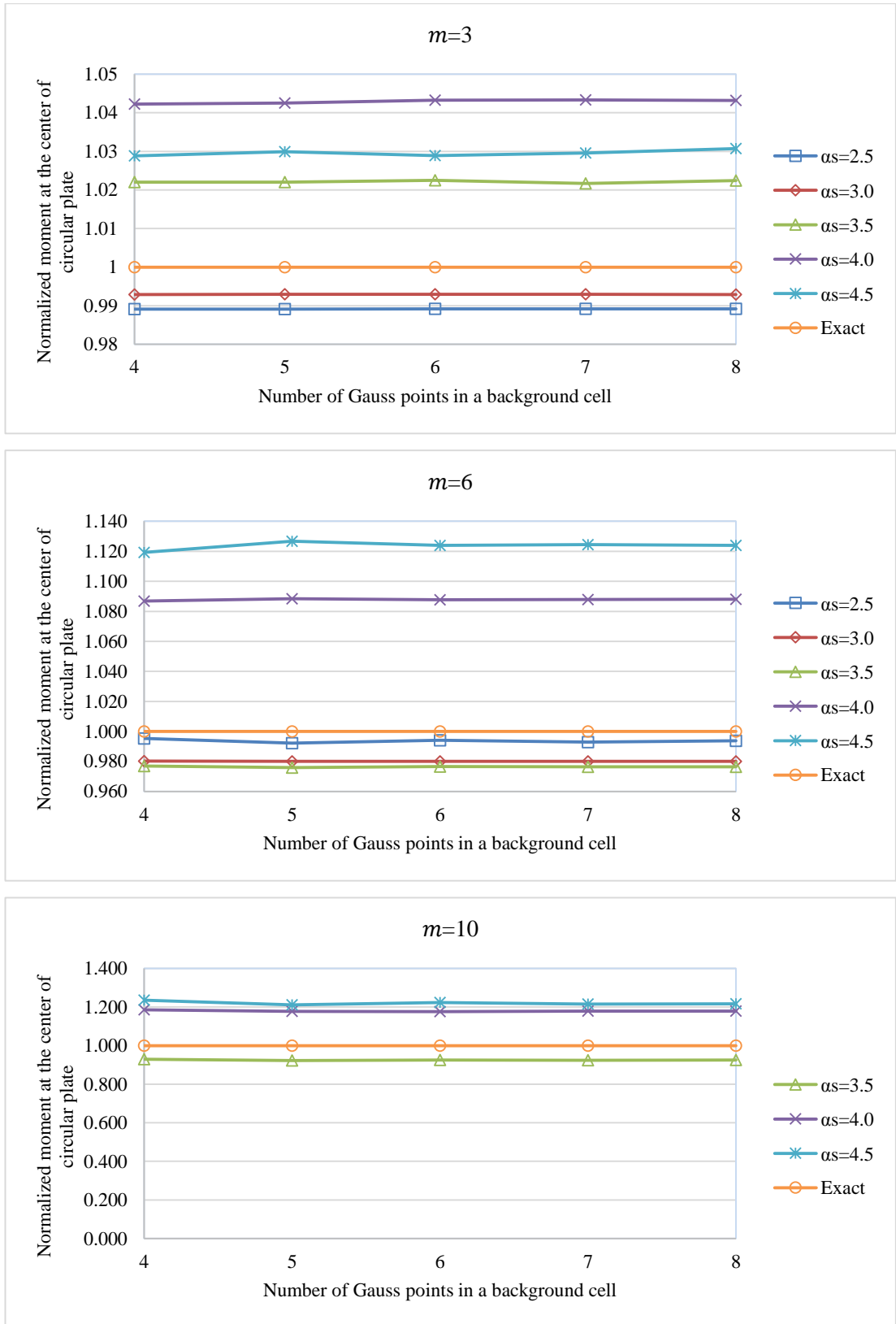


**Figure 5.32.** Variations of normalized central moments  $M_c / \left( \frac{pL^2}{10} \right)$  against  $n_g$  for clamped circular plate subjected to uniform load using cubic spline weight functions and regular node distribution with  $\alpha_p = 6$ .



**Table 5.27.** Normalized central deflections  $w_c / \left( \frac{pL^4}{100D} \right)$  of clamped circular plate subjected to uniform load for irregular node distribution using cubic spline weight function with  $\alpha_p = 6$ .

Number of monomials	Number of gauss points	Dimensionless size of support domain ( $\alpha_s$ )					Exact
		2.5	3.0	3.5	4.0	4.5	
<b>3</b>	4×4	0.184961	0.184999	0.185052	0.185027	0.185085	0.184821
	5×5	0.184954	0.184973	0.185003	0.185002	0.185039	
	6×6	0.184956	0.184965	0.184983	0.184990	0.185011	
	7×7	0.184955	0.184968	0.184981	0.184990	0.185013	
	8×8	0.184954	0.184964	0.184977	0.184987	0.185010	
<b>6</b>	4×4	0.184966	0.184966	0.184987	0.185008	0.185038	
	5×5	0.184963	0.184965	0.184989	0.184991	0.185006	
	6×6	0.184962	0.184965	0.184972	0.184991	0.185000	
	7×7	0.184962	0.184965	0.184972	0.184987	0.185004	
	8×8	0.184961	0.184964	0.184971	0.184988	0.185001	
<b>10</b>	4×4	0.188267	0.184985	0.184986	0.185033	0.185091	
	5×5	0.185844	0.184972	0.184982	0.185016	0.185046	
	6×6	0.185682	0.184970	0.184980	0.185013	0.185042	
	7×7	0.185487	0.184970	0.184979	0.185010	0.185035	
	8×8	0.185302	0.184968	0.184978	0.185010	0.185036	

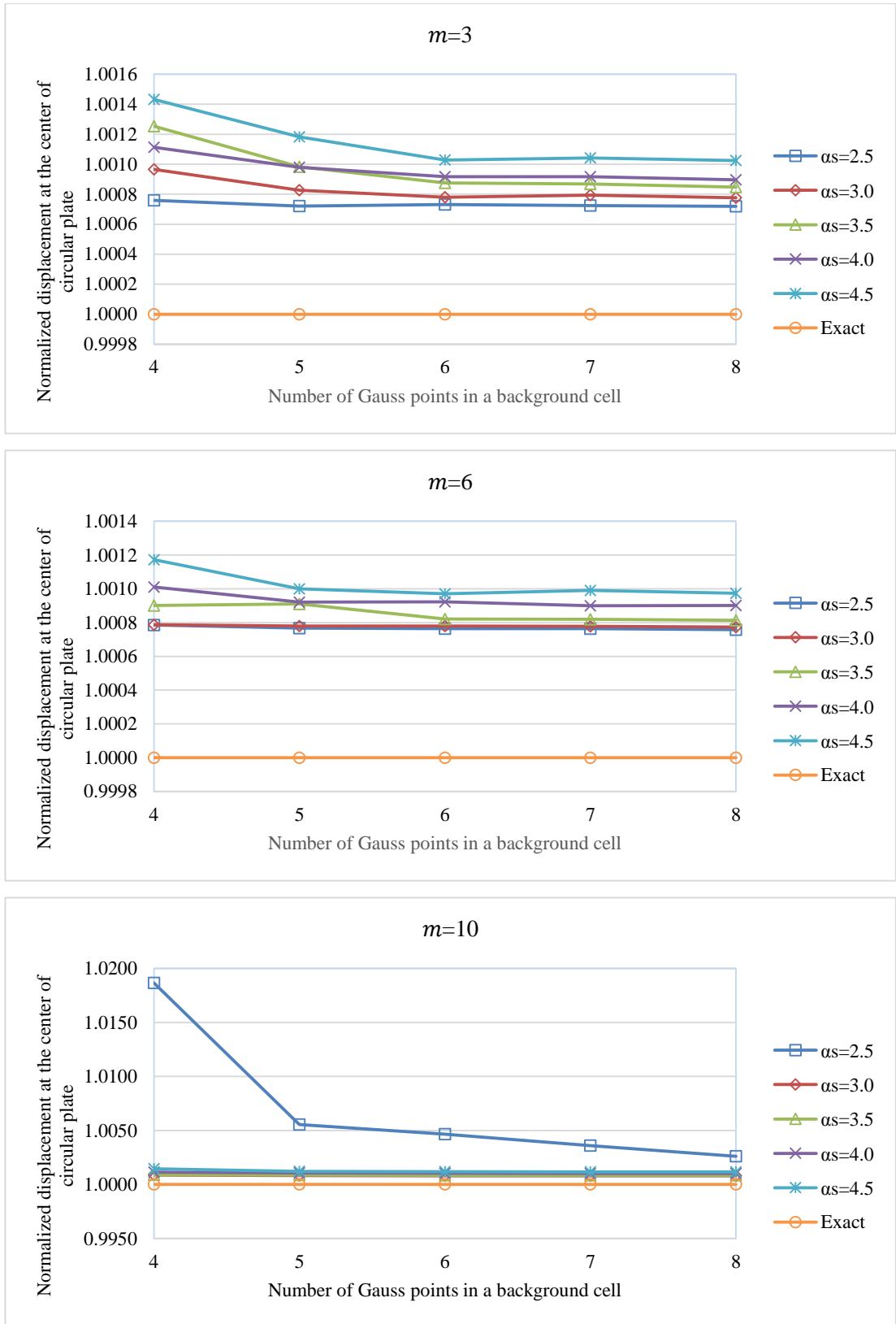


**Figure 5.33.** Variations of normalized central deflections  $w_c / \left( \frac{pL^4}{100D} \right)$  against  $n_g$  for clamped circular plate subjected to uniform load using cubic spline weight functions and irregular node distribution with  $\alpha_p = 6$ .

**Table 5.28.** Normalized central moments  $M_c / \left( \frac{pL^2}{10} \right)$  of clamped circular plate subjected to uniform load for irregular node distribution using cubic spline weight function with  $\alpha_p = 6$ .

Number of monomials	Number of gauss points	Dimensionless size of support domain ( $\alpha_s$ )					Exact
		2.5	3.0	3.5	4.0	4.5	
<b>3</b>	4×4	0.810929	0.808854	0.795776	0.805922	0.809077	0.812520
	5×5	0.808365	0.812443	0.814607	0.808698	0.810368	
	6×6	0.811051	0.809849	0.811728	0.813395	0.811228	
	7×7	0.809719	0.810609	0.810031	0.809654	0.811775	
	8×8	0.810014	0.810338	0.811581	0.811285	0.812268	
<b>6</b>	4×4	0.806641	0.811434	0.800688	0.788342	0.795006	
	5×5	0.814408	0.810984	0.812821	0.821233	0.811036	
	6×6	0.817937	0.811097	0.807876	0.813258	0.808849	
	7×7	0.819794	0.810510	0.807278	0.810308	0.809998	
	8×8	0.814991	0.810326	0.808130	0.812057	0.809152	
<b>10</b>	4×4	14.83234	0.840634	0.814480	0.762316	0.799567	
	5×5	5.042916	0.824141	0.771214	0.815158	0.826136	
	6×6	2.420183	0.809614	0.794258	0.790916	0.804838	
	7×7	1.393982	0.814234	0.787720	0.795260	0.811654	
	8×8	0.975245	0.805078	0.792068	0.794044	0.806382	

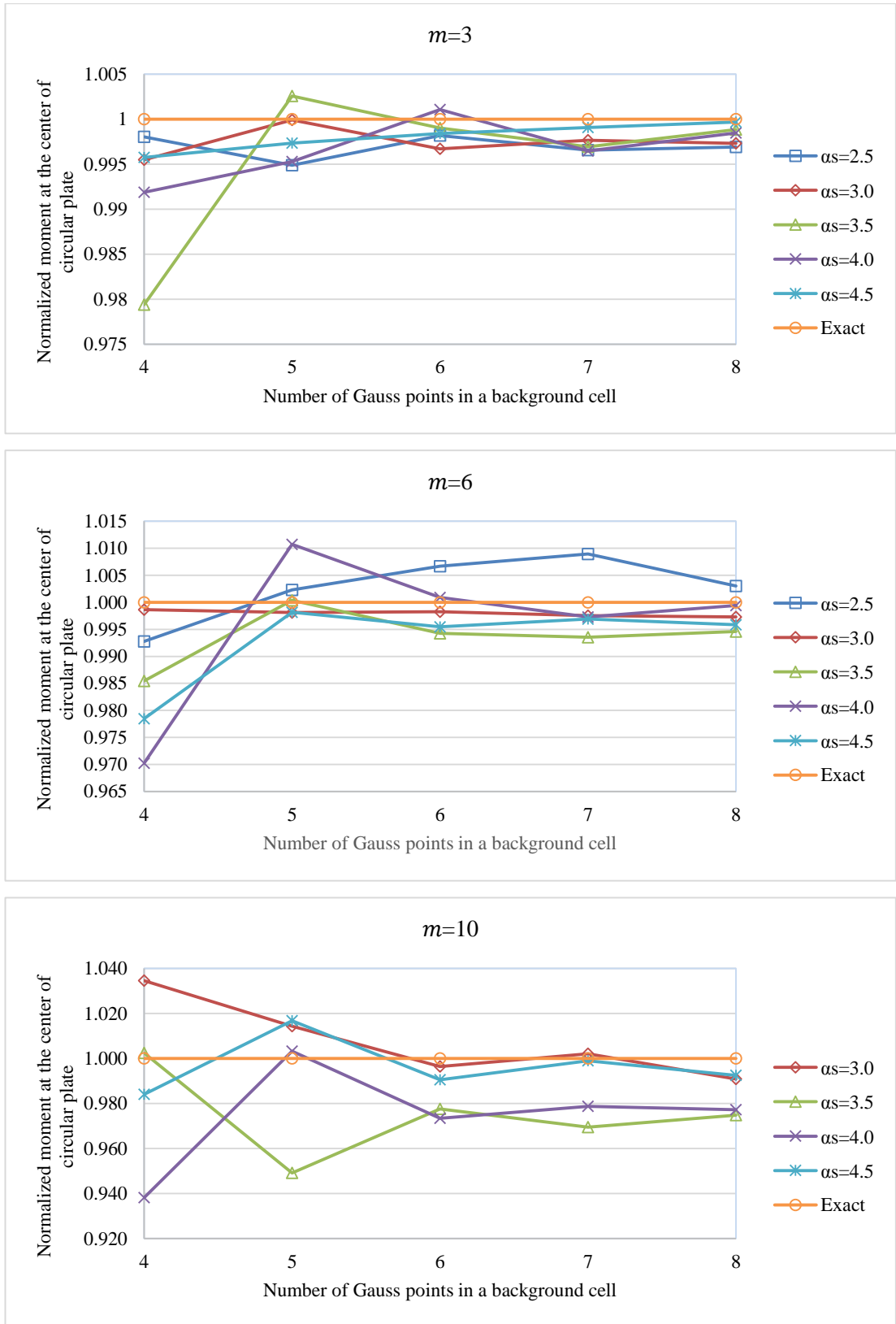


**Figure 5.34.** Variations of normalized central moments  $M_c / \left( \frac{pL^2}{10} \right)$  against  $n_g$  for clamped circular plate subjected to uniform load using cubic spline weight functions and irregular node distribution with  $\alpha_p = 6$ .

**Table 5.29.** Variations of normalized central deflections  $w_c / \left( \frac{pL^4}{100D} \right)$  of clamped circular plate subjected to uniform load using regular node distribution using cubic spline weight function with  $n_g = 5$ .

Number of monomials	Value of penalty coefficient	Dimensionless size of support domain ( $\alpha_s$ )					Exact
		2.5	3.0	3.5	4.0	4.5	
<b>3</b>	6	0.185249	0.185321	0.185573	0.185747	0.185768	0.184821
	7	0.185249	0.185321	0.185573	0.185747	0.185769	
	8	0.185249	0.185321	0.185573	0.185746	0.185770	
	9	0.185249	0.185321	0.185573	0.185811	0.185977	
	10	0.185250	0.185321	0.185590	0.185802	0.185436	
	11	0.185251	0.185323	0.185776	0.186681	0.185336	
<b>6</b>	6	0.185256	0.185264	0.185378	0.185772	0.185841	
	7	0.185256	0.185264	0.185378	0.185772	0.185841	
	8	0.185256	0.185264	0.185378	0.185772	0.185840	
	9	0.185256	0.185264	0.185378	0.185771	0.185830	
	10	0.185257	0.185264	0.185375	0.185777	0.185822	
	11	0.185259	0.185261	0.185382	0.185763	0.185288	
<b>10</b>	6	0.012204	0.016623	0.185365	0.185837	0.186014	
	7	0.293270	1.829059	0.185365	0.185837	0.186014	
	8	0.031030	0.019366	0.185365	0.185837	0.186014	
	9	0.144117	0.178680	0.185365	0.185838	0.186015	
	10	0.012006	0.150918	0.185366	0.185837	0.186021	
	11	0.000414	5.429067	0.185368	0.185763	0.186054	

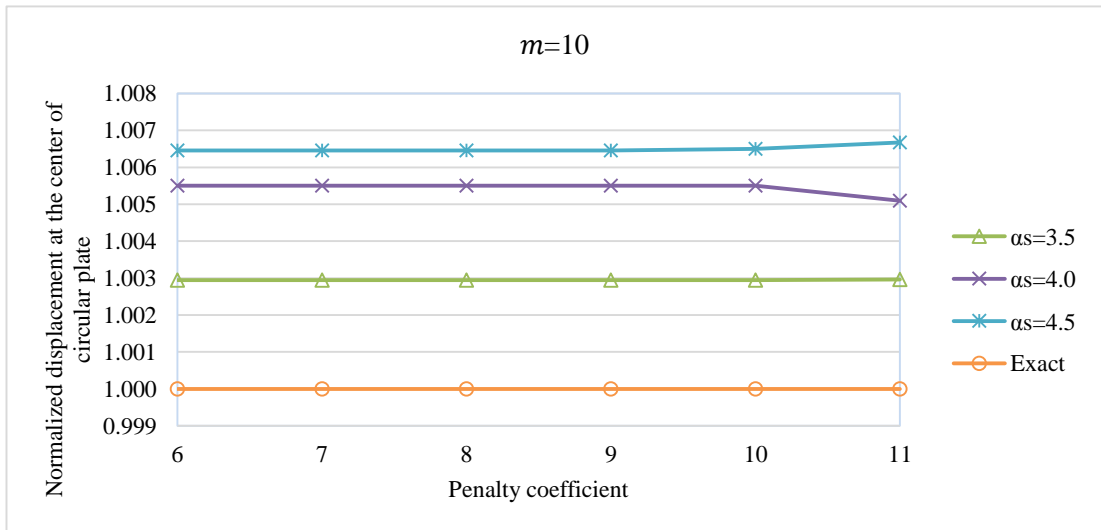
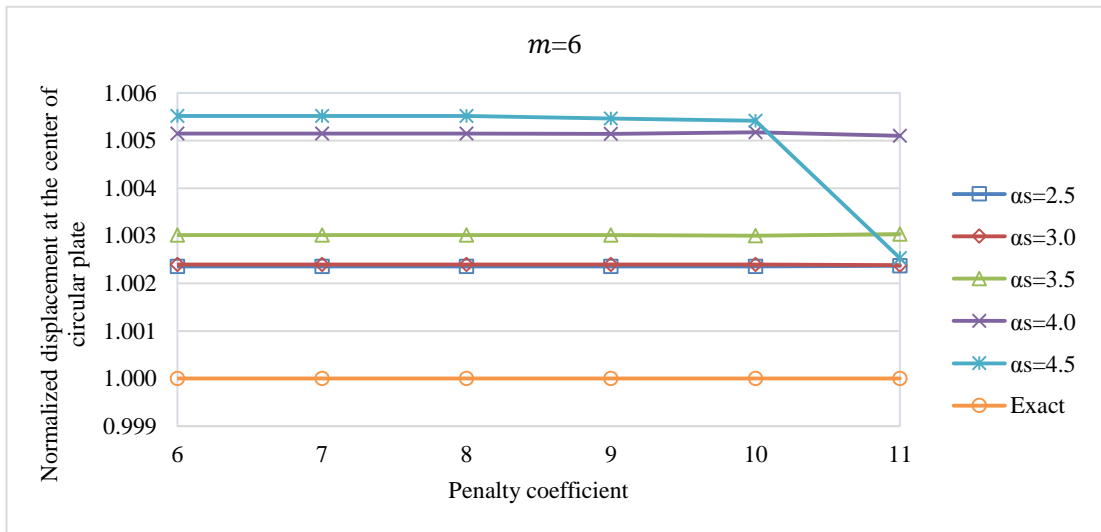
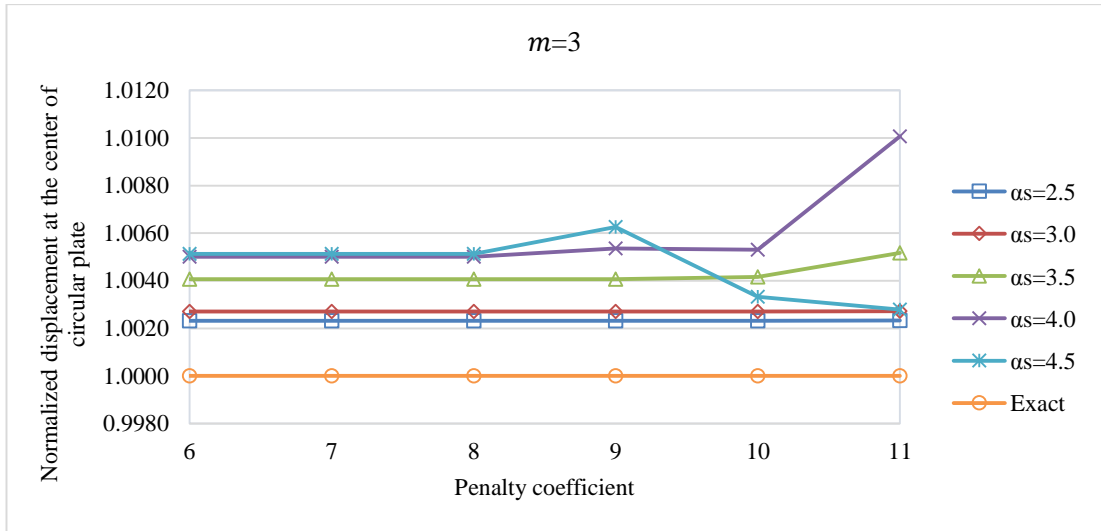


**Figure 5.35.** Variations of normalized central deflections  $w_c / \left( \frac{\rho L^4}{100D} \right)$  against  $\alpha_p$  for clamped circular plate subjected to uniform load using cubic spline weight functions and regular node distribution with  $n_g = 5$ .

**Table 5.30.** Variations of normalized central moments  $M_c / \left( \frac{pL^2}{10} \right)$  of clamped circular plate subjected to uniform load using regular node distribution using cubic spline weight function with  $n_g = 5$ .

Number of monomials	Value of penalty coefficient	Dimensionless size of support domain ( $\alpha_s$ )					Exact
		2.5	3.0	3.5	4.0	4.5	
<b>3</b>	6	0.793561	0.796388	0.825787	0.850086	0.838228	0.81252
	7	0.793562	0.796388	0.825789	0.850072	0.838263	
	8	0.793563	0.796388	0.825777	0.849728	0.838316	
	9	0.793565	0.796380	0.825856	0.857181	0.846872	
	10	0.793692	0.796490	0.826983	0.893778	0.800843	
	11	0.793583	0.795175	0.861890	0.836395	0.817878	
<b>6</b>	6	0.805522	0.792724	0.786690	0.881132	0.914100	
	7	0.805523	0.792724	0.786688	0.881133	0.914108	
	8	0.805518	0.792723	0.786698	0.881098	0.913649	
	9	0.805474	0.792770	0.786643	0.880908	0.913589	
	10	0.805580	0.792700	0.787733	0.878576	0.986539	
	11	0.807486	0.798771	0.789675	0.860875	0.568828	
<b>10</b>	6	1.013229	-0.396900	0.748127	0.954821	0.989044	
	7	-6.858128	-57.192240	0.748127	0.954814	0.989024	
	8	-0.039958	-0.658937	0.748126	0.954852	0.988741	
	9	1.337568	2.697877	0.748397	0.955136	0.990875	
	10	0.555053	0.653587	0.747854	0.949300	1.016872	
	11	0.312506	26.801572	0.733828	0.943248	0.779644	

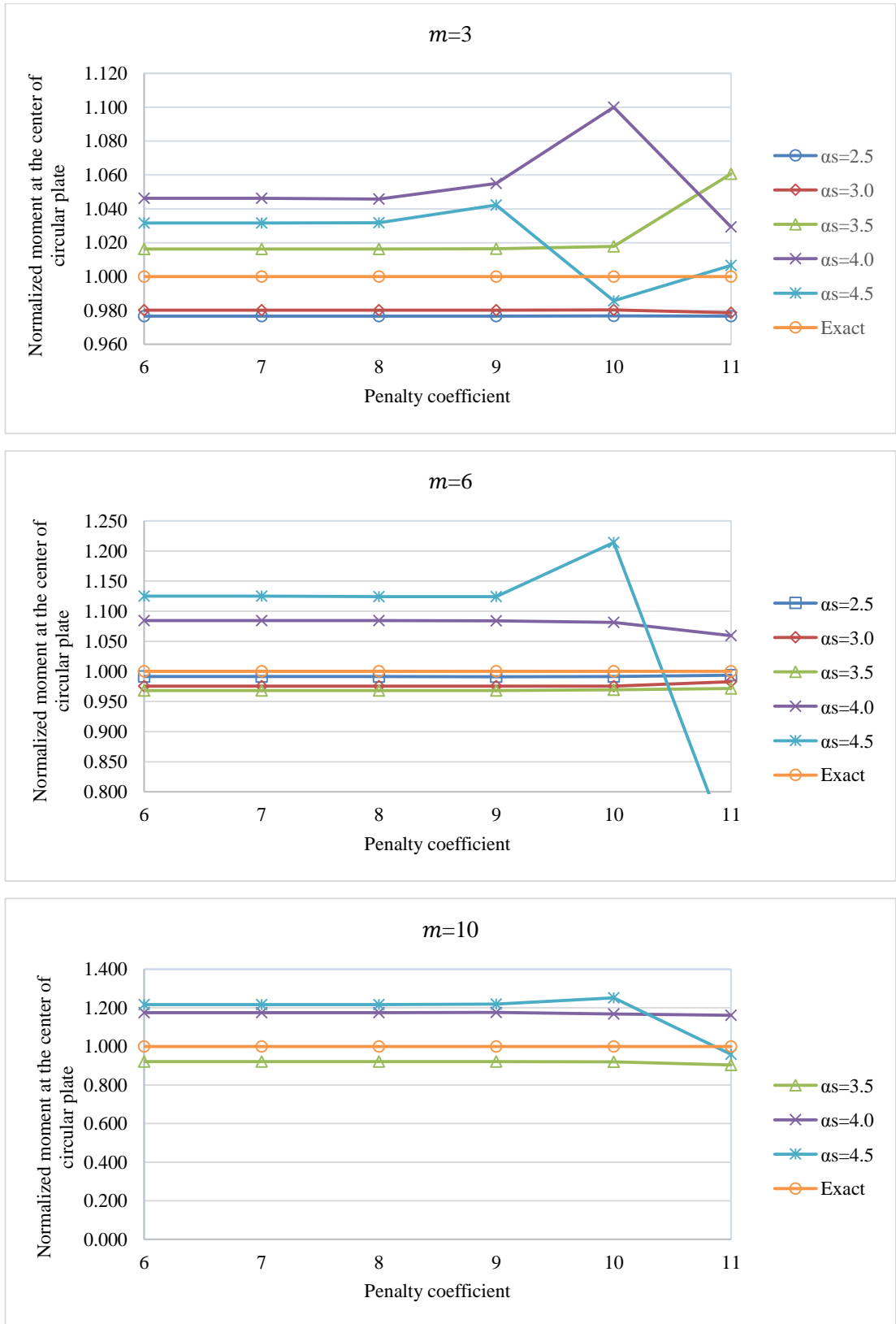


**Figure 5.36.** Variations of normalized central moments  $M_c/\left(\frac{pL^2}{10}\right)$  against  $\alpha_p$  for clamped circular plate subjected to uniform load using cubic spline weight functions and regular node distribution with  $n_g = 5$ .



**Table 5.31.** Variations of normalized central deflections  $w_c / \left( \frac{pL^4}{100D} \right)$  of clamped circular plate subjected to uniform load using irregular node distribution using cubic spline weight function with  $n_g = 5$ .

Number of monomials	Value of penalty coefficient	Dimensionless size of support domain ( $\alpha_s$ )					Exact
		2.5	3.0	3.5	4.0	4.5	
<b>3</b>	6	0.184954	0.184973	0.185003	0.184579	0.185039	0.184821
	7	0.184954	0.184973	0.185003	0.185002	0.185039	
	8	0.184954	0.184973	0.185003	0.185002	0.185039	
	9	0.184954	0.184973	0.185003	0.185002	0.185040	
	10	0.184954	0.184973	0.185002	0.185001	0.185982	
	11	0.184954	0.184974	0.185000	0.184989	0.185074	
<b>6</b>	6	0.184963	0.184965	0.184973	0.184991	0.185006	
	7	0.184963	0.184965	0.184973	0.184991	0.185006	
	8	0.184963	0.184965	0.184973	0.184991	0.185006	
	9	0.184963	0.184965	0.184973	0.184991	0.185005	
	10	0.184962	0.184965	0.184973	0.184991	0.185016	
	11	0.184965	0.184967	0.184972	0.184988	0.185195	
<b>10</b>	6	0.194294	0.184972	0.184982	0.185016	0.185046	
	7	0.194956	0.184972	0.184982	0.185016	0.185046	
	8	0.193388	0.184972	0.184982	0.185016	0.185046	
	9	0.225898	0.184972	0.184982	0.185017	0.185046	
	10	0.612754	0.184971	0.184982	0.185015	0.185044	
	11	3.991302	0.184966	0.184977	0.185007	0.185061	

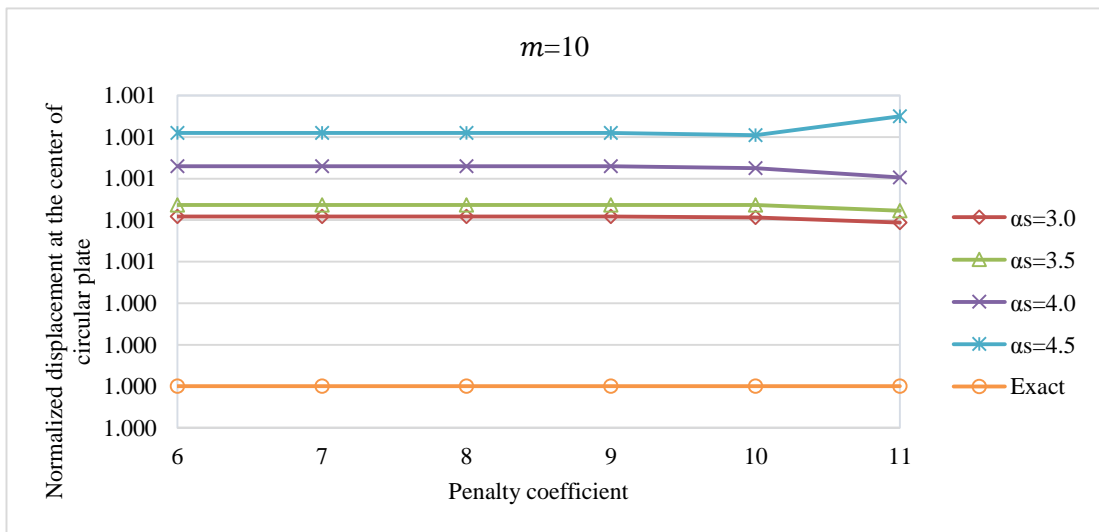
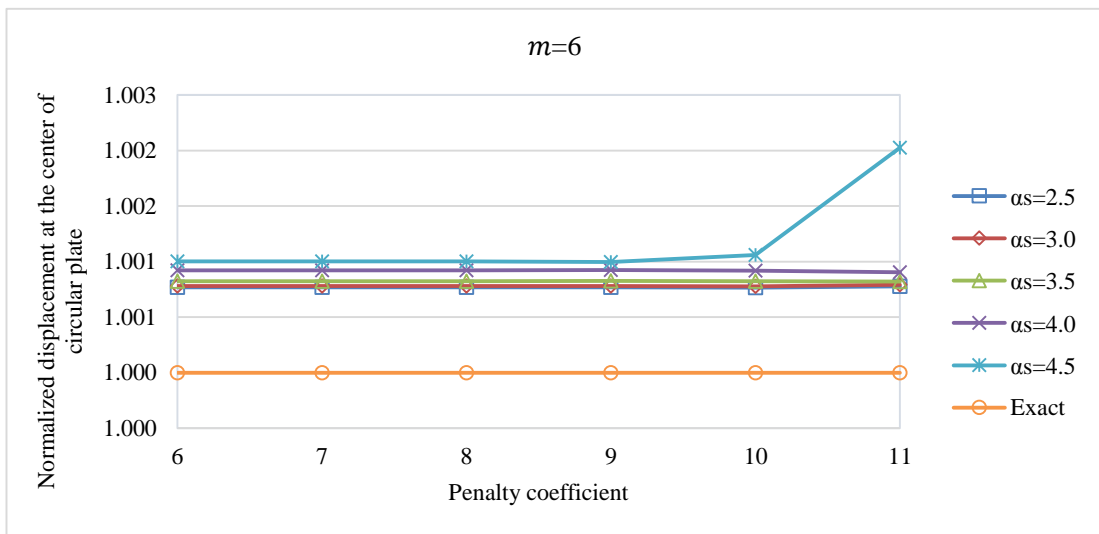
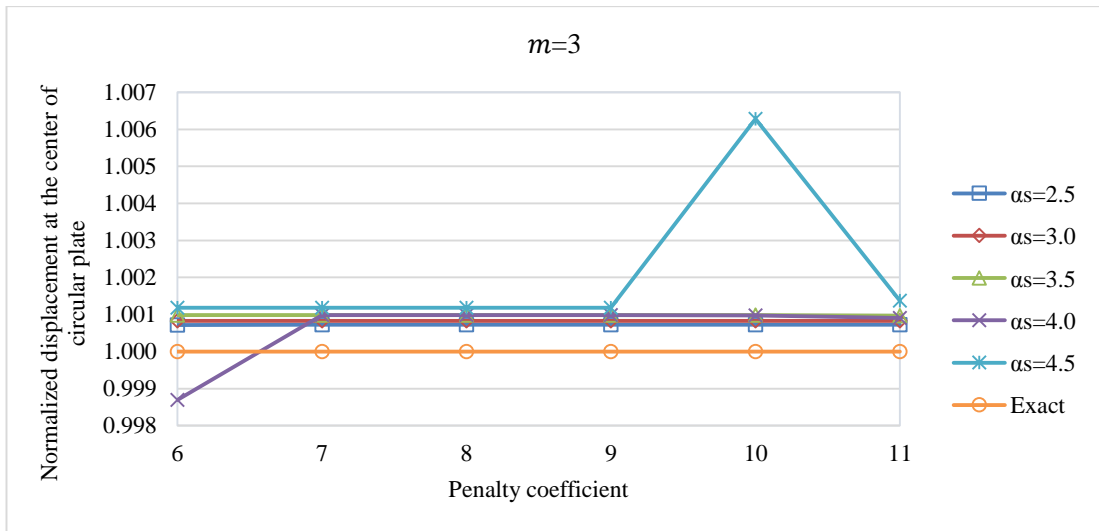


**Figure 5.37.** Variations of normalized central deflections  $w_c / \left( \frac{\rho L^4}{100D} \right)$  against  $\alpha_p$  for clamped circular plate subjected to uniform load using cubic spline weight functions and irregular node distribution with  $n_g = 5$ .

**Table 5.32.** Variations of normalized central moments  $M_c / \left( \frac{pL^2}{10} \right)$  of clamped circular plate subjected to uniform load using irregular node distribution using cubic spline weight function with  $n_g = 5$ .

Number of monomials	Value of penalty coefficient	Dimensionless size of support domain ( $\alpha_s$ )					Exact
		2.5	3.0	3.5	4.0	4.5	
<b>3</b>	6	0.806297	0.807521	0.809430	0.808711	0.810942	0.81252
	7	0.806298	0.807521	0.809431	0.808711	0.810942	
	8	0.806298	0.807531	0.809428	0.808708	0.810939	
	9	0.806256	0.807446	0.809409	0.808713	0.810897	
	10	0.806448	0.807646	0.808948	0.808606	0.808491	
	11	0.802864	0.813909	0.808067	0.812605	0.816746	
<b>6</b>	6	0.815844	0.809876	0.807320	0.810871	0.807294	
	7	0.815844	0.809876	0.807320	0.810871	0.807294	
	8	0.815848	0.809918	0.807326	0.810819	0.807301	
	9	0.816026	0.809768	0.807197	0.810514	0.807252	
	10	0.814844	0.808537	0.807092	0.809416	0.808359	
	11	0.818396	0.819513	0.804920	0.799838	0.821350	
<b>10</b>	6	-	0.805180	0.791402	0.793544	0.805440	
	7	-4.873900	0.805181	0.791399	0.793561	0.805439	
	8	-4.834712	0.805126	0.791389	0.793772	0.805431	
	9	-5.647452	0.804704	0.790996	0.793589	0.805426	
	10	-15.31885	0.803400	0.794435	0.794284	0.802448	
	11	99.782560	0.791174	0.765158	0.775530	0.805649	

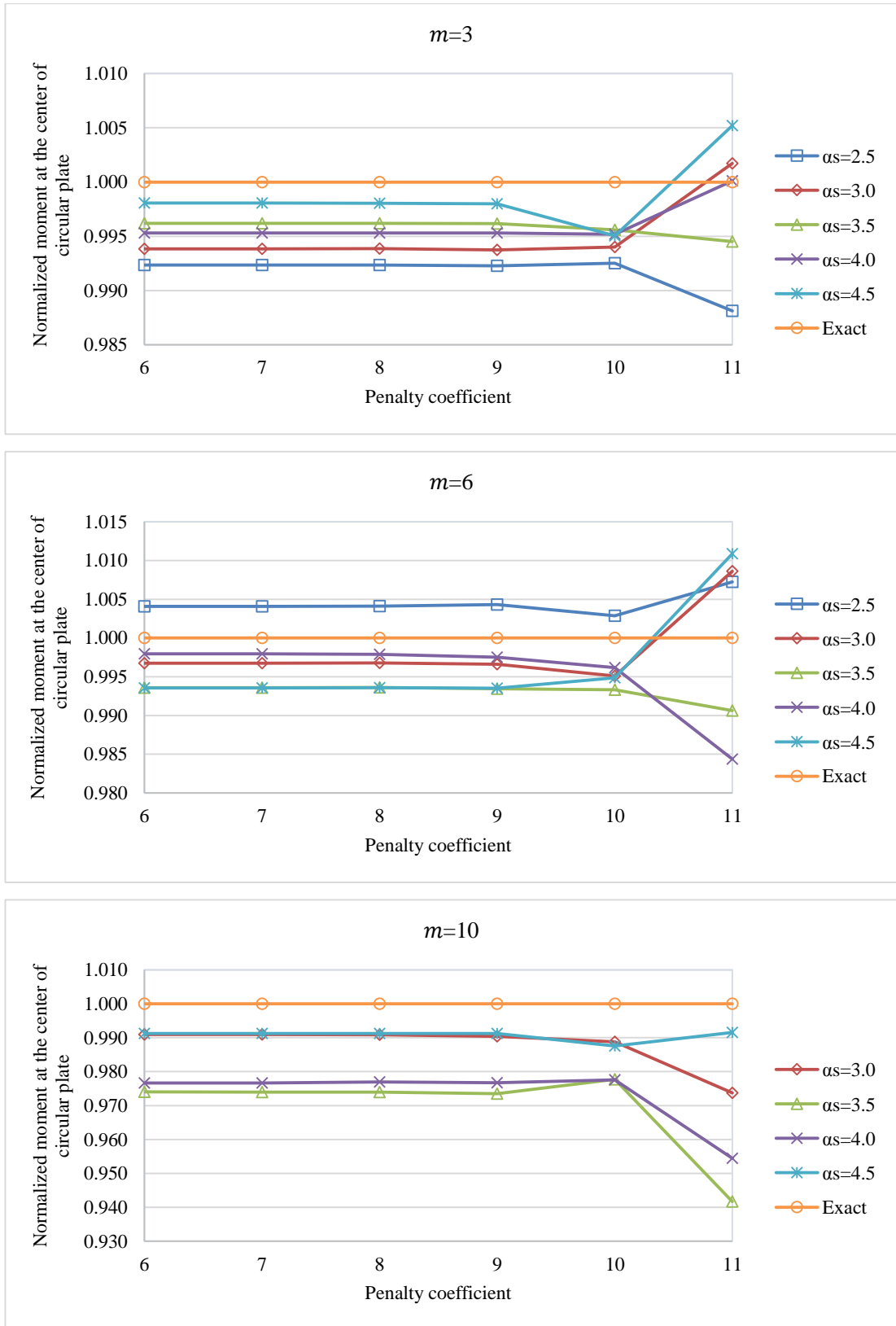


**Figure 5.38.** Variations of normalized central moments  $M_c/\left(\frac{pL^2}{10}\right)$  against  $\alpha_p$  for clamped circular plate subjected to uniform load using cubic spline weight functions and irregular node distribution with  $n_g = 5$ .

**Table 5.33.** Variations of normalized central deflections  $w_c/(pL^4/100D)$  of clamped circular plate subjected to uniform load using regular node distribution using quartic spline weight function with  $\alpha_p = 6$ .

Number of monomials	Number of gauss points	Dimensionless size of support domain ( $\alpha_s$ )					Exact
		2.5	3.0	3.5	4.0	4.5	
<b>3</b>	4×4	0.184979	0.185018	0.185092	0.185065	0.185230	0.184821
	5×5	0.184982	0.185022	0.185099	0.185065	0.185237	
	6×6	0.184980	0.185021	0.185093	0.185064	0.185236	
	7×7	0.184981	0.185021	0.185097	0.185065	0.185236	
	8×8	0.184980	0.185020	0.185094	0.185063	0.185263	
<b>6</b>	4×4	0.184968	0.185002	0.185203	0.185209	0.185281	
	5×5	0.184967	0.185002	0.185198	0.185210	0.185270	
	6×6	0.184967	0.185002	0.185202	0.185209	0.185275	
	7×7	0.184967	0.185002	0.185199	0.185210	0.185272	
	8×8	0.184966	0.185001	0.185200	0.185208	0.185272	
<b>10</b>	4×4	0.073116	3.204494	0.185167	0.185542	0.185588	
	5×5	0.587254	0.018966	0.185164	0.185533	0.185573	
	6×6	0.255416	0.881927	0.185159	0.185534	0.185575	
	7×7	0.001037	0.088467	0.185161	0.185533	0.185575	
	8×8	0.001275	0.207537	0.185159	0.185531	0.185574	

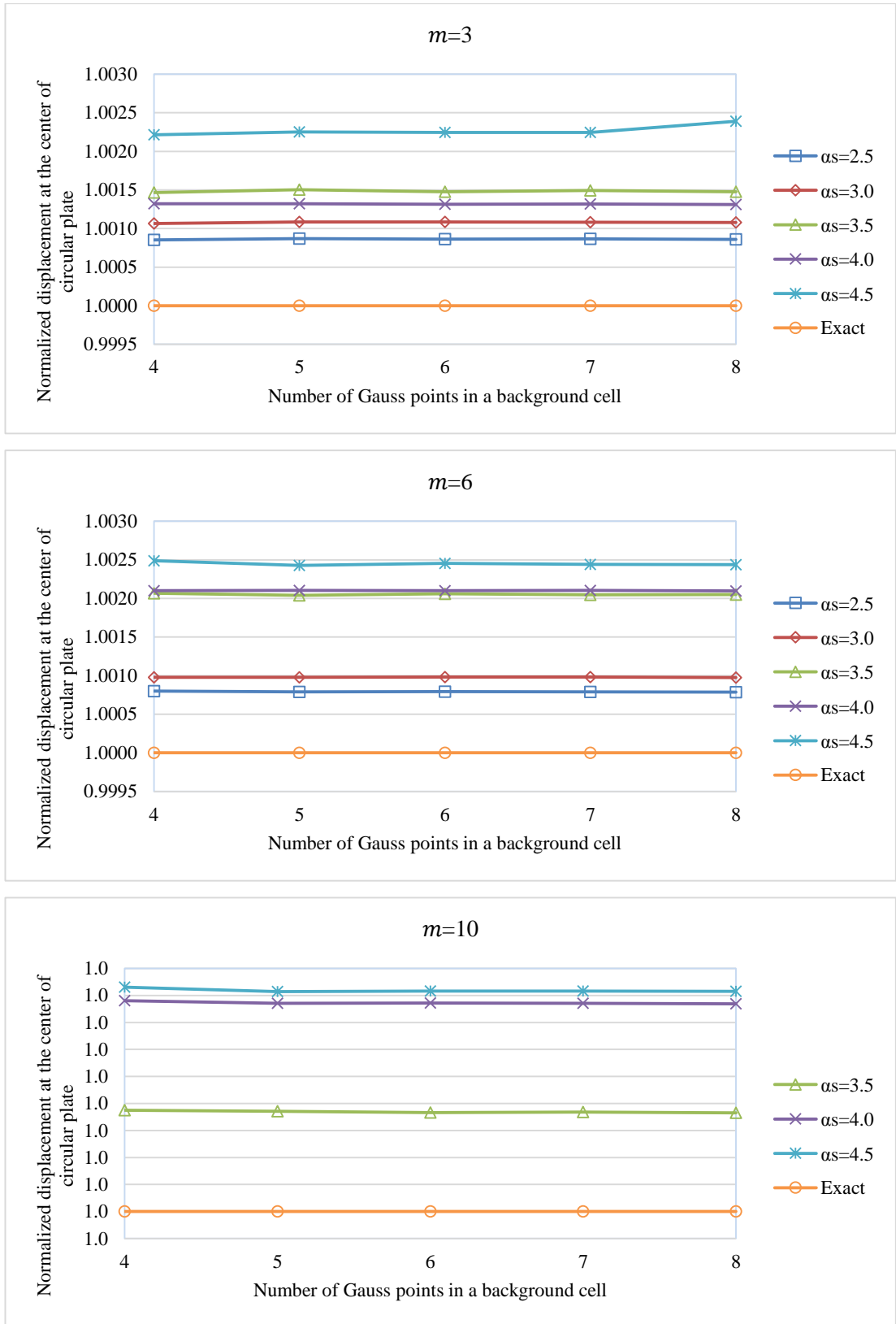


**Figure 5.39.** Variations of normalized central deflections  $w_c / \left( \frac{pL^4}{100D} \right)$  against  $n_g$  for clamped circular plate subjected to uniform load using quartic spline weight functions and regular node distribution with  $\alpha_p = 6$ .

**Table 5.34.** Variations of normalized central moments  $M_c / \left( \frac{pL^2}{10} \right)$  of clamped circular plate subjected to uniform load using regular node distribution using quartic spline weight function with  $\alpha_p = 6$ .

Number of monomials	Number of gauss points	Dimensionless size of support domain ( $\alpha_s$ )					Exact
		2.5	3.0	3.5	4.0	4.5	
<b>3</b>	4×4	0.803216	0.807935	0.812038	0.811658	0.815952	0.812520
	5×5	0.803409	0.808044	0.812407	0.811622	0.816192	
	6×6	0.803395	0.808066	0.812097	0.811561	0.816113	
	7×7	0.803357	0.808029	0.812311	0.811604	0.816105	
	8×8	0.803412	0.808028	0.812171	0.811592	0.816606	
<b>6</b>	4×4	0.808403	0.785755	0.816451	0.812367	0.826805	
	5×5	0.803875	0.785271	0.815545	0.813038	0.826578	
	6×6	0.806252	0.785532	0.816040	0.812943	0.826437	
	7×7	0.804720	0.785431	0.815930	0.812971	0.826502	
	8×8	0.805755	0.785372	0.815736	0.812914	0.826489	
<b>10</b>	4×4	31.251156	-839.6852	0.805688	0.965372	0.906891	
	5×5	4.7317120	-1.231550	0.806454	0.951697	0.899088	
	6×6	244.81044	213.328960	0.803503	0.949618	0.902025	
	7×7	-15.090472	321.223240	0.805454	0.953758	0.900464	
	8×8	-12.727712	388.400040	0.805672	0.952396	0.900643	

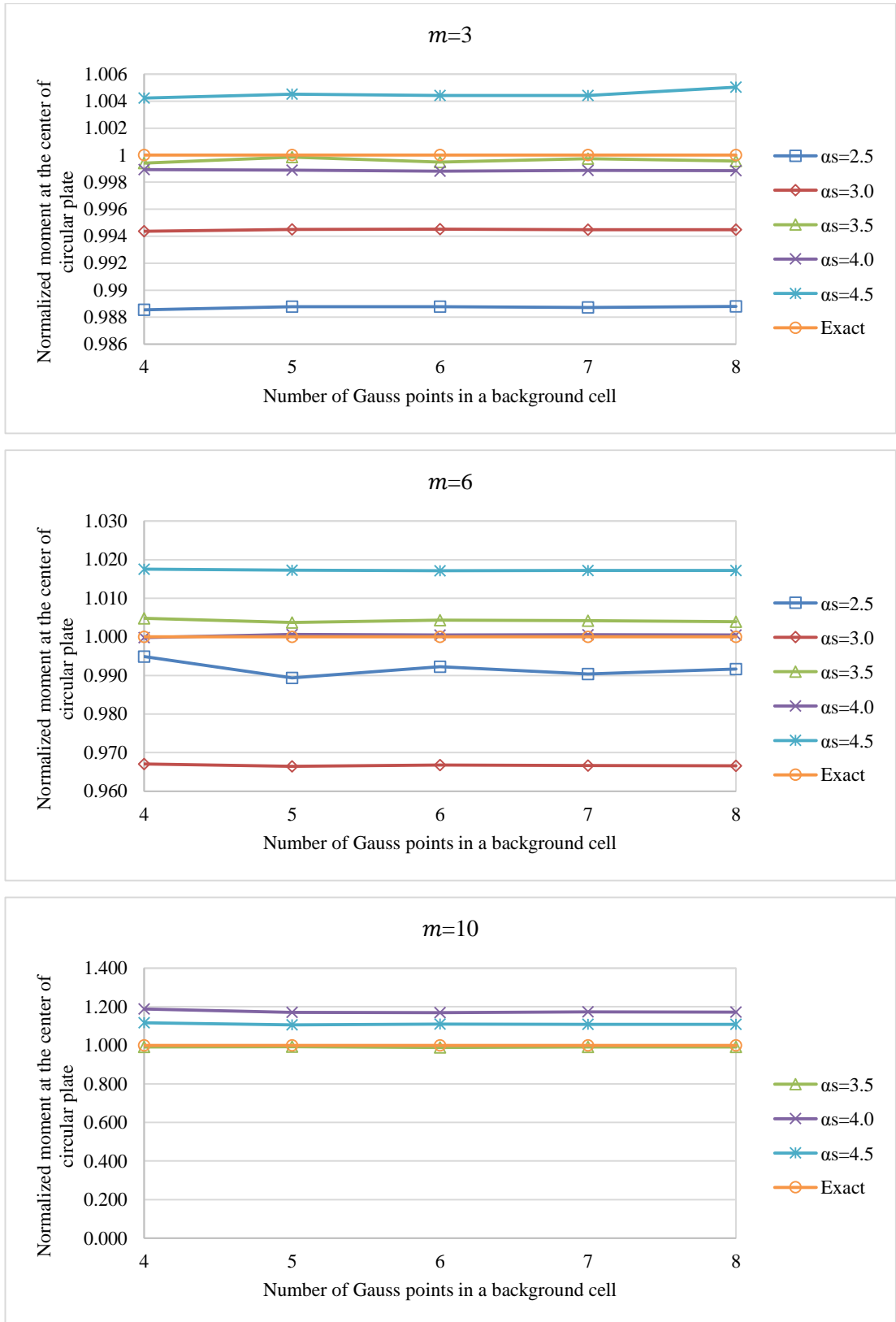


**Figure 5.40.** Variations of normalized central moments  $M_c/\left(\frac{pL^2}{10}\right)$  against  $n_g$  for clamped circular plate subjected to uniform load using quartic spline weight functions and regular node distribution with  $\alpha_p = 6$ .



**Table 5.35.** Variations of normalized central deflections  $w_c / \left( \frac{pL^4}{100D} \right)$  of clamped circular plate subjected to uniform load using irregular node distribution using quartic spline weight function with  $\alpha_p = 6$ .

Number of monomials	Number of gauss points	Dimensionless size of support domain ( $\alpha_s$ )					Exact
		2.5	3.0	3.5	4.0	4.5	
<b>3</b>	4×4	0.184954	0.184991	0.184997	0.185010	0.185061	0.184821
	5×5	0.184957	0.184973	0.184981	0.184978	0.184994	
	6×6	0.184952	0.184966	0.184972	0.184975	0.184987	
	7×7	0.184953	0.184968	0.184972	0.184973	0.184984	
	8×8	0.184951	0.184965	0.184970	0.184972	0.184984	
<b>6</b>	4×4	0.184974	0.184976	0.184998	0.185022	0.185043	
	5×5	0.184965	0.184969	0.184983	0.185007	0.185007	
	6×6	0.184963	0.184968	0.184980	0.185002	0.185001	
	7×7	0.184964	0.184969	0.184980	0.185000	0.185000	
	8×8	0.184962	0.184967	0.184979	0.185000	0.184998	
<b>10</b>	4×4	0.188686	0.185024	0.185021	0.185083	0.185098	
	5×5	0.186088	0.184983	0.185015	0.185037	0.185062	
	6×6	0.185740	0.184979	0.185005	0.185031	0.185053	
	7×7	0.185560	0.184976	0.185002	0.185026	0.185050	
	8×8	0.185348	0.184974	0.185000	0.185026	0.185049	

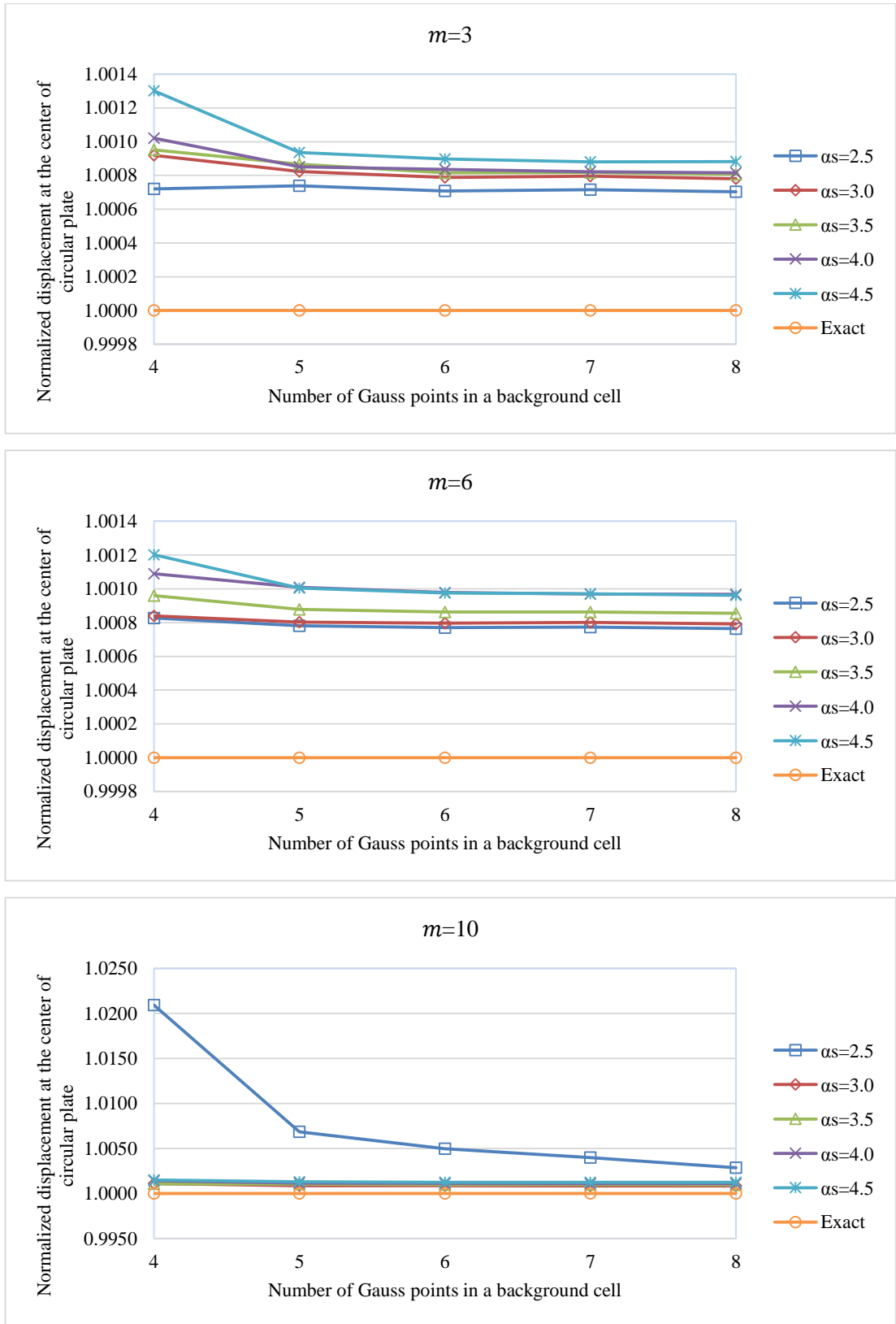


**Figure 5.41.** Variations of normalized central deflections  $w_c / \left( \frac{pL^4}{100D} \right)$  against  $n_g$  for clamped circular plate subjected to uniform load using quartic spline weight functions and irregular node distribution with  $\alpha_p = 6$ .

**Table 5.36.** Variations of normalized central moments  $M_c / \left( \frac{pL^2}{10} \right)$  of clamped circular plate subjected to uniform load using irregular node distribution using quartic spline weight function with  $\alpha_p = 6$ .

Number of monomials	Number of gauss points	Dimensionless size of support domain ( $\alpha_s$ )					Exact
		2.5	3.0	3.5	4.0	4.5	
<b>3</b>	4×4	0.804040	0.802575	0.808092	0.813732	0.819422	0.812520
	5×5	0.811428	0.811770	0.811144	0.810076	0.811360	
	6×6	0.808846	0.808862	0.811272	0.812296	0.813214	
	7×7	0.809623	0.809502	0.811158	0.810939	0.812107	
	8×8	0.808738	0.809311	0.810990	0.811592	0.812608	
<b>6</b>	4×4	0.802242	0.791169	0.803957	0.790910	0.806595	
	5×5	0.809645	0.802359	0.801746	0.812815	0.807682	
	6×6	0.816418	0.798713	0.801013	0.805444	0.808402	
	7×7	0.819568	0.798002	0.799454	0.806072	0.808520	
	8×8	0.811520	0.797916	0.800636	0.805559	0.807921	
<b>10</b>	4×4	0.800306	0.800306	0.851540	0.751181	0.816967	
	5×5	0.731032	0.818052	0.731032	0.814384	0.804134	
	6×6	0.772068	0.804206	0.772068	0.795138	0.791816	
	7×7	0.758465	0.817425	0.758465	0.795084	0.799176	
	8×8	0.766742	0.796136	0.766742	0.793900	0.792316	

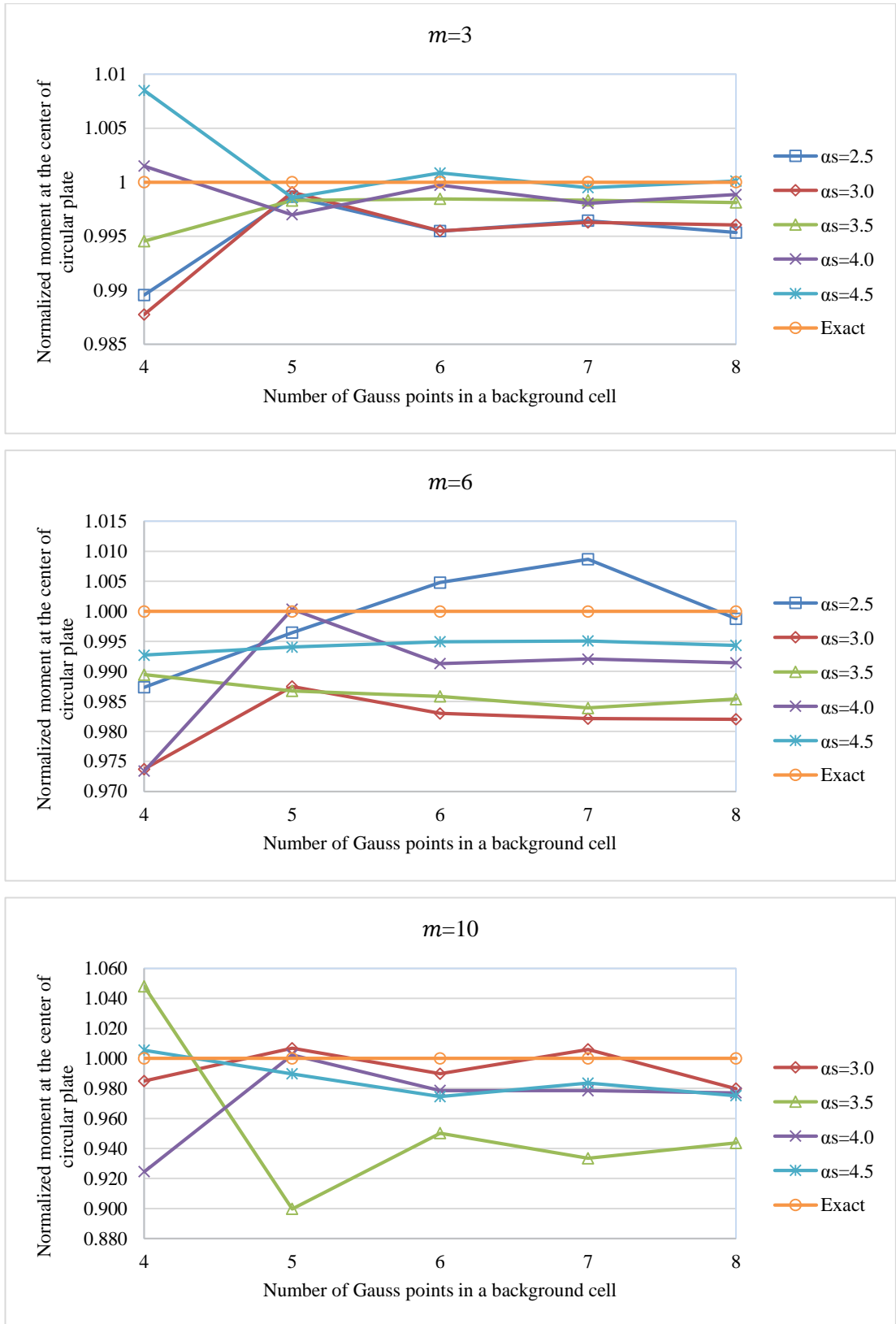


**Figure 5.42.** Variations of normalized central moments  $M_c / \left( \frac{pL^2}{10} \right)$  against  $n_g$  for clamped circular plate subjected to uniform load using quartic spline weight functions and irregular node distribution with  $\alpha_p = 6$ .

**Table 5.37.** Variations of normalized central deflections  $w_c / \left( \frac{pL^4}{100D} \right)$  of clamped circular plate subjected to uniform load using regular node distribution using quartic spline weight function with  $n_g = 5$ .

Number of monomials	Value of penalty coefficient	Dimensionless size of support domain ( $\alpha_s$ )					Exact
		2.5	3.0	3.5	4.0	4.5	
<b>3</b>	6	0.184982	0.185022	0.185099	0.185065	0.185237	0.184821
	7	0.184982	0.185022	0.185099	0.185065	0.185237	
	8	0.184982	0.185022	0.185099	0.185065	0.185237	
	9	0.184982	0.185022	0.185099	0.185065	0.185238	
	10	0.184982	0.185022	0.185099	0.185066	0.185259	
	11	0.184982	0.185018	0.185101	0.185063	0.185009	
<b>6</b>	6	0.184967	0.185002	0.185198	0.185210	0.185270	
	7	0.184967	0.185002	0.185198	0.185210	0.185270	
	8	0.184967	0.185002	0.185198	0.185210	0.185270	
	9	0.184967	0.185002	0.185198	0.185210	0.185270	
	10	0.184967	0.185002	0.185200	0.185210	0.185278	
	11	0.184966	0.185001	0.185198	0.185205	0.185299	
<b>10</b>	6	0.587254	0.018966	0.185164	0.185533	0.185573	
	7	0.046057	0.000554	0.185164	0.185533	0.185573	
	8	0.030590	0.131359	0.185164	0.185533	0.185573	
	9	0.032774	0.034070	0.185164	0.185532	0.185574	
	10	0.201877	0.056659	0.185164	0.185534	0.185573	
	11	0.062664	0.038410	0.185164	0.185545	0.185577	

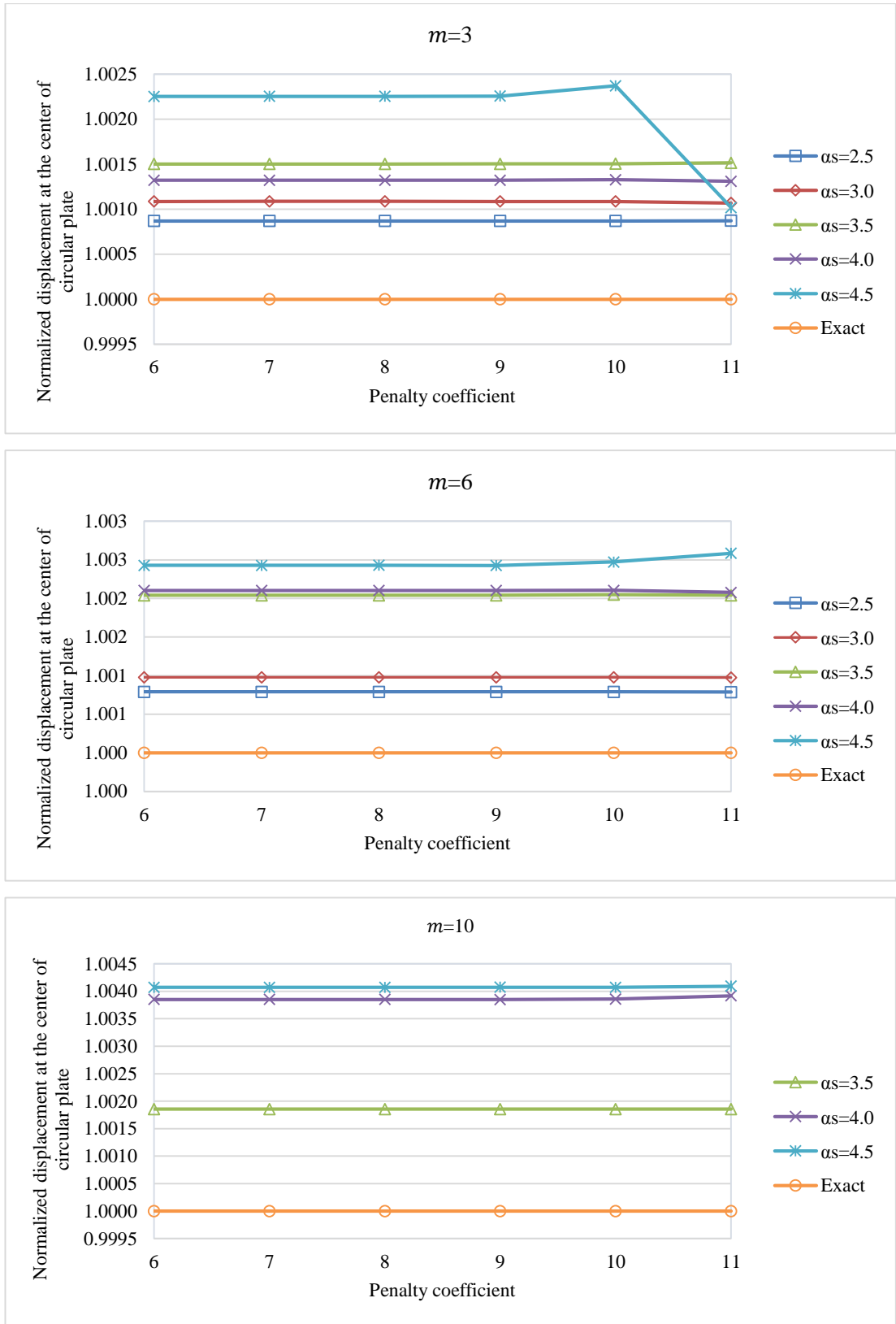


**Figure 5.43.** Variations of normalized central deflections  $w_c / \left( \frac{pL^4}{100D} \right)$  against  $\alpha_p$  for clamped circular plate subjected to uniform load using quartic spline weight functions and regular node distribution with  $n_g = 5$ .

**Table 5.38.** Variations of normalized central moments  $M_c/\left(\frac{pL^2}{10}\right)$  of clamped circular plate subjected to uniform load using regular node distribution using quartic spline weight function with  $n_g = 5$ .

Number of monomials	Value of penalty coefficient	Dimensionless size of support domain ( $\alpha_s$ )					Exact
		2.5	3.0	3.5	4.0	4.5	
<b>3</b>	6	0.793561	0.796388	0.825787	0.850086	0.838228	0.81252
	7	0.793562	0.796388	0.825789	0.850072	0.838263	
	8	0.793563	0.796388	0.825777	0.849728	0.838316	
	9	0.793565	0.796380	0.825856	0.857181	0.846872	
	10	0.793692	0.796490	0.826983	0.893778	0.800843	
	11	0.793583	0.795175	0.861890	0.811790	0.817878	
<b>6</b>	6	0.805522	0.792724	0.786690	0.881132	0.914100	
	7	0.805523	0.792724	0.786688	0.881133	0.914108	
	8	0.805518	0.792723	0.786698	0.881098	0.913649	
	9	0.805474	0.792770	0.786643	0.880908	0.913589	
	10	0.805580	0.792700	0.787733	0.878576	0.986539	
	11	0.807486	0.798771	0.789675	0.860875	0.568828	
<b>10</b>	6	4.731712	-1.231550	0.748127	0.954821	0.989044	
	7	-4.077584	-14.86779	0.748127	0.954814	0.989024	
	8	10.518148	372.40796	0.748126	0.954852	0.988741	
	9	27.793320	55.000480	0.748397	0.955136	0.990875	
	10	960.83960	130.99592	0.747854	0.949300	1.016872	
	11	-88.41152	-3.352686	0.733828	0.943248	0.779644	

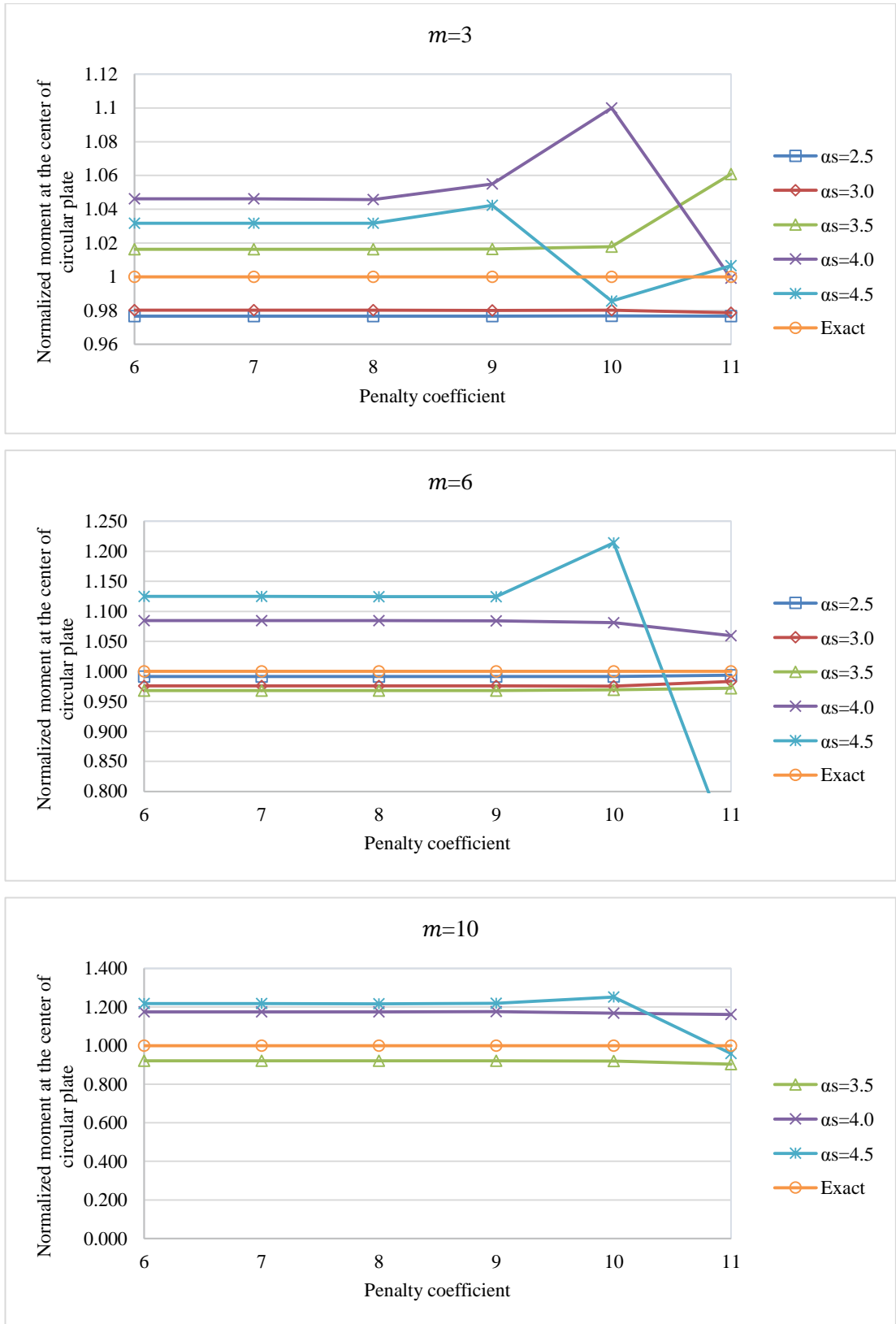


**Figure 5.44.** Variations of normalized central moments  $M_c/\left(\frac{pL^2}{10}\right)$  against  $\alpha_p$  for clamped circular plate subjected to uniform load using quartic spline weight functions and regular node distribution with  $n_g = 5$ .



**Table 5.39.** Variations of normalized central deflections  $w_c / \left( \frac{pL^4}{100D} \right)$  of clamped circular plate subjected to uniform load using irregular node distribution using quartic spline weight function with  $n_g = 5$ .

Number of monomials	Value of penalty coefficient	Dimensionless size of support domain ( $\alpha_s$ )					Exact
		2.5	3.0	3.5	4.0	4.5	
<b>3</b>	6	0.184957	0.184973	0.184981	0.184978	0.184994	0.184821
	7	0.184957	0.184973	0.184981	0.184978	0.184994	
	8	0.184957	0.184973	0.184981	0.184978	0.184994	
	9	0.184957	0.184973	0.184981	0.184978	0.184994	
	10	0.184957	0.184973	0.184981	0.184978	0.184994	
	11	0.184957	0.184973	0.184981	0.184979	0.184990	
<b>6</b>	6	0.184965	0.184969	0.184983	0.185007	0.185007	
	7	0.184965	0.184969	0.184983	0.185007	0.185007	
	8	0.184965	0.184969	0.184983	0.185007	0.185007	
	9	0.184965	0.184969	0.184983	0.185007	0.185007	
	10	0.184965	0.184969	0.184983	0.185007	0.185006	
	11	0.184966	0.184968	0.184984	0.185007	0.185008	
<b>10</b>	6	0.186088	0.184983	0.185015	0.185037	0.185062	
	7	0.184983	0.184983	0.185015	0.185037	0.185062	
	8	0.184983	0.184983	0.185015	0.185037	0.185062	
	9	0.184983	0.184983	0.185015	0.185037	0.185062	
	10	0.184983	0.184983	0.185014	0.185039	0.185062	
	11	0.184979	0.184979	0.185019	0.185011	0.185076	

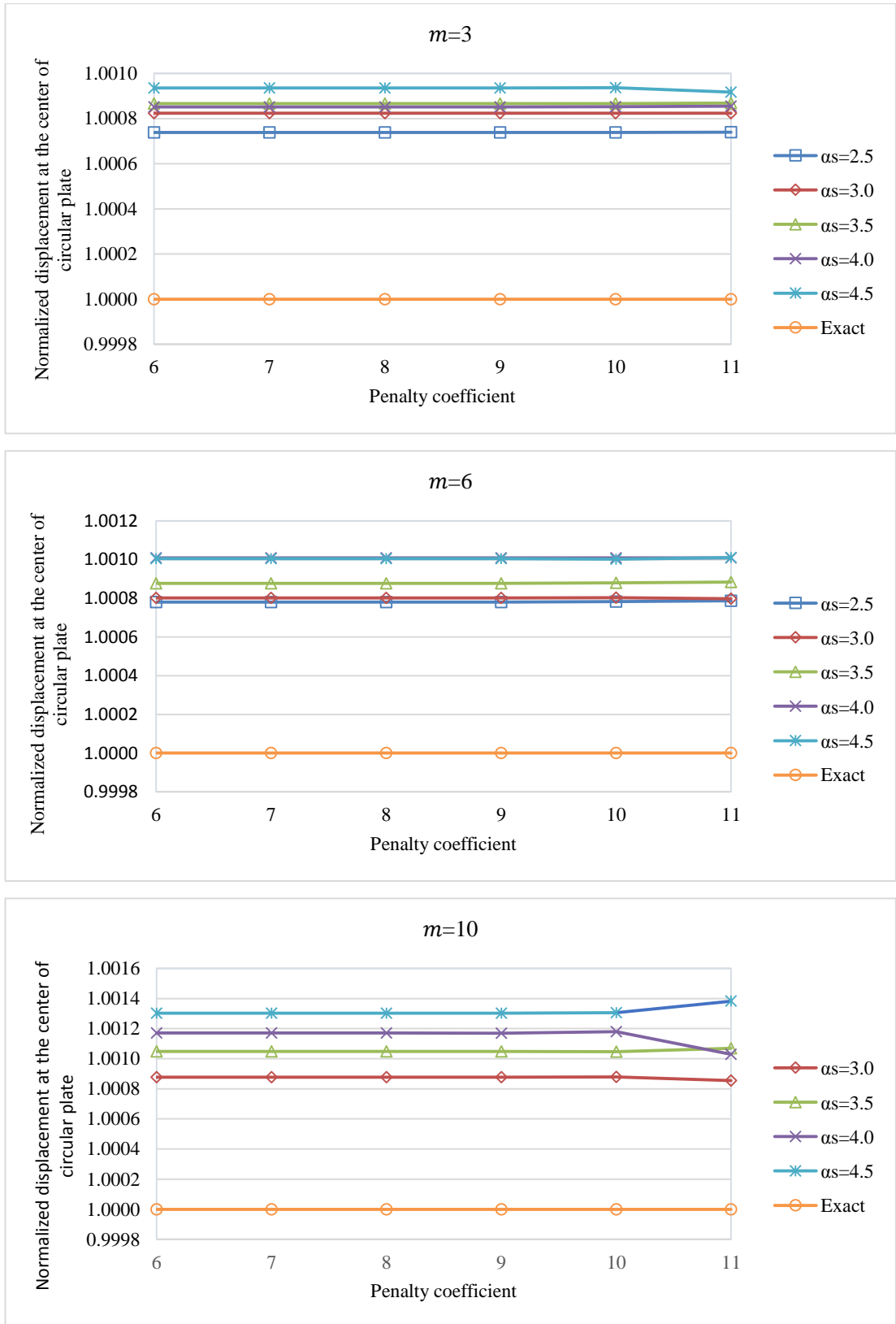


**Figure 5.45.** Variations of normalized central deflections  $w_c / \left( \frac{pL^4}{100D} \right)$  against  $\alpha_p$  for clamped circular plate subjected to uniform load using quartic spline weight functions and irregular node distribution with  $n_g = 5$ .

**Table 5.40.** Variations of normalized central moments  $M_c / \left( \frac{pL^2}{10} \right)$  of clamped circular plate subjected to uniform load using irregular node distribution using quartic spline weight function with  $n_g = 5$ .

Number of monomials	Value of penalty coefficient	Dimensionless size of support domain ( $\alpha_s$ )					Exact
		2.5	3.0	3.5	4.0	4.5	
<b>3</b>	6	0.806297	0.807521	0.809430	0.808711	0.810942	0.81252
	7	0.806298	0.807521	0.809431	0.808711	0.810942	
	8	0.806298	0.807531	0.809428	0.808708	0.810939	
	9	0.806256	0.807446	0.809409	0.808713	0.810897	
	10	0.806448	0.807646	0.808948	0.808606	0.808491	
	11	0.802864	0.813909	0.808067	0.812605	0.816746	
<b>6</b>	6	0.815844	0.809876	0.807320	0.810871	0.807294	
	7	0.815844	0.809876	0.807320	0.810871	0.807294	
	8	0.815848	0.809918	0.807326	0.810819	0.807301	
	9	0.816026	0.809768	0.807197	0.810514	0.807252	
	10	0.814844	0.808537	0.807092	0.809416	0.808359	
	11	0.818396	0.819513	0.804920	0.799838	0.821350	
<b>10</b>	6	-7.026600	0.805180	0.791402	0.793544	0.805440	
	7	-6.999436	0.805181	0.791399	0.793561	0.805439	
	8	-6.925176	0.805126	0.791389	0.793772	0.805431	
	9	-3.056648	0.804704	0.790996	0.793589	0.805426	
	10	12.080536	0.803400	0.794435	0.794284	0.802448	
	11	256.58380	0.791174	0.765158	0.775530	0.805649	

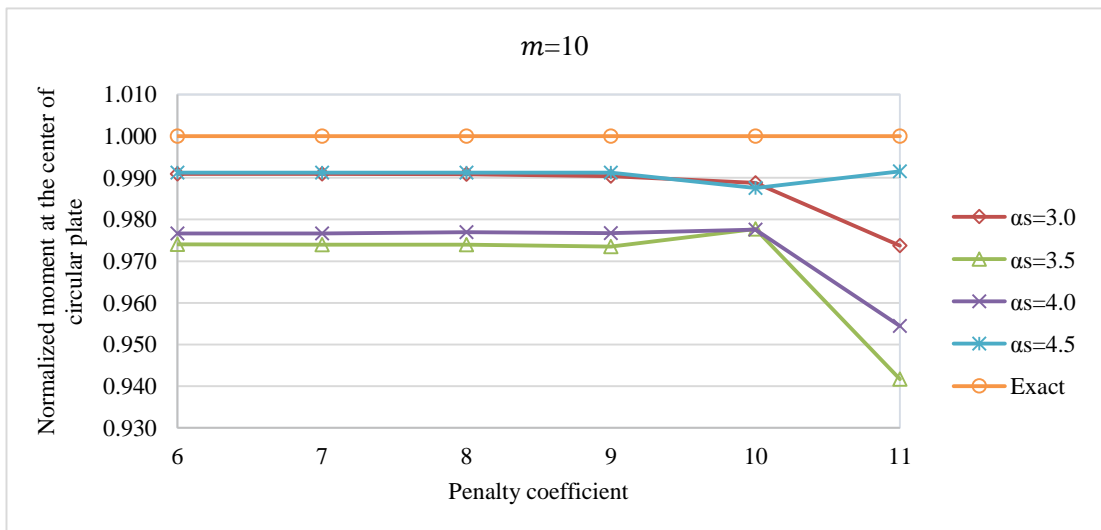
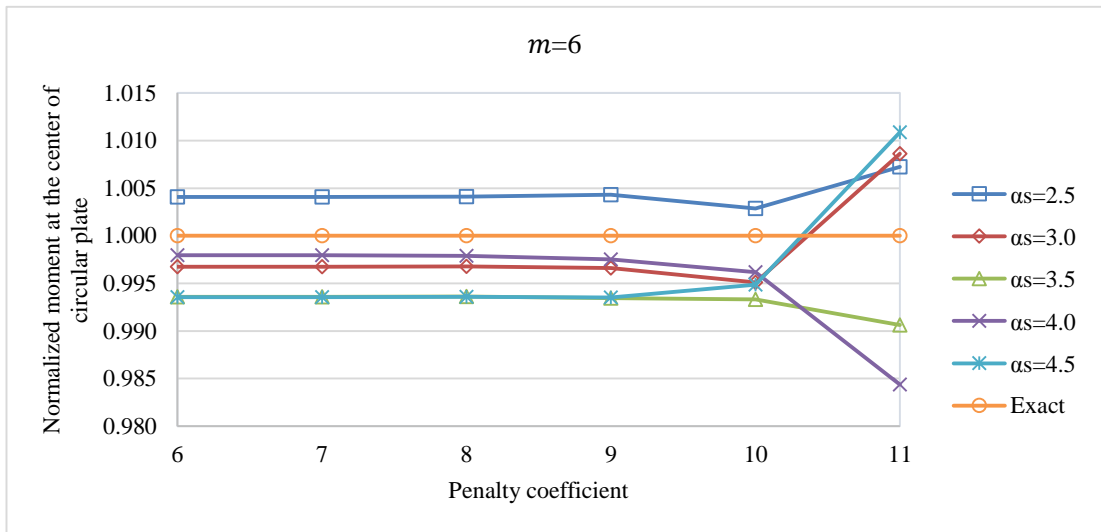
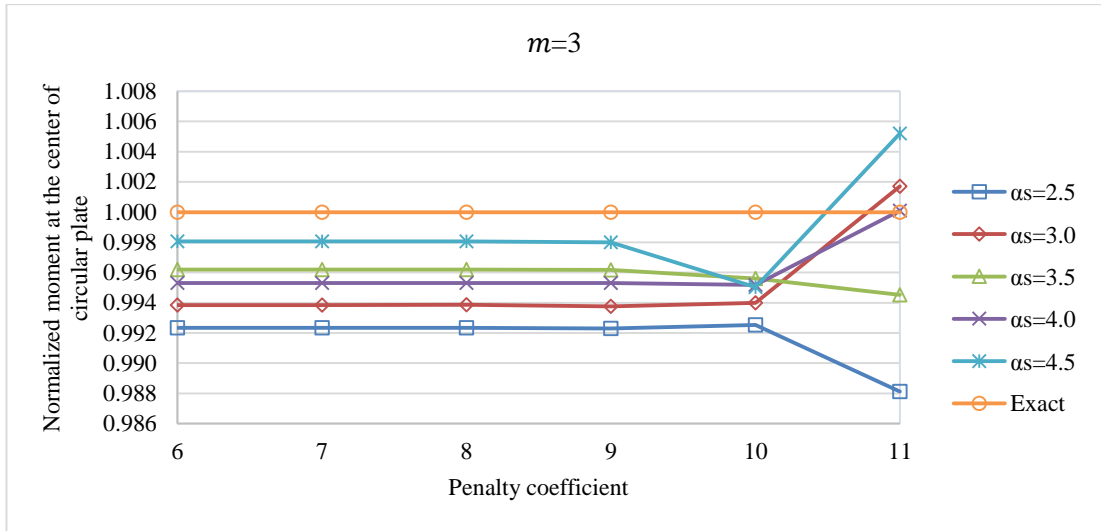


**Figure 5.46.** Variations of normalized central moments  $M_c / \left( \frac{pL^2}{10} \right)$  against  $\alpha_p$  for clamped circular plate subjected to uniform load using quartic spline weight functions and irregular node distribution with  $n_g = 5$ .

## CHAPTER 6

### CONCLUSIONS AND RECOMMENDATIONS

The effects of selectable parameters: size of support domain, number of monomials, type of weight function, number of integration points in a background cell and value of penalty coefficient, on the accuracy of the EFGM solution of the Reissner-Mindlin plate bending are investigated. Three plate bending problems which are accepted as benchmark problems are solved using regular and irregular node distributions. The results of the problems show that small support domains give more accurate and more stable results. It is shown that the number of gauss points in a background cell, at the examined range, don't have so much effect on the accuracy of results. Also, the value of penalty coefficient does not exhibit any accuracy loss or fluctuation up to  $1 \times 10^8$ . There are some differences found between cubic spline and quartic spline weight functions and it seems that quartic spline weight function is more stable and less sensitive to values of selectable parameters. These assessments are valid for both displacement and moment. However, it is shown that the accuracy of displacement results are higher than the accuracy of moment results.

According to the results of problems;  $3.0, 5 \times 5, 1 \times 10^6$  can be suggested for dimensionless size of support domain, number of gauss points in a background cell, and value of penalty coefficient, respectively. These values may not be the optimum values for every situation, however, in general, give the results with sufficient accuracy.

## REFERENCE

- [1] Lucy, L. B. (1977). A numerical approach to the testing of the fission hypothesis. *Astronomical Journal*, **82**(12), 1013–1024.
- [2] Gingold, R. A. and Monaghan, J. J. (1977). Smoothed particle hydrodynamics - Theory and application to non-spherical stars. *Monthly notices of the royal astronomical society*, **181**,375-389.
- [3] Breitkopf, P. et al. (2004). Integration constraint in diffuse element method. *Computer methods in applied mechanics and engineering*, **193**, 1203-1220.
- [4] Belytschko, T. et al. (1996). Meshless Methods An Overview and Recent Developments. *International Journal for Numerical Methods in Engineering*, **38**, 1655-1679.
- [5] Memar Ardestani, M. et al. (2014). Analysis of functionally graded stiffened plates based on FSDT utilizing reproducing kernel particle method. *Elsevier journal*, **112**, 231–240.
- [6] Liu, G.R. and Gu, Y.T. (2003). A matrix triangularization algorithm for the polynomial point interpolation method. *Computer methods in applied mechanics and engineering*, **192**, 2269–2295.
- [7] Atluri, S. N. and Zhu, T. (1998). A new meshless local petrov-galerkin (mlpg) approach in computational mechanics, *Computational Mechanics*. 22, 117–127.
- [8] Shahrokhbadi, Sh.et al. (2014). Hybrid of Natural Element Method (NEM) with Genetic Algorithm (GA) to find critical slip surface. *Alexandria Engineering Journal*, **53**, 373–383.
- [9] Yu, Y. et al. (2013). Multi-snap-through and dynamic fracture based on Finite Particle Method. *Journal of Constructional Steel Research*, **82**, 142–152.

- [10] William E. B. and Richard C. D. (2001). Elementary Differential Equations and Boundary Value Problems. *Library of Congress Cataloging in Publication Data*, 0-47.
- [11] PEDLEY, T.J. (1977). Introduction to Fluid Dynamics. *Scientia marina*, **61**, (Supl. 1): 7-24.
- [12] Liu, M. B. et al. (2003). Smoothed particle hydrodynamics for numerical simulation of underwater explosion. *Springer-Verlag*, 106–118.
- [13] Li, SH. and Liu, W.K. (2002). Meshfree and particle methods and their applications. *American Society of Mechanical Engineers*, **55**, 10.1115
- [14] Sticko, S. (2013). Smooth Particle Hydrodynamics Applied to Fracture Mechanics. *Uppsala university*, 1401-5757.
- [15] Blyth, M. G. and Pozrikidis, C. (2005). A Lobatto interpolation grid over the triangle. *Journal of Applied Mathematics*, **10**, 1093.
- [16] Huerta, A. et al. (2004). Meshfree Methods. *Encyclopedia of Computational Mechanics*.
- [17] Lima, N. Z. and Mesquita, R. C. (2013). Point Interpolation Methods based on Weakened-Weak Formulations. *Journal of Microwaves, Optoelectronics and Electromagnetic Applications*, **12(2)**, 2179-1074.
- [18] BOYD, J. P. (1985). Complex Coordinate Methods for Hydrodynamic instabilities and Sturm-Liouville Eigen problems with an Interior Singularity. *Journal of computational physics*, **57**, 454-471.
- [19] Liu R. and Gu. Y.T. (2003). A matrix triangularization algorithm for the polynomial point interpolation method. *Proceedings of the Asia-Pacific Vibration Conference*, **192(19)**, 2269–2295.
- [20] Kanber, B. and Bozkurt, O. Y. (2008). A diagonal offset algorithm for the polynomial point interpolation method, *Numerical method in biomedical engineering*, **24(12)**, 1909-1922.

- [21] Liu, G.R. (2003). Mesh Free Methods Moving beyond the finite element method. *Taylor and Francis Group*, 0-8493-1238-8.
- [22] Liu, G.R. and GU, Y.T. (2005). An Introduction to Meshfree Methods and Their Programming. *Springer Dordrecht*, **10**, 1-4020-3228-5.
- [23] Singh, S. et al. (2012). Buckling of laminated composite plates subjected to mechanical and thermal loads using meshless collocations. *Journal of mechanical science and technology*, **27**, 327-336.
- [24] Lear, M.H. (2003). Numerical Simulation of Adiabatic Shear Bands and Crack Propagation in Thermoviscoplastic Materials. *Engineering Mechanics*.
- [25] Sladek, V. et al. (2013). Physical decomposition of thin plate bending problems and their solution by mesh-free methods. *Slovakia engineering analysis with boundary elements*, **37(2)**, 348–365.
- [26] Zhu, P. and Liew, K.M. (2011). Free vibration analysis of moderately thick functionally graded plates by local Kriging meshless method, *Journal of Elsevier*, **93(13)**, 2925–2944.
- [27] Liu, G.R. et al. (2008). Static and free vibration analysis of laminated composite plates using the conforming radial point interpolation method. *Journal of Elsevier*, **68(2)**, 354–366.
- [28] Atluri, S. N. and Shen, SH. (2002). The Meshless Local Petrov-Galerkin (MLPG) Method: A Simple & Less-costly Alternative to the Finite Element and Boundary Element Methods. *Tech Science Press*. **3**, 1.11-51.
- [29] Li, Q. et al. (2003). Application of Meshless Local Petrov-Galerkin (MLPG) to Problems with Singularities, and Material Discontinuities in 3-D Elasticity. *Tech Science Press*, **4(5)**, 571-585.
- [30] Sladek, J. et al. (2004). Meshless Local Petrov-Galerkin Method in Anisotropic Elasticity. *Tech Science Press*, **6(5)**, 477-489.



- [31] Lin, H. and Atluri, S.N. (2001). The Meshless Local Petrov-Galerkin (MLPG) Method for Solving Incompressible Navier-Stokes Equations. *Tech Science Press*, **2(2)**, 117-142.
- [32] Batra, R.C. and Porfir, M. (2008). Analysis of rubber-like materials using meshless local Petrov-Galerkin (MLPG) method. *Wiley InterScience*, **24**, 1781-1804.
- [33] Batra, R.C. and Ching, H.K. (2002). Analysis of Elastodynamic Deformations near a Crack/Notch Tip by the Meshless Local Petrov-Galerkin (MLPG). *Tech Science Press*, **3(6)**, 717-730.
- [34] Yu, SH. T. et al. (2013). An element-free Galerkin (EFG) method for generalized Fisher equations (GFE). *China Phys*, **22(6)**, 060210
- [35] Yin, Y. et al. (2003). A 3D shell-like approach using element-free Galerkin method for analysis of thin and thick plate structures. *Springer*, **29(1)**, 85-98.
- [35] De, S. and Bathe, K. J. (2000). The method of finite spheres. *Computational Mechanics*, **25**, 329-345.
- [36] Byrd, R. H. et al. (2007). Steering Exact Penalty Methods for Nonlinear Programming. *Optimization Technology Center Northwestern University*.
- [37] Trench, W.F. (2013). The method of lagrange multipliers. *Department of MathematicsTrinity University*.
- [38] Fries, T.P. and Matthies, H.G. (2004). Stabilized and Coupled FEM/EFG Approximations for Fluid Problems. *Computational Mechanics*, **65**, D-38106.
- [39] Shyan, Ch. and Ping, W. (2000). New boundary condition treatments in meshfree computation of contact problems. *Computer methods in applied mechanics and engineering*, **187**,441±468.
- [40] Beissel S, Belytschko T. (1996). Nodal integration of the element-free Galerkin method. *Computer Methods in Applied Mechanics and Engineering*. 139, 49-74.

- [41] Samimi, S. and Pak, A. (2012). Three-dimensional simulation of fully coupled hydro-mechanical behavior of saturated porous media using Element Free Galerkin (EFG) method. *Computers and Geotechnics*, **46**, 75–83.
- [42] Li, Y. et al. (2009). Fracture analysis of cracked 2D planar and axisymmetric problems of magneto–electro-elastic materials by the MLPG coupled with FEM. *Computer Methods in Applied Mechanics and Engineering*, **198**, 2347–2359.
- [43] Wu, C.H. and Chiu, K. (2011). RMVT-based meshless collocation and element-free Galerkin methods for the quasi-3D free vibration analysis of multilayered composite and FGM plates. *Composite Structures*, **93**, 1433–1448.
- [44] Wu, C.H. et al. (2011). RMVT-based meshless collocation and element-free Galerkin methods for the quasi-3D analysis of multilayered composite and FGM plates. *Composite Structures*, **93**, 923–943.
- [45] LIU, G. R. and CHEN, X. L. (2001). A Mesh-free Method For Static And Free Vibration Analyses Of Thin Plates Of Complicated Shape. *Journal of Sound and vibration*, **241**, 839-855.
- [46] Froehle, B. and Persson, P. (2014). A high order discontinuous Galerkin method for fluid–structure interaction with efficient implicit–explicit time stepping. *Journal of Computational Physics*, **272**, 455–470.
- [47] Ferrer, E. and Willden, R. (2012). A high order Discontinuous Galerkin – Fourier incompressible 3D Navier–Stokes solver with rotating sliding meshes. *Journal of Computational Physics*, **231**, 7037–7056.
- [48] Zhang, L. et al. (2011). The coupling of element-free Galerkin method and molecular dynamics for the incompressible flow problems. *Springer link journal*, **10**(4), 809-820.
- [49] Park, Y. and Leap, D. (2000). Modeling groundwater flow with a free and moving boundary using the element-free Galerkin (EFG) method. *Springer link journal*, **4**(3), 243-249.

- [50] Miyamoto, N. and Yamashita, H. (2002). Element-free Galerkin method for electromagnetic field computations, *Browse Journals & Magazines*, **34**(5), 3236-3239.
- [51] Louaï, F.Z. and et al. (2007). Implementation of an efficient element-free Galerkin method for electromagnetic computation. *Engineering Analysis with Boundary Elements*, **31**, 191–199.
- [52] Cheng, R.J. and Liew, K.M. (2012). Analyzing modified equal width (MEW) wave equation using the improved element-free Galerkin method. *Engineering Analysis with Boundary Elements*, **36**, 1322–1330.
- [53] Liu, X. et al. (2007). Element-Free Galerkin Method in Electromagnetic Scattering Field Computation. *Journal of Electromagnetic Waves and Applications*, **21**(14), 1915-1923.
- [54] Louaï, F. et al. (2006). Numerical Analysis Of Electromagnetic Axisymmetric Problems Using Element Free Galerkin Method. *Journal of Electrical Engineering*, **57**(2):9–104.
- [55] Rao, B.N. and Rahman, S. (2000). An efficient meshless method for fracture analysis of cracks. *Computational Mechanics*, **26**,398-408.
- [56] Rahman, S. and Rao, B.N. (2000). An efficient meshless method for fracture analysis of cracks. *Computational Mechanics*, **26**,398-408.
- [57] Swathi, B. (2007). Technical Article Overview of Meshless Methods. Academia.com.
- [58] Belytschko, T. et al. (1994). Element-free Galerkin methods, *International Journal for Numerical Methods in Engineering*, **37**, 2, 229–256.
- [59] Liew, K.M. et al. (2011). A review of meshless methods for laminated and functionally graded plates and shells. *Composite Structures*, **93**, 2031–2041.
- [60] Bui, T.Q. et al. (2011). Buckling analysis of Reissner–Mindlin plates subjected to in-plane edge loads using a shear-locking-free and meshfree method. *Engineering Analysis with Boundary Elements*, **35**, 1038–1053.

- [61] Liew, K. M. et al. (2002). Analysis of laminated composite beams and plates with piezoelectric patches using the element-free Galerkin method. *Computational Mechanics(Springer)*, **29**, 486–497.
- [62] Tiago, C.and Pimenta, P. (2008). An EFG method for the nonlinear analysis of plates undergoing arbitrarily large deformations. *Engineering Analysis with Boundary Elements*, **32**, 494–511.
- [63] Swaminathan, K. et al. (2014). Stress, vibration and buckling analyses of FGM plates - A state-of-the-art Review. *Composite Structures*, **120**, 10–31.
- [64] Tinh Quoc, B. et al. (2011). An efficient meshfree method for vibration analysis of laminated composite plates. *Computer Mechanic*, **48**:175–193.
- [65] Li, D.M. .et.al. (2014). An improved complex variable element-free Galerkin method for two-dimensional large deformation elastoplasticity problems. *Journal of Elsevier*, **269**, 72–86.
- [66] Goudarzi, M. and Mohammadi, S. (2014). Analysis of cohesive cracking in saturated porous media using an extrinsically enriched EFG method. *Computers and Geotechnics*, **63**, 183–198.
- [67] Tiago, C. and Leitao, V. (2007). Eliminating Shear – Locking in Meshless Method: A Critical Overview and a New Framework for Structural Theories. *Computaitional method in applied sciences*, **5**, 123-145.
- [68]Kiasat, A. et al. (2006). Application Of High Order Basis Functions In Solid Mechanics By Element Free Galerkin (EFG) Method. *Computaitional methods*, 1453-1457.
- [69] Emre Erkmen, R. and Bradford, M. (2010). Elimination of slip-locking in composite beam-column analysis by using the element-free Galerkin method. *Computational Mechanics*, **46**,911–924.
- [70] Owen D.R., and Hinton E. (1980). Finite Elements in Plasticity. *Swensea, Pineridge Pres Limited*,